TRP and TRPL Channels in Synaptic Transmission in *Drosophila* Photoreceptors

Tesis

Entregada a la

Universidad de Chile

en Cumplimiento Parcial de los Requisitos

Para Optar al Grado de

Doctor en Ciencias con Mención en Biología Molecular, Celular Y Neurociencias

Facultad De Ciencias

Por

Guadalupe Lorenia Astorga Rodríguez

Junio, 2010

Directores de Tesis:

Dr. Juan Bacigalupo
Dra. Magdalena Sanhueza

FACULTAD DE CIENCIAS

UNIVERSIDAD DE CHILE

INFORME DE APROBACION

TESIS DE DOCTORADO

Se informa a la Escuela de Postgrado de la Facultad de Ciencias que la Tesis de Doctorado presentada por la candidata.

GUADALUPE LORENIA ASTORGA RODRIGUEZ

Ha sido aprobada por la comisión de Evaluación de la tesis como requisito para optar al grado de Doctor en Ciencias con mención en Biología Molecular Celular y Neurociencias, en el examen de Defensa Privada de Tesis rendido el día 26 de mayo de 2010.

Director de Tesis:
Dr. Juan Bacigalupo .....

Directora de Tesis:
Dra. Magdalena Sanhueza .....

Comisión de Evaluación de la Tesis

Dra. Jimena Sierralta .....

Dr. Andrés Couve .....

Dr. John Ewer .....

Dr. Bernardo Morales .....

Agradecimientos

A mi abuelo Enrique y su pasión por los claveles blancos...

" y a los claveles ¿qué les digo agradeciendo su fragancia?"
Pablo Neruda

Y al universo, ¿ cómo le agradezco su inmensidad
y la oportunidad que me brinda de esbozar su silueta
con el pincel mágico del conocimiento?

Quiero comenzar este capítulo, reconociendo que la culminación de esta importante etapa de mi vida profesional es producto no solo de mi infatigable esfuerzo y perseverancia, sino también del apoyo cálido y solidario de muchos profesores y personas que han sembrado conocimientos y cariños en mi espíritu.

Agradezco al Laboratorio de Fisiología Celular de la Facultad de Ciencias de la Universidad de Chile, por haberme formado y brindado el espacio para desarrollar esta tesis. Agradezco a mis tutores Juan Bacigalupo, por haber confiado en mis propuestas y permitirme desarrollarlas con libertad e independencia, y Magdalena Sanhueza, por sus agudas intervenciones y asertivas propuestas. Quiero reconocer especialmente el valioso aporte que ha realizado Ricardo Delgado en mi formación profesional, desde que crucé el umbral del Laboratorio hasta hoy. Agradezco también a Jeannette Bravo y Danny Acevedo por su incondicional colaboración, en el mantenimiento de mis cultivos de *Drosophila* y en esos pequeños detalles que han sido imprescindibles.

A mis queridas amigas y compañeras de Laboratorio, junto a las que me he formado, Carolina González, María Graciela Delgado, Lorena Sulz, Karen Castillo, por haberme apoyado y estar siempre ahí en los momentos difíciles.

Quiero agradecer también a Álvaro Glavic, John Ewer y Jimena Sierralta por su asesoría en Genética de *Drosophila* y por las cepas que generosamente me facilitaron. Así mismo, a Steffen Hartel, Omar Ramírez y Carmen Gloria Lemus por su importante asesoría en análisis y cuantificación de imágenes.

A Roger Hardie por facilitarnos los mutantes necesarios para la realización de este proyecto. A Craig Montell y Charles Zuker por facilitarnos los anticuerpos requeridos.

Cómo dejar de mencionar a mis queridos amigos de OPA ("los malos"), que me han acompañado en los últimos 7 años en mis experiencias y aventuras lúdicas y espirituales.

A mis queridas "bichitas" con las cuales hemos forjado una especial y linda amistad, fundamental cuando el agobio golpea la puerta o cuando compartimos la alegría de ir avanzando juntas en nuestros sueños.

Agradezco a toda mi familia; a mi padre por su inteligencia, su ejemplo y su locura, y por mostrarme distintas facetas de la vida; a mi madre por su elocuencia y vivacidad; a mis hermanos porque siempre sé que cuento con ellos. Como no agradecer la compañía y ternura de mi perrito Alerce, con sus largas y suaves orejas, su brillante pelaje color plateado, su estilo de gran caballero y cazador y sobretodo: su lealtad a toda prueba.

Por último, quiero agradecer a las instituciones que han financiado esta tesis: CONICYT, por sus becas: Doctoral y de Apoyo a Tesis (AT-24080134), MIDEPLAN ICM P05-001F y Proyecto Fondecyt 1100730.

INDEX

LIST OF FIGURES

ABREVIATIONS

- a.u.: arbitrary units
- CDA: confined displacement algorithm
- Ch: channel
- CICR: calcium induced calcium release
- DAG: diacylglycerol
- ER: endoplasmic reticulum
- ERG: electroretinogram
- ES: extracellular solution
- EPSCs: excitatory postsynaptic currents
- Fl: fluorescence
- FM4-64: N-(3-triethylammoniumpropyl)-4-(6-(diethylamino)phenyl)hexatrienyl)pyridinium dibromide
- GFP: green fluorescent protein
- GMR: glass multimeric reporter
- GS: gelatinous substance
- IDL: Interactive Data Language
- InaD: inactivation-no-afterpotential D
- IP_3: inositol 1,4,5-trisphosphate
- IP_3R: IP_3 receptor
- LNA: linolenic acid
- *m*-3M3FBS: 2,4,6-trimethyl-N-(meta-3-trifluoromethyl-phenyl)-benezenesulfonamide
- NCBI: National Center for Biotechnology
- NMJ: neuromuscular junction
- NINAC: neither inactivation nor afterpotential C
- NORPA (norpA): no-receptor-potential A

- PDFs: probability density functions
- PKC: protein kinase C
- PLC: phospholipase C
- PLTX-II: plectreurys toxin II
- PIP_2: phosphatidylinositol bisphosphate
- PM: plasma membrane
- PUFAS: polyunsaturated fatty acids
- Rh1: rhodopsin1
- ROI: region of interest
- RBO: rolling blackout
- Ry: ryanodine
- RyR: ryanodine receptors
- SERCAs: sarcoplasmic/endoplasmic reticulum calcium ATPases
- SCIAN: scientific image analysis
- Syb: synaptobrevin
- SV: synaptic vesicles
- SOCE: store operated calcium entry
- SOC: store operated channels
- STIM: stromal interaction molecule
- Thg: thapsigargin
- TRP: transient receptor potential
- TRPL: transient receptor potential-like
- UAS: upstream activation sequence
- VGCC: voltage-gated calcium channels

RESUMEN

Los canales TRP y TRPL de *Drosophila* pertenecen a la familia canales iónicos de potencial de receptor transitorio (TRP). Estas proteínas permeables a Ca^{2+} son el blanco final de la cascada de fototransducción y su activación está mediada por la vía de señalización de PLC_{β}. En los fotorreceptores estos canales están localizados en los rabdómeros junto a todos los componentes moleculares de la cascada de fototransducción. En estas neuronas sin espigas (o de potencial graduado), la liberación de neurotransmisor es tónica y está linealmente relacionada con la intensidad del estímulo. De esta manera, la homeostasis de Ca^{2+} en estos terminales sinápticos debe ser finamente regulada.

En este trabajo, una novedosa preparación de rebanadas de cerebro de *Drosophila* fue desarrollada para estudiar la distribución y propiedades fisiológicas de TRP y TRPL en el sistema visual. Ambos canales, junto a otras proteínas de la cascada de fototransducción, tales como PLC, PKC, G-protein and InaD, fueron encontrados en las dos neuropilas (lámina y médula) donde los fotorreceptores proyectan sus axones. A través de un análisis cuantitativo se reveló que los canales TRP están distribuidos en dominios confinados, mientras que TRPL están dispersos aleatoriamente sobre las proyecciones de los fotoreceptores. PLC y PKC fueron encontradas en mayor proporción que la proteína G e InaD en la lámina y médula.

Imágenes de Ca^{2+} y de FM4-64 en las rebanadas de cerebro revelaron que la exocitosis de vesículas en la lámina parece estar controlada por dos vías complementarias

de Ca^{2+}: una es activada por despolarización y es llevada por los canales de Ca^{2+} dependientes de voltaje, Cacophony y la otra implica actividad de PLC y reservorios intracelulares de Ca^{2+}. Bajo continua estimulación, estos reservorios de Ca^{2+} podrían vacíarse. La propuesta de esta tesis es que el rol fisiológico de los canales TRP y TRPL en la lámina se relaciona con el relleno de Ca^{2+} en reservorios sensibles a Thg en el RE, cuando éstos están vacios. Este crítico rol sería desempañado a través de una regulación tipo SOC de la actividad de TRP/TRPL en la lámina. Estos hallazgos son consistentes con reportes previos que muestran una potenciación presináptica en los terminales de los fotorreceptores, relacionada con liberación de Ca^{2+} desde reservorios intracelulares. Los resultados mostrados en esta tesis pueden abrir nuevas ideas acerca de la liberación tónica de neurotransmisores en neuronas de potencial graduado.

ABSTRACT

Drosophila TRP and TRPL belong to the transient receptor potential (TRP) family of ion channels. These Ca^{2+}-permeant proteins are the final target of the phototransduction cascade and their activation is mediated by the PLC_{β} signaling pathway. In photoreceptors these channels are located in the rhabdomers, together with all the molecular components of the phototransduction cascade. In these non-spiking (or graded potentials) neurons, neurotransmitter release is tonic and linearly related to stimulus intensity. Therefore, Ca^{2+} homeostasis at these synaptic terminals must be finely regulated.

In the present work, a novel preparation of *Drosophila* brain slices was developed to study the distribution and physiological properties of TRP and TRPL in the visual system. Both channels, together with other proteins of the phototransduction pathway, namely PLC, PKC, G-protein and InaD, were found at the two neuropiles (lamina and medulla) where the photoreceptors project their axons. A detailed quantitative analysis revealed that TRP channels are distributed in confined domains, while TRPL are randomly dispersed over the photoreceptors axonal projections. PLC and PKC were found in a higher proportion than G-protein and InaD in the lamina and medulla.

Ca^{2+} and FM4-64 imaging in brain slices revealed that vesicle exocytosis at the lamina seems to be controlled by two complementary Ca^{2+} pathways: one is activated by depolarization and is carried by Cacophony voltage-dependent Ca^{2+} channels and the other implies PLC activity and intracellular Ca^{2+} reservoirs. Under sustained stimulation,

these Ca^{2+} stores may be depleted. It is proposed that the physiological role of TRP and TRPL channels in the lamina relates to Ca^{2+} refilling of Thg-sensitive stores in the ER when they are depleted. This critical role would be achieved by a SOC regulation of TRP/TRPL activity in the lamina. These findings are consistent with previous reports that showed a presynaptic potentiation related to Ca^{2+} release from intracellular reservoirs in photoreceptor terminals. The results showed in this thesis shall give new lights into tonic neurotransmitter release in non-spiking neurons.

1. INTRODUCTION

1.1 *Drosophila* visual system

In the visual system, light stimuli are decoded by neurons organized in discrete functional units capable of transducing photonic inputs into bioelectrical signals. In *Drosophila melanogaster*, this system is arranged in morphological columns that preserve their structural and functional organization along the layers of the visual system. In the outermost part of the compound eye, roughly 800 ommatidia shape the retina (Fig. 1A). Each ommatidium is a cylindrical structure formed by 20 cells, including the somata of eight different photoreceptors (R1-R8), pigment cells and other cells important for cohesion and lens structure (Meinertzhagen & O'Neil, 1991). Photoreceptors are highly specialized sensory neurons which continuously encode light contrast into graded membrane potential changes. In vertebrates and invertebrates, these neurons generate graded potentials instead of action potentials in response to light intensity changes. Graded potentials operate in shorter distances than action potentials and their amplitude is proportional to the intensity of the stimulus.

Two types of chemical synapses are present in vertebrate and invertebrate retinas: conventional and ribbon synapses. The latter one presents a distinctive ribbon structure (with a "T" shape, seen in cross sections) in the presynaptic sites and serves to direct synaptic vesicles (SV) to the plasmalema prior to exocytosis. Regarding their functionality, multiple postsynaptic elements (four in *Drosophila*) are present opposite

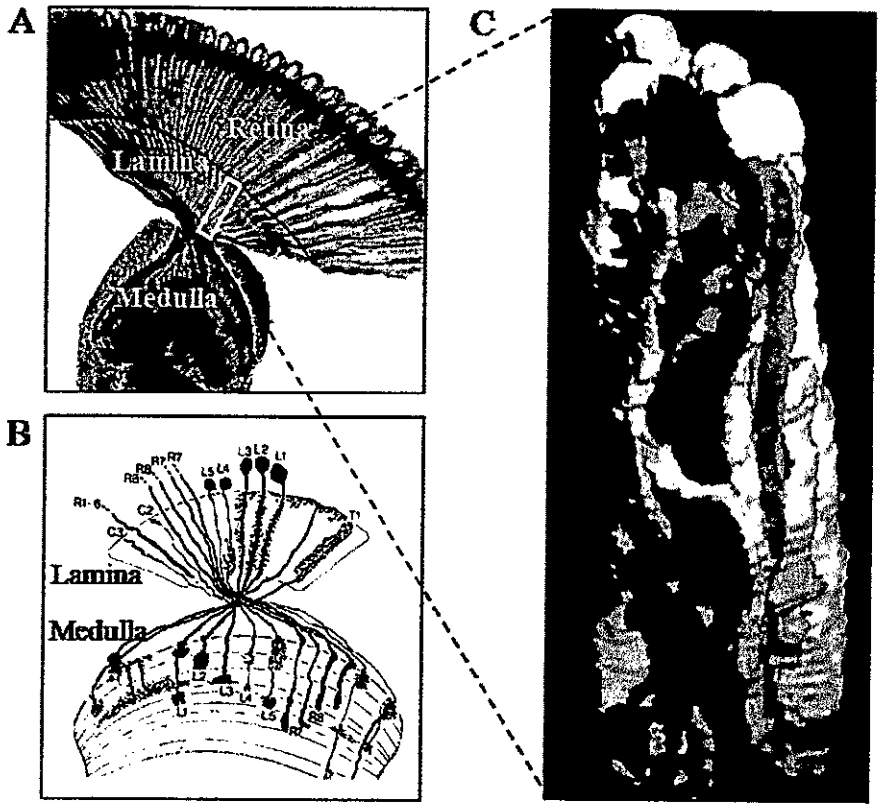

Figure 1. *Drosophila* visual system.

A. Horizontal section of the *Drosophila* visual system. Photoreceptors present in the retina and the two neuropiles: lamina and medulla are shown (from Meinertzhagen 1991). **B**. Golgi impregnations showing the photoreceptors axonal projections in the lamina (R1-R6) and beyond the lamina, into the medulla (R7-8). The somata of the laminar interneurons or large monopolar cells (L1-L5) are in the outermost part of the lamina and the high density of terminals in these cells is clearly appreciated. **C**. Three-dimensional reconstruction of electron micrographies showing synaptic connectivity in the lamina cartridges (Adapted from I. Meinertzhagen and E. Sorra, 2001).

to the site of the presynaptic ribbon. This arrangement provides a rich network of synaptic microcircuits in the retina (Meinertzhagen & O'Neil, 1991).Photoreceptor ribbon synapses posess a characteristic topology specialized for coding graded presynaptic signals into tonic neurotransmitter release. This mechanism allows the transmission of signals at much higher rates (5-fold) than spiking synapses and transmitter release is linearly correlated to Ca^{2+} influx into the active zone (Juusola *et al.*, 1996).

A significant advantage of graded potentials as a strategy for coding stimuli is that the operating range is much wider than for action potentials and can be dynamically modulated. A change from dim to bright light causes a 10-fold increase in the voltage response over baseline depolarization (contrast gain) and a significant reduction in voltage noise. This signal enhancement improves the signal to noise ratio. Therefore, the dynamic range of photoreceptors light response may cover a broad range, from dim light stimuli (small depolarizations) to bright light (large depolarizations). In a typical spiking synapse of the giant squid, the activation curve of Ca^{2+} channels varies sigmoidaly from -30 to -10 mV. In vertebrate retinal bipolar neurons the dynamic range of the cell response (which present graded synapses) extends beyond this range, linearly from -80 to 0 mV (Juusola *et al.*, 1996).

In order to achieve high rates of sustained neurotransmitter release, ribbon synapses have two main sources of SV: docked or tethered to the ribbon structure, constituting the ultrafast and ready releasable pool, respectively. This last one represents the pool for sustained release and is typically fivefold larger than the docked pool available for fast release.

Information processing in graded potential neurons and synapses provides significant signal optimization. During signal transmission, tonic transmitter release is augmented by voltage-dependent mechanisms in the photoreceptor axons. This can be observed as fast voltage transients added to the initial depolarizing phase of the photoreceptor response. A predictive model for this contrast enhancing behaviour agrees with the theory of maximizing sensory information (Juusola *et al.*, 1995). This theory proposes that early sensory processing maximises the information rate between the photoreceptors to the central parts of the brain.

In *Drosophila* visual system, the photoreceptor cell bodies are located in the retina and their synaptic terminals in two high-density neuropiles: the lamina and the medulla (Fig. 1B). R1-R6 project their axons to the lamina and R7-R8 to the medulla. R1-R6 make multiple dyads and triads synaptic contacts with amacrine and three different large monopolar cells (LMC), L1-L3. Approximately 1200 synapses transmit the signals from six photoreceptors located in 6 different ommatidia, to one LMC. In the lamina, there is a geometric array of cylindrical structures called cartridges (Fig. 1C), which include axons from 13 different photoreceptor, laminar, amacrinal and glial cells (Miller & Ripps, 2001). The neurotransmitter released from the photoreceptors is histamine and it activates hyperpolarizing (Gengs *et al.*, 2002) postsynaptic ionotropic chloride channels in LMC (Hardie, 1989). From the medulla, the visual information is conducted to higher processing centers in the optic lobe.

In electroretinogram (ERG) recordings, postsynaptic activity of LMC is manifested as the on and off transients, while the long lasting depolarization reflects the photoreceptor response to light stimulation.

Modification of synaptic transmission by adaptation is a powerful feature of graded synapses. The photoreceptor-LMC synapse is an adaptive filter, whose neurotransmitter release frequency changes with mean stimulus intensity; from low pass filtering at dim light intensities to band pass at higher levels of illumination (Juusola *et al.*, 1995).

1.2 Visual transduction in *Drosophila*

Photons are the basic units of light. Photoreceptors might be viewed as digital-analogue converters as they sample discrete events (photon absorptions) and transduce them into graded voltage responses (Juusola *et al.*, 1995). The effective absorption of a single photon generates discrete fast responses known as quantum bumps. These represent the simultaneous activation of about 15 light-sensitive channels, generating an inward current of ~10 pA (Hardie *et al.*, 2002). Each quantum bump represents the activity of one microvillus from a total of approximately 30,000 tightly packed microvilli that form the rhabdomere. The elements of the phototransduction cascade are located in these structures. The signaling process starts when a photon isomerizes rhodopsin and activates a heteromeric G-Protein (G_q), which releases its alpha subunit and activates a phospholipase C ($PLC_{\beta 4}$ isoform) encoded by the *norpA* gene. This enzyme catalyzes the hydrolysis of the membrane phospholipid phosphatidyl inositol bisphosphate (PIP_2) into inositol trisphosphate (IP_3) and diacylglycerol (DAG). By a highly controversial mechanism, activation of PLC_β leads to the opening of at least two classes of Ca^{2+} permeable channels, TRP and TRPL (Hardie & Minke, 1992), (Niemeyer

et al., 1996),(Reuss *et al.*, 1997). ERG recordings in the *trp;trpl* double mutant and in PLC_{β} hypomorphic flies exhibit no light response (Liu *et al.*, 2007a), indicating an essential role for these components in light transduction (Bloomquist *et al.*, 1988).

The contribution of one of the PLC_{β} products, IP_3, as the signal causing channel activation, has been discarded, since the null mutant for the IP_3 receptor shows a normal ERG and photorelease of caged IP_3 has no effect (Acharya *et al.*, 1997; Raghu *et al.*, 2000). The role of DAG has been highly debated. It has been observed that this lipid and its metabolic products, the polyunsaturated fatty acids (PUFAs), induce TRP and TRPL channel activity in whole-cell (Chyb *et al.*, 1999) and excised patch recordings (Delgado & Bacigalupo, 2009). External application of the PUFA linolenic acid (LNA) in the dark induced an inward current with similar properties to that activated by light (Chyb *et al.*, 1999). However, it is not clear if these lipids act directly on the channels or by changing the membrane fluidity around them.

The best known target of DAG is Protein Kinase C (PKC), which is present in *Drosophila* photoreceptors and negatively regulates PLC_{β} activity by phosphorylation. Null mutants for this enzyme respond to light, but the kinetics of the response termination is significantly slower than for wild-type flies (Smith *et al.*, 1991), (Hardie *et al.*, 1993). This observation suggests that PKC participates in response termination, probably by mediating PLC_{β} inhibition (Gu *et al.*, 2005).

The phototransduction proteins are organized in membrane signalling complexes known as signalplexes. These multiprotein associations are gathered by protein-protein interactions between TRP channels and the scaffolding protein INAD (Pak & Leung,

2003). INAD contains five 90 amino acid PDZ motifs, which are characteristic domains for protein-protein interactions, present in a diversity of signalling, cell adhesion, and cytoskeleton proteins. In *Drosophila* photoreceptors, this dynamic signalling complex includes rhodopsin, PLC_{β}, calmodulin, TRP and the kinase proteins PKC and NINAC (Minke & Cook, 2002). TRP association into transduction complexes with its upstream activator, PLC_{β}, and its potential regulator, PKC, may increase the speed and efficiency of transduction events. Moreover, it has been shown that TRP plays a major role anchoring the signalling complex to its subcellular site in the microvilli (Tsunoda *et al.*, 2001).

All the genes coding for the phototransduction cascade components have been identified and clone and mutant flies for all the identified signalling proteins are available. On the other hand, no specific blockers have been discovered for TRP channels. For the reason that they have never been crystallized, the design of specific inhibitors remains poorly developed. The genetic tools available in *Drosophila* make it a valuable model for signal transduction research.

1.2.1 Function of TRP and TRPL channels in *Drosophila*

TRP and TRPL channels are the key targets of the phototransduction pathway and are essential for light response in flies. Flies carrying a mutant *trp* allele present a transient rather than maintained receptor potential in response to a sustained light stimulus (Cosens & Manning, 1969). For this reason, the gene was termed transient receptor potential or *trp*. This mutation causes a ~10-fold reduction in the light induced

Ca^{2+} influx to the photoreceptor (Minke, 1977; Montell *et al.*, 1985). According to the Goldman-Hodgkin-Katz equation, the relative permeability to Ca^{2+} with respect to Na^{+} (pCa^{2+}:pNa^{+}) for TRP channel is 100:1 and for TRPL, 3:1. This high Ca^{2+} permeability of the channels is critical to initiate photoreceptor depolarization in rhabdomeres.

1.3 Classes of TRP Channels

The widest ion channel functional and structural diversity is found in the TRP family of channels. Once the *Drosophila trp* gene was cloned, many homologues were found in vertebrates and invertebrates including yeasts, worms, insects, fishes, birds, and mammals (Venkatachalam & Montell, 2007). Most TRP channels are key elements in sensory cells, responding to a broad range of external (light, sound, chemicals, temperature, touch) and internal stimuli (osmolarity changes, oxidative stress). In mammals, they are present in a wide range of organs and cells, including central and peripheral nervous system.

TRP channels have been divided into two major groups according to their topological similarities and into seven subfamilies by sequence homology. Group 1 is formed by TRPC (canonical, includes *Drosophila* TRP and TRPL), TRPV (vanilloid), TRPM (melastatine), TRPN (NOMP or no mechanoreceptor potential) and TRPA (ankyrin). Group 2 is formed by TRPP (polycystin) and TRPML (mucolipin) subfamilies. They have been poorly characterized and were included in a separate group due to their low sequence and topological similarities with Group 1 channels. TRPC channels comprise nine members, TRPC (1-7) in worms and mammals plus *Drosophila* TRP and TRPL. In mammals, they are found in brain, retina, heart, testis, ovaries, lung,

endothelia and adrenal glands. Their activity has been implicated in multiple physiological functions such as neuronal excitability in Purkinje cells, acrosome reaction in sperm cells, pheromone response, vasorelaxation, neurotransmitter release and Ca^{2+} oscillations in multiple cell kinds.

In *Drosophila* genome, there are 13 different TRP genes and splice variants, including members of groups 1 and 2. In the eye, where TRP, TRPL and their splice variants are highly expressed, there is a third channel which shares high sequence homology with TRP, known as TRP-gamma. This channel is highly enriched in the photoreceptor cells and forms a heteromultimeric regulated cation channel preferentially with TRPL *in vitro* and *in vivo* (Xu *et al.*, 2000). *Drosophila* TRP and TRPL channels share structural and topological characteristics, such as Ca^{2+}-Calmodulin binding sites (one in TRP and two in TRPL) and a proline-rich sequence in the C-terminal (Phillips *et al.*, 1992). This sequence is also important for interactions with other proteins. Since several members of the TRP family hold multiple protein-protein interaction sites, they may be key elements for anchoring and localization of functional signal transduction complexes (Venkatachalam & Montell, 2007).

Although the crystal structure of TRP channels has not been resolved, they are believed to form tetrameric assemblies (Kedei *et al.*, 2001; Kuzhikandathil *et al.*, 2001) with different subunit composition (homo and heterotetramers). The members of this family display a predicted topology of six transmembrane segments (S1-S6), a pore forming loop between S5 and S6 and intracellular NH2 and COOH termini domains.

The members of Group 1 TRP channels share a significant sequence identity (70%) in their transmembrane domains. TRPC, TRPM and TRPN channels (except for

Drosophila NOMPC) include a characteristic TRP domain with no ascribed role. This domain consists of a highly conserved sequence of 23-25 amino acids, located C-terminal to the 6th transmembrane domain.

Other relevant characteristic of Group 1 channels (except for TRPM) is the presence of at least three ankyrin repeats in the N-terminal domain. Ankyrin repeats are 33 amino acid sequences that participate in protein-protein interactions (Sedgwick & Smerdon, 1999) and cytoskeleton anchorage (Michaely & Bennett, 1993).

1.4 TRP channel regulation

Most TRP channels can be regulated by serine/threonine kinases, such as PKC. The charged residues that normally participate in voltage sensing in the fourth segment (S4) of voltage-gated channels are replaced by non-charged amino acids in TRP channels. Hence, TRP channels are not voltage-gated, although some of them display voltage regulation or acquire voltage dependence properties through pore blocking by divalent cations like Ca^{2+} and Mg^{2+}. Voltage-dependence of TRP channels is a matter of intense ongoing discussions (Venkatachalam & Montell, 2007).

1.4.1 Store operated activity

TRPC channel gating mechanism is related to PLC_{β} activity, although there are other factors that regulate TRPC channel opening. These include channel plasma membrane coupling to endoplasmic reticulum (ER) membrane, such that its gating is linked to Ca^{2+} depletion of the store, exhibiting properties of store operated channels

(SOC) (Ong *et al.*, 2007; Worley *et al.*, 2007; Pani *et al.*, 2009). Other TRPC channels are activated by plasma membrane insertion from intracellular vesicular compartments (TRPC3, TRPC4 and TRPC5). This activation might be related to proton regulation in these channels (Venkatachalam & Montell, 2007).

TRP and TRPL cDNAs have been heterologously expressed in insect and vertebrate cell lines in order to characterize their electrophysiological properties. Nevertheless, in the heterologous membranes, TRP channels show a different behaviour than in their native membranes. *Drosophila* TRP channels heterologously expressed in HEK 293 and 293T cells can be activated by store depletion induced by thapsigargin treatment (Xu *et al.*, 1997). This behaviour has not been found in whole-cell recordings of photoreceptor somata. On the other hand, the TRPL channel preserves its native electrophysiological properties when expressed in other systems, with the difference that it is constitutively active (Xu *et al.*, 1997; Harteneck *et al.*, 2000). Remarkably, in heterologous systems TRPL activity can also be significantly increased by thapsigargin treatment suggesting a SOC function (Xu *et al.*, 1997). Co-expression of TRP and TRPL suppresses the mentioned constitutive activity of TRPL channel (Gillo *et al.*, 1996; Xu *et al.*, 1997), but on the other hand results in a SOC activity of the channels.

TRPC1-5 channels display a SOC behaviour when expressed in heterologous membranes or in their native tissue (Minke & Cook, 2002). It has been reported that different types of TRP contribute to the Ca^{2+} influx mechanism in several synapses modulating the dynamic range of presynaptic Ca^{2+} signalling. This may be achieved through a SOC-mediated or metabotropic mechanism (De Petrocellis & Di Marzo, 2009).

In vertebrate photoreceptors, this mechanism may contribute to sustained calcium signalling in darkness and light adapted conditions by extending the dynamic range of the light response beyond the operation range of VGCC in the synaptic terminals (Szikra *et al.*, 2008).

1.5 TRP channels in synaptic transmission

Evidence relating TRP channels to synaptic transmission increase year by year. In presynaptic terminals on neurons of the rat substantia gelatinosa (SG) of the spinal cord, TRPA1 channels have been shown to facilitate inhibitory and excitatory synaptic transmission by enhancing glutamate release. This central modulation of sensory signals may be associated with physiological and pathological pain sensations (Kosugi *et al.*, 2007). This channel has also been reported to increase glutamate release in presynaptic terminals at nucleus tractus solitarii neurons of the brain stem (Sun *et al.*, 2009). In the same way, presynaptic activation of TRPV1 in primary nociceptive afferent neurons that innervate the SG enhances glutamatergic spontaneous excitatory synaptic transmission (Yang *et al.*, 1998; Tominaga & Caterina, 2004; Jiang *et al.*, 2009).

The contribution of TRP channels to pain sensation and disease makes them very attractive targets for medical research and the design of novel analgesic drugs (Kim *et al.*, 2009). Group I channels TRPV1-4, TRPM8 and TRPA1 are expressed in sensory neurons of the dorsal root ganglia and play important roles in nociception, by favouring and modulating glutamatergic afferent transmission onto partially overlapping but distinct neuron populations (Wrigley *et al.*, 2009).

In the *Drosophila* neuromuscular junction, TRPML has been shown to play a very important role in synaptic transmission. *trpml* mutants exhibit a significant decrement in synaptic transmission (Venkatachalam *et al.*, 2008).

Like invertebrates, vertebrate photoreceptors release neurotransmitter in a tonic manner. These synapses are specialized for sustained Ca^{2+} entry and transmitter release, allowing their operation in a graded fashion over a wide dynamic range. In vertebrate photoreceptors, the dynamic range of the cone output extends beyond the activation threshold for voltage-operated calcium entry. This is achieved by SOCs and is responsible for the generation of sustained excitatory signals across the first retinal synapse (Szikra *et al.*, 2009). Store depletion directly activates a TRPC1-dependent Ca^{2+} entry that stimulates exocytosis and maintains baseline Ca^{2+} in rod synaptic terminals. This store-operated Ca^{2+} entry (SOCE) is not dependent on voltage-operated Ca^{2+} entry and is essential for photoreceptor-mediated synaptic inputs to horizontal basal cells in the two extremes of light intensity range: dim and adapting light.

In *Drosophila* photoreceptors, TRP spatial distribution is not restricted to the rhabdomere. Pollock et al (1995) described the presence of this channel along the axon of photoreceptors, in the lamina and medulla neuropiles by immunofluorescences performed with an antibody developed by the authors. Nevertheless, unlike the extensively studied rhabdomeric channels, the axonal presence of TRP has not been further examined.

Considering the physiological similarities between vertebrate and invertebrate photoreceptors regarding graded potentials and tonic neurotransmitter release, it is

reasonable to question whether *Drosophila* synaptic TRP channels could be involved in the sustained Ca^{2+} entry associated to transmitter release in these synaptic terminals.

In the present work, the synaptic presence and function of TRP and TRPL channels was examined.

2. HYPOTHESIS

TRP and TRPL channels participate in synaptic transmission in *Drosophila* photoreceptors.

3. OBJECTIVES

3.1 General Objective

Study the role of TRP and TRPL channels in synaptic transmission in *Drosophila* photoreceptors.

3.2 Specific Objectives

1. Investigate the presence of TRP and TRPL channels in synaptic terminals of *Drosophila* photoreceptors.
2. Investigate the signalling pathway mediating the activation of TRP and TRPL channels in synaptic terminals.
3. Determine if TRP and TRPL contribute to the Ca^{2+} rise occurring in photoreceptor synaptic terminals.
4. Establish whether TRP and TRPL contribute to synaptic transmission.

4. MATERIALS AND METHODS

4.1 *Drosophila* fly strains

The following fly strains were used for experimentation:

- Wild type (*wt*) Oregon Red *Drosophila melanogaster*
- *w;trp*^{343} (null for TRP channels)
- *w;trpl*^{302} (null for TRPL channels)
- *w,cn,trp*^{CM}*,trpl,* (null for TRP and TRPL channels)
- *w,trpl*^{302}*, trp*^{343} (null for TRP and TRPL channels)
- Recombinant GMR-Gal4/UAS-mCD8-GFP (Green Fluorescent Protein)
- UAS-Syb-GFP (express GFP fused to synaptobrevin)
- GMR-Gal4/CyO
- UAS-GCaMP flies were crossed to GMR-Gal4/CyO and the progeny of 2-4 days post eclosion was used for experiments.

4.2 *Drosophila* brain slices

Adult *Drosophila* were anesthetized in CO_2 and kept on ice for dissection with a vibratome (Vibratome, 1000 plus). For each experiment, around 10 flies were stuck to the stainless steel tray with 1 µL of cyanoacrylate ester glue. Flies were immersed in chilled extracellular solution containing in mM: 120 NaCl, 5 KCl, 8 $MgSO_4$, 1.5 $CaCl_2$, 25 L-Proline, 0.5 EGTA, 1.25 NaH_2PO_4 and 25 $NaHCO_3$. This solution was oxygenated with a mixture of 95% O_2-5% CO_2 maintaining the pH at 7.15.

Flies were sectioned into 200 μm thickness slices, obtaining one optimal slice per fly. The slices were kept in iced Ringer for Ca^{2+} or FM4-64 *in vivo* imaging for no longer than 2 hours. Only slices with a visible preservation of the visual system structure were used.

4.3 Immunohistochemistry

Flies were anesthetized in CO_2 and fixed for 48h in 4% formaldehyde in PBS at 4°C. 200 μm thick horizontal head sections were cut with a vibratome in chilled PBS. The sections were incubated for 2 h at room temperature in blocking solution containing: 50% goat serum, 10% BSA in PBST (PBS + 0.1% Triton X-100; Sigma). Primary antibodies were incubated overnight at the appropriate dilution in blocking solution at 4°C (α-TRP 1:200, α-TRPL 1:1000, α-Gprot, α-PLC and α-InaD 1:300). Slices were washed 4 x 20 min in PBS and incubated with secondary antibody (1:200) for 1 h at room temperature. Either goat anti-rabbit AlexaFluor594 or goat anti-mouse AlexaFluor546 conjugated IgG antibodies were used. Sections were then washed (4x20 min) in PBS and stored in glycerol at 4°C. For imaging, slices were enclosed by two coverglasses and immersed in mounted media (Fluoromount, Electron Microscopy Sciences) and 20% glycerol.

4.4 Ca^{2+} imaging

Drosophila slices were covered by low melting point Agarose (type IX-A, Sigma-Aldrich). The system was constantly perfused at 1ml/min by normal extracellular

solution and a glass micropipette positioned on the lamina was used for local application of LNA and high K^+ extracellular solution (in mM: 35 NaCl, 90 KCl, 8 $MgSO_4$, 1.5 $CaCl_2$, 25 L-Proline, 0.5 EGTA, 1.25 NaH_2PO_4 and 25 $NaHCO_3$, pH 7.15). The extracellular solution was oxygenated with a mixture of 95% O_2-5% CO_2.

For each experiment, z-stacks were recorded in the lamina before, during and after the stimuli. Images were deconvoluted as described below and z-projections were used for subsequent analysis using Image J software (National Institutes of Health). Fluorescence intensity represents the integrated density of the pixels in a selected region of interest (ROI).

4.5 Vesicle exocytosis (FM4-64 imaging)

Wild-type and mutant *Drosophila* brain slices were stimulated with high K^+ extracellular solution in the presence of FM4-64 on ice and darkness for 10 minutes. Slices were then washed for 5 minutes in normal extracellular solution on ice and darkness. In other experiments, slices were stimulated with the PLC activator 100 µM *m*-3M3FBS for 12 minutes at room temperature. This compound activates all PLC isotypes. In experiments with Thapsigargin (Thg) or Ryanodine (Ry), *m*-3M3FBS and FM4-64 were applied after 8 min of Thg and Ry pretreatment. For all Ca^{2+} and FM4-64 experiments only healthy slices with a well preserved tissue were used. Due to the high density of synaptic boutons in the medulla, it was difficult to discriminate individual units. Because of it higher structural clarity, only the lamina was imaged.

Images were taken in 1 channel with an excitation wavelength λexc = 543nm and long pass emission λem = 615 nm. For each experiment, slices were imaged for a maximum of 2 h after dissection. Z-stacks were recorded in the lamina and images were deconvoluted. 10 image Z-projections were used for analysis. Fluorescently labelled synaptic terminals with a signal to noise (S/N) ratio over 10 were selected with Interactive Data Language (IDL) tools (ITT, Boulder, CO), by segmentation with the filters mentioned above. The number and area of the selected ROIs in each z-projection were quantified.

4.6 Image capture and analysis

Images were acquired in 8 bits with a Zeiss LSM Meta 510 confocal microscope using LSM 5 3.2 image capture and analysis software. Objectives 20x/0.5, 40x/0.75, 63x/1.4 Oil digital zoom (4x) and 100x/1.3 oil digital zoom (3x) were used.

Two-channel fluorescent image stacks (intensity $I(x,y,z) \in [0,255]$, voxel size $\Delta x/\Delta y/\Delta z$ =70/70/300 nm) were recorded in the multi-track mode. Channel-1 with an excitation/emission wavelength λexc/λem = 488/505-530 nm, and channel-2 with λexc/λem = 543/560-590 or 543/590-615 nm. I(x,y,z) did not saturate and image background was slightly above zero by adjusting the laser power, detector gain and detector offset. Raw confocal image stacks were deconvolved by Huygens Scripting software (Scientific Volume Imaging, Hilversum, Netherlands) using an algorithm based on the Classic Maximum Likelihood Estimator (CMLE). Deconvolution improves the signal to noise ratio and is essential for a reliable analysis of colocalization coefficients.

Image-processing routines were developed in SCIAN laboratory (www.scian.cl) based on IDL. These comprise visualization, segmentation routines to select ROIs, calculation of Manders colocalization coefficients and statistical validation of these coefficients. For ROI segmentation in the lamina, gradient filters were applied to deconvolved images and threshold values were selected from gradient histograms. Image gradient resolves object contours and separation of homogeneous regions. Cartridges, axons and active zones were consistently selected with this procedure in the lamina. For the colocalization analysis, segmented cartridges were used to define the displacement area. The reliability of the segmentation was examined by overlaying the original fluorescent images with the mask in each channel. The same segmentation criterion was applied to all images within the lamina.

Colocalization was measured with an approach based on Costes et al., 2004 using Manders coefficients M1 and M2 (Costes *et al.*, 2004; Espinosa *et al.*, 2009). For colocalization quantification we calculated M1 and M2 between ROIs 1 and 2, by the following definition:

$$M1_{ROI} = \frac{\sum_{ij} I_{Ch1(ROI1(xi,yj) \cap ROI2(xi,yj))}}{\sum_{ij} I_{Ch1(ROI1(xi,yj))}} \qquad M2_{ROI} = \frac{\sum_{ij} I_{Ch2(ROI1(xi,yj) \cap ROI2(xi,yj))}}{\sum_{ij} I_{Ch2(ROI2(xi,yj))}} \quad \text{Eq. 1A and B)}$$

M1 and M2 sum up the contribution of the respective fluorescence intensities in the colocalizing region ICh1/2(ROI1 ∩ ROI2) and are divided by the sum of the fluorescence intensities ICh1/Ch2 inside of the segmented regions ICh1 (ROI1) or ICh2 (ROI2). ROI1 and ROI2 are segmented as previously described. M1 and M2 can be

understood as the amount of colocalizing signal in each channel relative to the total segmented signal.

With correlation techniques (Omar Ramírez & Härtel, 2010) it is possible to shift one channel and its corresponding image mask (which confines radial displacement to the defined axonal section) relative to the second channel. This 2D image correlation technique calculates M1 ROI (d) and M2 ROI (d) as a function of radial displacements d:

$$M1_{ROI}(d) = M1_{ROI}\left(x', y' \middle| \sqrt{x'^2+y'^2} = d\right) = \frac{\sum_{ij} I_{Ch1(ROI1(xi,yj) \cap ROI2(xi+x', yj+y'))}}{\sum_{ij} I_{Ch1(ROI1(xi,yj))}} \qquad \text{(Eq. 2A)}$$

$$M2_{ROI}(d) = M2_{ROI}\left(x', y' \middle| \sqrt{x'^2+y'^2} = d\right) = \frac{\sum_{ij} I_{Ch2(ROI1(xi,yj) \cap ROI2(xi+x', yj+y'))}}{\sum_{ij} I_{Ch2(ROI2(xi+x', yj+y'))}} \qquad \text{(Eq. 2B)}$$

New values for M1ROI(d) and M2ROI(d) are calculated for each displacement radius. The radial displacements are restricted to xy-planes due to PSF elongation in the z-axis in confocal images. For a maximum displacement d', pixel shifts are applied for all x' and y' within $\sqrt{x'^2+y'^2} \leq d'$: $x' \in [-d', d']$, $y' \in [-d', d']$. For each shift $[x', y']$ one data value is obtained as a function of the Euclidian distance $d = \sqrt{x'^2+y'^2}$. Successive shifts lead to one value for d = 0, four values for d = 1, $d = \sqrt{2}$, and d = 2, eight values for $d = \sqrt{5}$, etc.

With increasing displacement (d), $M1/2_{ROI}$ (d) approaches values that represent random scenarios for a given signal distribution. Probability density functions (PDFs) (Costes *et al.*, 2004) can be calculated from these values, in order to test whether the

colocalization coefficients that were calculated at the original image position ($M1/2_{ROI}(d = 0)$) are statistically different from a random population in terms of *p* values (Sanchez *et al.*, 2008).

The statistical significance of colocalizing structures was evaluated by P-values ($P < 0.05$); which test if M1/M2 values calculated at the original channel positions (d=0)) are significantly greater than M1/M2-values calculated for successive displacements. One- and two-way ANOVA with Dunnett's and Bonferroni post test statistical analysis was performed using the GraphPad Prism version 4 for Windows (GraphPad Software, San Diego California USA).

4.6.1 Quantification of FM4-64 labelled synaptic boutons

In order to quantify the number of synaptic boutons in an unbiased manner, it was necessary to develop a semi-automated analysis. After image deconvolution, segmentation routines based on IDL were applied for ROIs selection. These include isotropic Laplace filters with a radius r = 10 to select membrane contours, followed by intensity thresholds to select only high S/N ratio structures.

The diameters of the synaptic terminals observed in *Drosophila* lamina vary from 0.9 to 1.1 μm. According to these data, their areas should fit the range between 0.4-0.7 μm^2. A size selection filter was used to select objects within these values. The quality of the segmentation was controlled by superposition of the original images over the ROIs. The same parameters were applied to all images and ROI quantification was performed in an automated mode with IDL.

4.7 Antibodies and Reagents

The α-TRP monoclonal antibody MAb83F6 developed by Seymour Benzer was obtained from the "Developmental Studies Hybridoma Bank (DSHB) under the auspices of the NICHD and maintained by The University of Iowa, Department of Biological Sciences, Iowa City, IA 52242". A second α-TRP monoclonal antibody was kindly provided by Craig Montell (Chevesich *et al.*, 1997). α-TRPL policlonal antibody AB5912 was obtained from Chemicon. Policlonal antibodies directed against InaD, G_q-Protein, Rh1 and PLC, where kindly provided by Charles Zuker (Smith *et al.*, 1991). Alexa-Fluor546 conjugated goat α-mouse and goat α-rabbit, Texas Red-X phalloidin, Bodipy TR-X thapsigargin, TO-PRO-3 iodide Alexa 633 and the calcium ionophore A-23187 from Molecular Probes, Invitrogen. The PLC activator, *m*-3M3FBS was obtained from Calbiochem. The spider toxin Plectreurys toxin II (PLTX-II) was obtained from Alomone Labs.

5. RESULTS

5.1 *Drosophila* brain slices

The organization of the visual system of *Drosophila* (Fig. 2A) has been described in detail by electronmicroscopy studies showing the structure of ribbon synapses and the connectivity in the lamina (Meinertzhagen & O'Neil, 1991). However, the physiological properties of photoreceptor synapses in the visual system of *Drosophila* have only been studied in the entire fly, by intracellular recordings in the somata of laminar interneurons (Pantazis *et al.*, 2008), (Niven *et al.*, 2007).

With the purpose of elucidating the distribution of TRP and TRPL in the photoreceptor axon terminals and their possible implication in synaptic transmission, it was necessary to develop a novel methodology for structural and physiological studies. A preparation of *Drosophila* brain slices was implemented, where the integrity of photoreceptors axonal terminals in the two neuropiles was largely preserved. Moreover, the different components of the visual system are easily identified and accessible to experimental manipulation (Fig. 2B). The flies were immersed in a chilled and oxygenized extracellular solution and cut with a vibratome, horizontally along the antero-posterior axis (see Materials and Methods) in sections of 200 μm of thickness. One optimal brain slice was obtained per fly and only those with a clear structural preservation of the visual system were used for experimentation. These brain slices were suitable for both immunofluorescence and functional analysis. In response to light

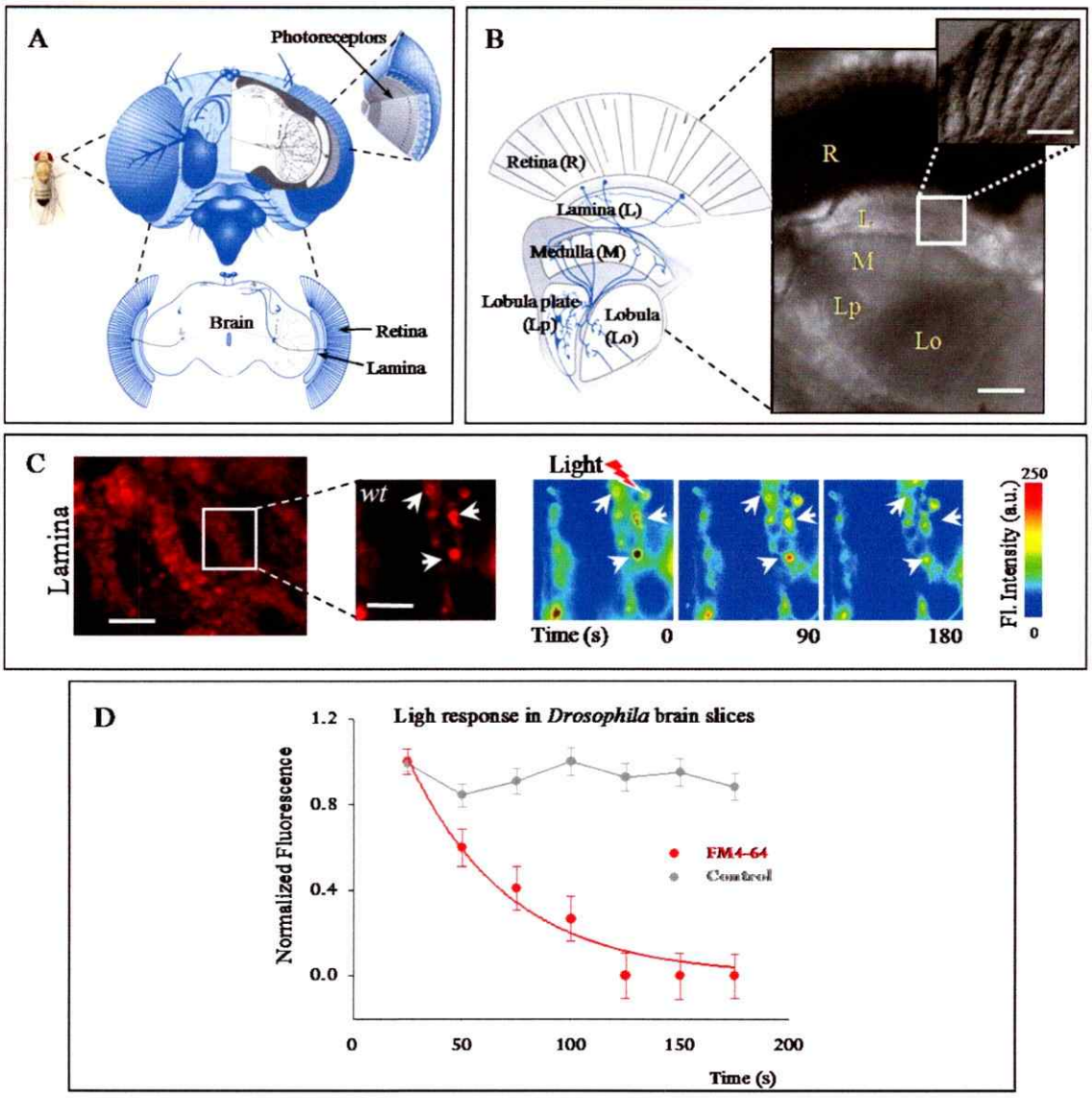

Figure 2. *Drosophila* brain slices.

A. Schematic representation of a frontal view of the fly's head showing the visual system (photoreceptors in the retina and the lamina neuropile). Adapted from (Greenspan, 2007). **B.** *in vivo* preparation of *Drosophila* brain slices with squematic representation of the retina and the lamina and medulla neuropiles. Bar: 50μm. The inset shows a detail of the cartridge structures in the lamina. Bar: 10μm. **C.** The left panel shows FM4-64 loading in the lamina of a *wt* brain slice, following depolarization by 90 mM KCl. The inset shows a detail of synaptic boutons labelled with FM4-64. In the right, time lapse confocal images screening light response in the lamina of *wt* flies. The fluorescence intensity of the pseudocolor images varies from 0 to 250 (a.u.). The decay in FM4-64 fluorescence reflects synaptic vesicle exocytosis from the terminals in the lamina. Bar: 5 μm. **D.** Quantification of FM4-64 fluorescence decay in time. The control FM4-64 fluorescence was acquired in the absence of light stimuli.

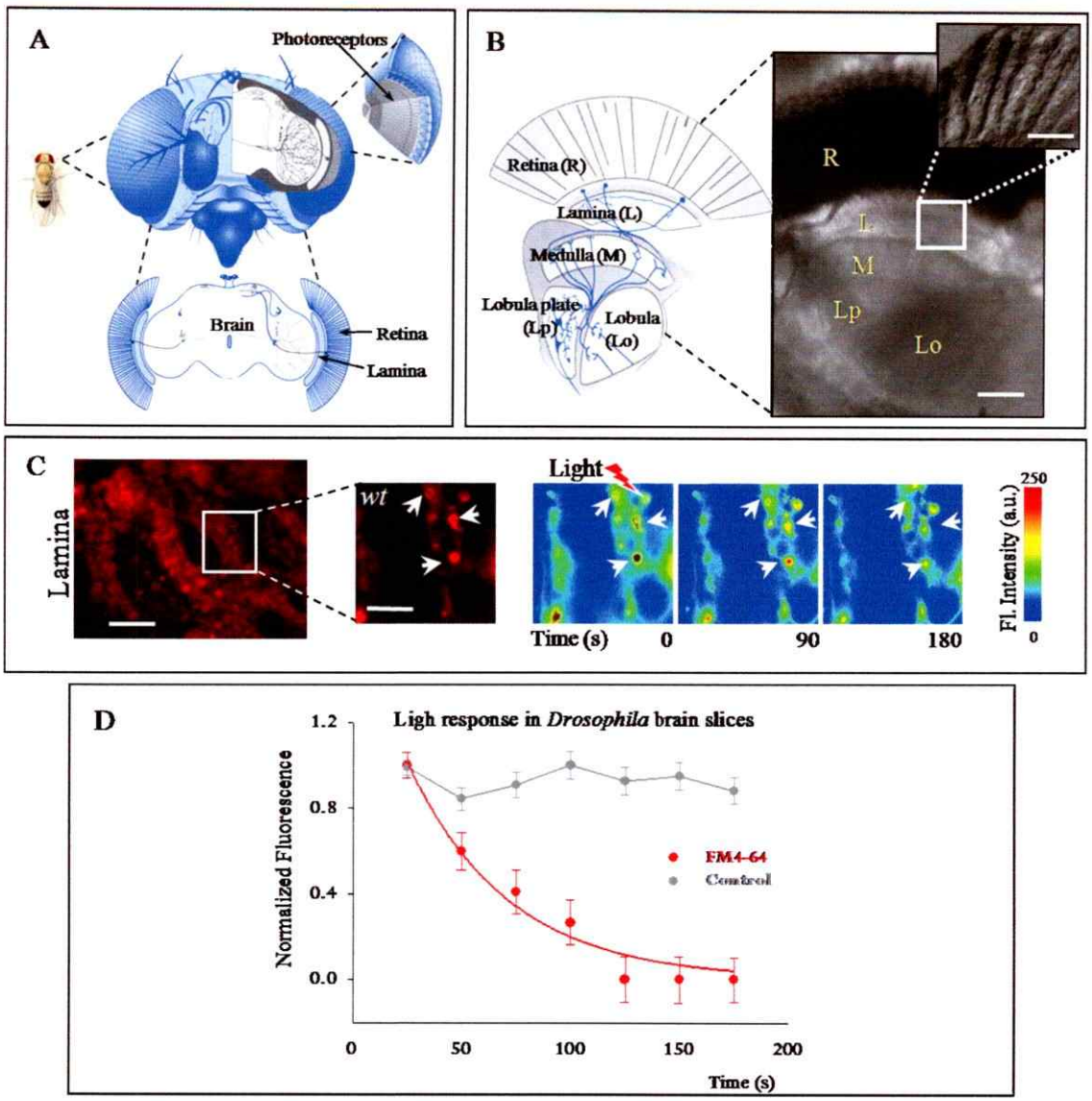

Figure 2. *Drosophila* brain slices.

A. Schematic representation of a frontal view of the fly's head showing the visual system (photoreceptors in the retina and the lamina neuropile). Adapted from (Greenspan, 2007). **B.** *in vivo* preparation of *Drosophila* brain slices with squematic representation of the retina and the lamina and medulla neuropiles. Bar: 50μm. The inset shows a detail of the cartridge structures in the lamina. Bar: 10μm. **C.** The left panel shows FM4-64 loading in the lamina of a *wt* brain slice, following depolarization by 90 mM KCl. The inset shows a detail of synaptic boutons labelled with FM4-64. In the right, time lapse confocal images screening light response in the lamina of *wt* flies. The fluorescence intensity of the pseudocolor images varies from 0 to 250 (a.u.). The decay in FM4-64 fluorescence reflects synaptic vesicle exocytosis from the terminals in the lamina. Bar: 5 μm. **D.** Quantification of FM4-64 fluorescence decay in time. The control FM4-64 fluorescence was acquired in the absence of light stimuli.

stimuli, activation of the phototransduction cascade depolarizes photoreceptors and massive neurotransmitter release occurs in the lamina.

In order to determine if *Drosophila* brain slices preserved their physiological activity, light responses were evaluated by imaging vesicle exocytosis in the lamina. *In vivo* imaging with the fluorescent dye, FM4-64 was performed in the lamina of *Drosophila* brain slices. The fluorescence quantum yield of this amphiphilic dye is nominal in water and is strongly increased by lipophilic interactions, when embedded in membranes (Gaffield & Betz, 2006). After neurons are stimulated, endocytosed SV exposed to this dye become fluorescently labelled. After a second round of stimulation, SV are released and exposed to the extracellular dye-free aqueous environment. This causes a decrease in the dye fluorescence and thus provides a quantitative measure of vesicle exocytosis (Betz & Bewick, 1992).

Drosophila brain slices were exposed to an extracellular solution containing high KCl (90 mM), as a depolarizing stimulus to induce FM4-64 (10 μM) loading into the lamina terminals (see section 5.8). Fluorescence decay of this dye, as a consequence of vesicle exocytosis from the terminals, was monitored over time. Confocal time lapse images were acquired in the lamina with a fixed size of 36.56 μm in the x/y axes. Application of a 20 s light stimulus on photoreceptors (at room temperature) induced the fluorescence decay of labelled boutons in *wt* brain slices (Fig. 2C and 2D, red trace). After 180 s, fluorescence declined to background levels. As a control, spontaneous vesicle exocytosis and photobleaching was measured by recording the fluorescence of FM4-64 loaded brain slices over time, in the absence of light stimulus (Fig. 2D, gray

trace). In this case, fluorescence intensity of the dye did not show a significant change after 180 minutes. These results show that the *in vivo* preparation of *Drosophila* brain slices preserves the ability to respond to light.

5.2 TRP and TRPL channels are present in the lamina and medulla

The *Drosophila* visual system is a complex arrangement of neuronal tissue. In the previously described brain slices, TRP and TRPL channel expression was scrutinized by immunofluorescence. In *wt* flies, the immunoreactivity of a previously reported monoclonal antibody directed against the C-terminal of TRP channels (Pollock *et al.*, 1995) was confirmed. In the visual system, a clear staining was observed in the retina and the lamina (Fig. 3A). In addition, a monoclonal antibody directed against a 15 amino acid peptide located in proximity to the C-terminal of TRPL, also revealed a high expression of this channel in both neuropiles (Fig 3B). TRP channel detection was confirmed using a second antibody directed against the C-terminal of TRP channel (Chevesich *et al.*, 1997). In this case, it was also possible to detect a high level of immunostaining in the retina, lamina and medulla (Fig. 3C). To test the specificity of TRP and TRPL antibodies, they were surveyed for immunoreactivity in the TRP and TRPL null double mutant $trpl^{302};trp^{343}$. In brain slices of this mutant, a weak immunostaining was detected that was comparable to the background signal (Fig. 3D). This control supports the idea that in *Drosophila* visual system, TRP and TRPL channels are present in the two neuropiles, in addition to the rhabdomere. As the photoreceptors axonal projections are located in the lamina and medulla, we examined whether TRP and TRPL channel are located in these or other cell types in these neuropiles. To assess

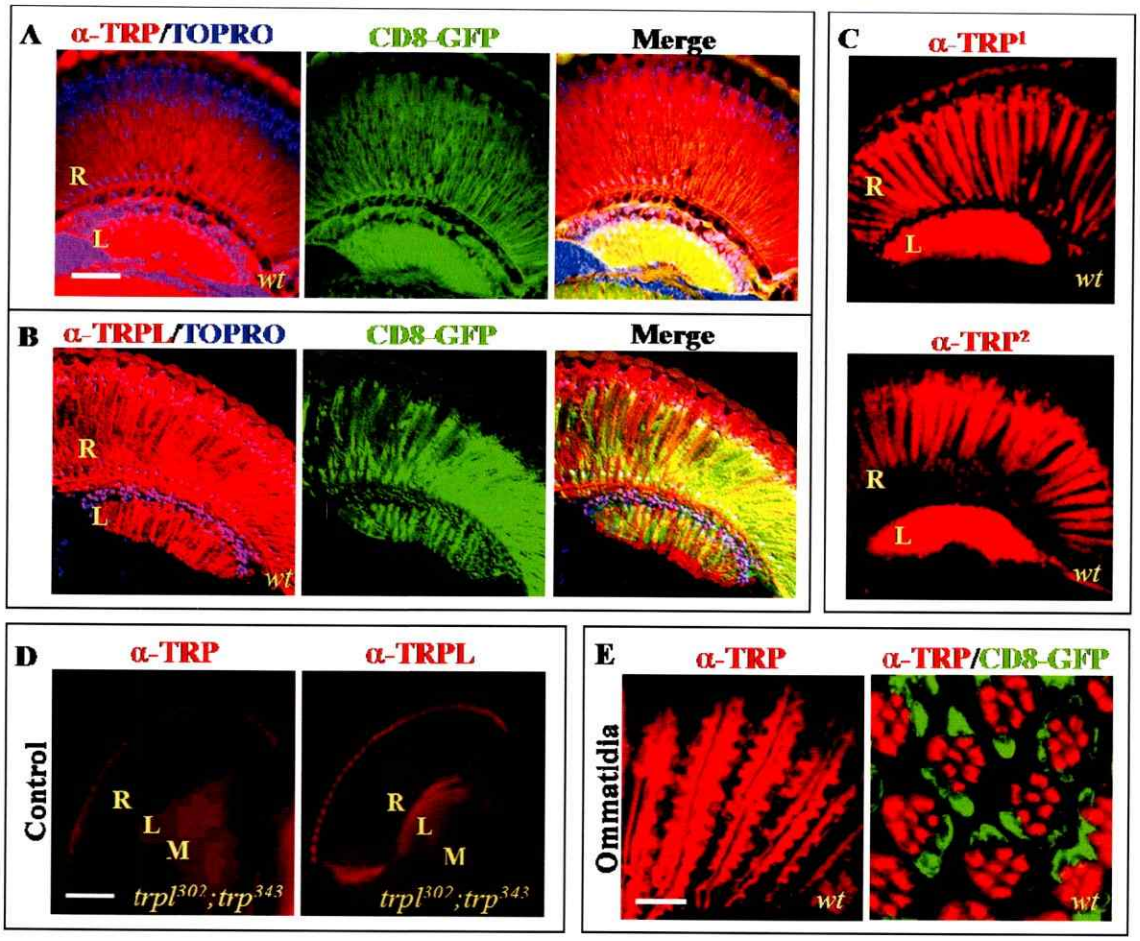

Figure 3. TRP and TRPL channels in the *Drosophila* visual system.
Confocal immunofluorescence images of TRP and TRPL in *wt* brain slices. **A**. TRP channel distribution in the retina (R) and lamina (L) (red) detected by monoclonal α-TRP antibody reactivity (Pollock *et al.*, 1995). Cell nuclei are stained with TOPRO (blue). Photoreceptors are labelled by ectopic expression of CD8-GFP (green). Bar: 50 μm. **B.** TRPL channel distribution in the retina and lamina detected by monoclonal α-TRPL antibody reactivity. **C.** TRP channel distribution in the retina and lamina detected by two different α-TRP^{1} (Pollock *et al.*, 1995) and α-TRP^{2} (Chevesich *et al.*, 1997) antibodies. **D.** Negative controls for α-TRP and α-TRPL antibodies where done in $trpl^{302};trp^{343}$ null double mutants. Bar: 80 μm. **E.** Horizontal (left) and cross (right) sections in the retina showing α-TRP reactivity in ommatidia. In the cross section, CD8-GFP is in the cytoplasm of photoreceptors cell bodies, while TRP is in the rhabdomers. Bar: 10 μm.

this question, the UAS-GAL4 expression system was used to specifically label photoreceptor neurons with a fluorescent marker. For the first purpose, the membrane protein mCD8 fused to GFP was ectopically expressed in photoreceptors under the glass multimeric reporter protein (GMR) promote (GMR-Gal4/UAS-mCD8-GFP). The mCD8-GFP protein is a membrane protein expressed in photoreceptor somata and axonal projections in the lamina and the medulla.

Regarding the distribution of TRP channels in photoreceptors somata in the retina, longitudinal sections show a confined distribution located predominantly in the rhabdomers (Fig. 3E, left image) and mCD8-GFP is localized to the cell bodies. In cross sections of the retina, this observation was clearly confirmed (Fig. 3E, right image). These observations confirmed the specificity of the TRP antibody in *Drosophila* photoreceptors. In the lamina and the medulla, the boundaries of photoreceptor axonal projections are clearly visualized by mCD8-GFP expression. By using α-TRP (Fig. 4A) or α-TRPL (Fig. 4B) antibodies and high magnification (63x objective), it was possible to clearly distinguish defined structures in both neuropiles, which are likely to be photoreceptor axonal projections (see section 5.3). In the medulla, larger structures are observed, corresponding to the big brush photoreceptor terminals in this neuropile, as have been shown in Golgi stainings (Meinertzhagen & O'Neil, 1991). Within these terminals in the medulla, TRP channels appear arranged in clusters. This spotted distribution of TRP channels suggests that they may be forming functional complexes with other signalling proteins (signalplex), like their rhabdomeric counterparts. In contrast, TRPL displays a homogeneous distribution and were observed in a subset of

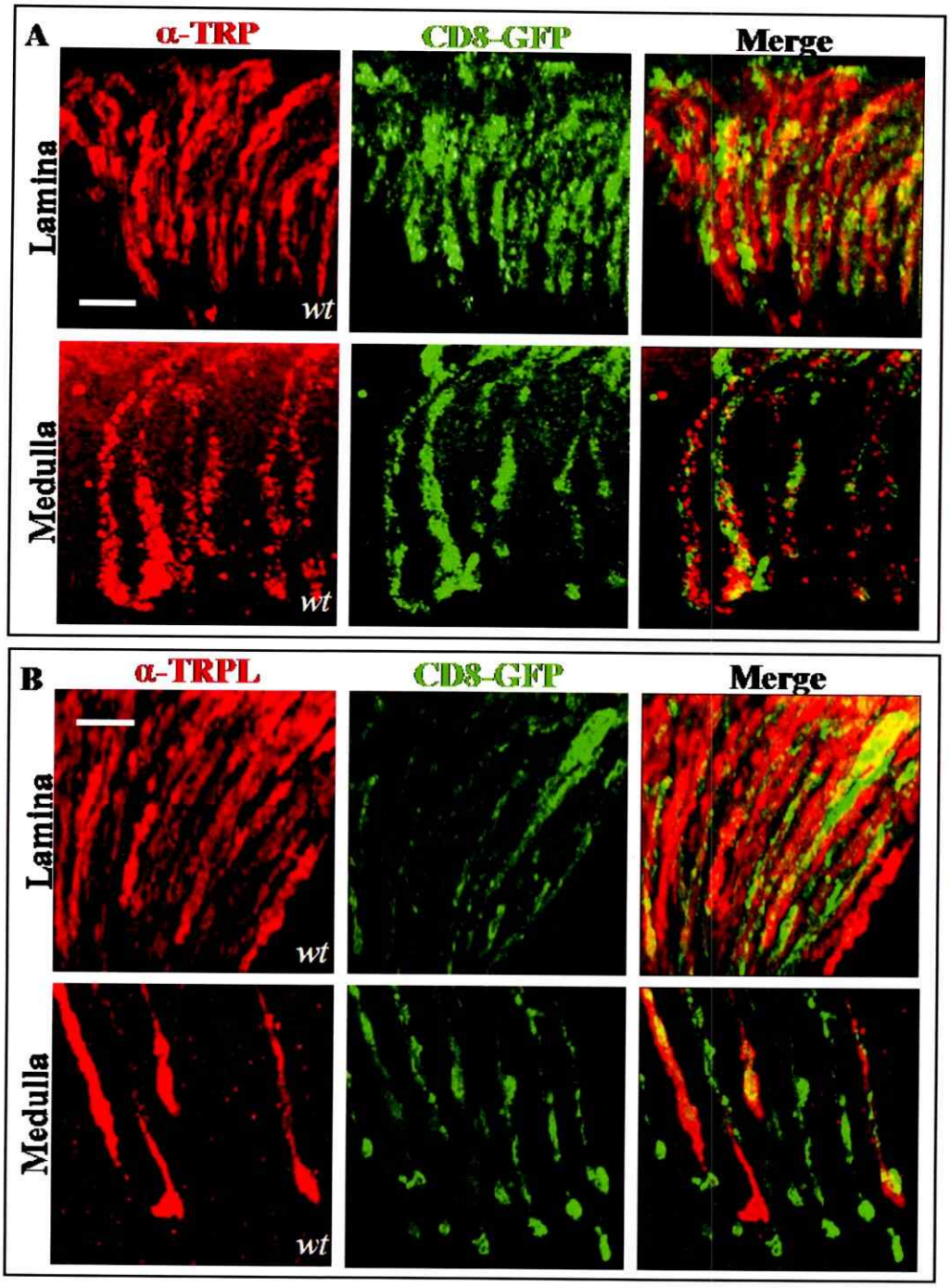

Figure 4. Distribution of TRP, TRPL in photoreceptor terminals. Confocal images of immunofluorescently labelled photoreceptors terminals within the lamina and medulla in *wt* brain slices. **A.** TRP channel distribution (red) within synaptic terminals in the lamina (left) and medulla (right). Photoreceptors are labelled with ectopic expression of CD8-GFP (green). **B.** TRPL channel distribution (red) within synaptic terminals in the lamina (left) and medulla (right). Photoreceptors are labelled with ectopic CD8-GFP expression (green). Bar: 10 μm

photoreceptor axons. This suggests that TRPL channels may be selectively expressed either in R7 or R8 axons. The expression pattern of TRP and TRPL channels can be correlated to that of mCD8-GFP. However, a precise colocalization analysis is crucial to further determine TRP and TRPL expression in photoreceptors axonal projections (see section 5.5).

5.3 TRP and TRPL channels are present in photoreceptor synaptic terminals in the lamina and medulla

In order to determine if TRP and TRPL channels are present in the active zone of photoreceptors axonal projections, expression of the synaptic vesicle protein Synaptobrevin fused to GFP (Syb-GFP) was driven to these neurons under the GMR promoter (GMR-Gal4/UAS-Syb-GFP) (Fig. 5A and 6A). The TRP and TRPL channels immunostaining distribution was compared to the expression pattern of Syb-GFP in the lamina (Fig. 5B and 6B) and in the medulla (Fig. 5C and 6C). The distribution of these signals in the lamina and medulla appears to be only partially correlated to Syb-GFP. In this case, a precise colocalization analysis is also crucial to further determine TRP and TRPL expression in the synaptic boundaries of photoreceptors axonal projections (see section 5.5).

5.4 Signalling transduction proteins in photoreceptor axons in the lamina and medulla

The presence of other signalling proteins of the phototransduction cascade of the rhabdomere was explored in the lamina and medulla, in an effort to determine the activation pathway of TRP and TRPL in the axonal projections in the lamina.

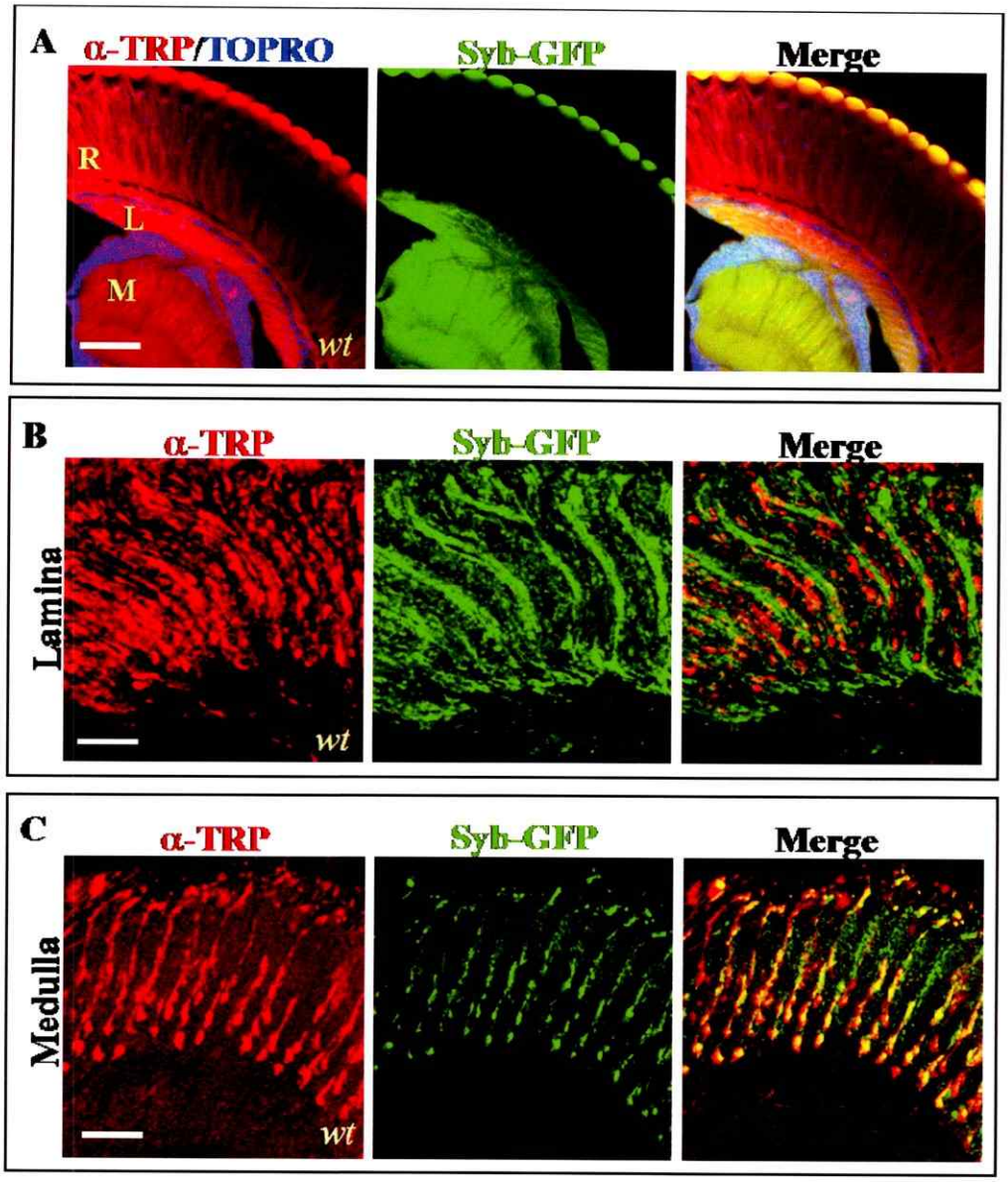

Figure 5. Distribution of TRP channels in photoreceptors active zone in the lamina and medulla. Confocal images of immunofluorescently labelled synaptic terminals within the lamina and medulla in *Drosophila* brain slices. **A.** TRP channel distribution in the retina and lamina (red) detected by monoclonal α-TRP antibody reactivity (Pollock *et al.*, 1995). Cell nuclei are stained with TOPRO (blue). Photoreceptors present ectopic expression of GFP fused to the synaptic vesicle protein, synaptobrevin (Syb-GFP). Bar: 50 μm. **B.** Details of images in A showing TRP channel distribution in synaptic terminals of the lamina. Bar: 10 μm. **C.** Details of images in A, showing TRP channel distribution in synaptic terminals in the medulla. Bar: 15 μm.

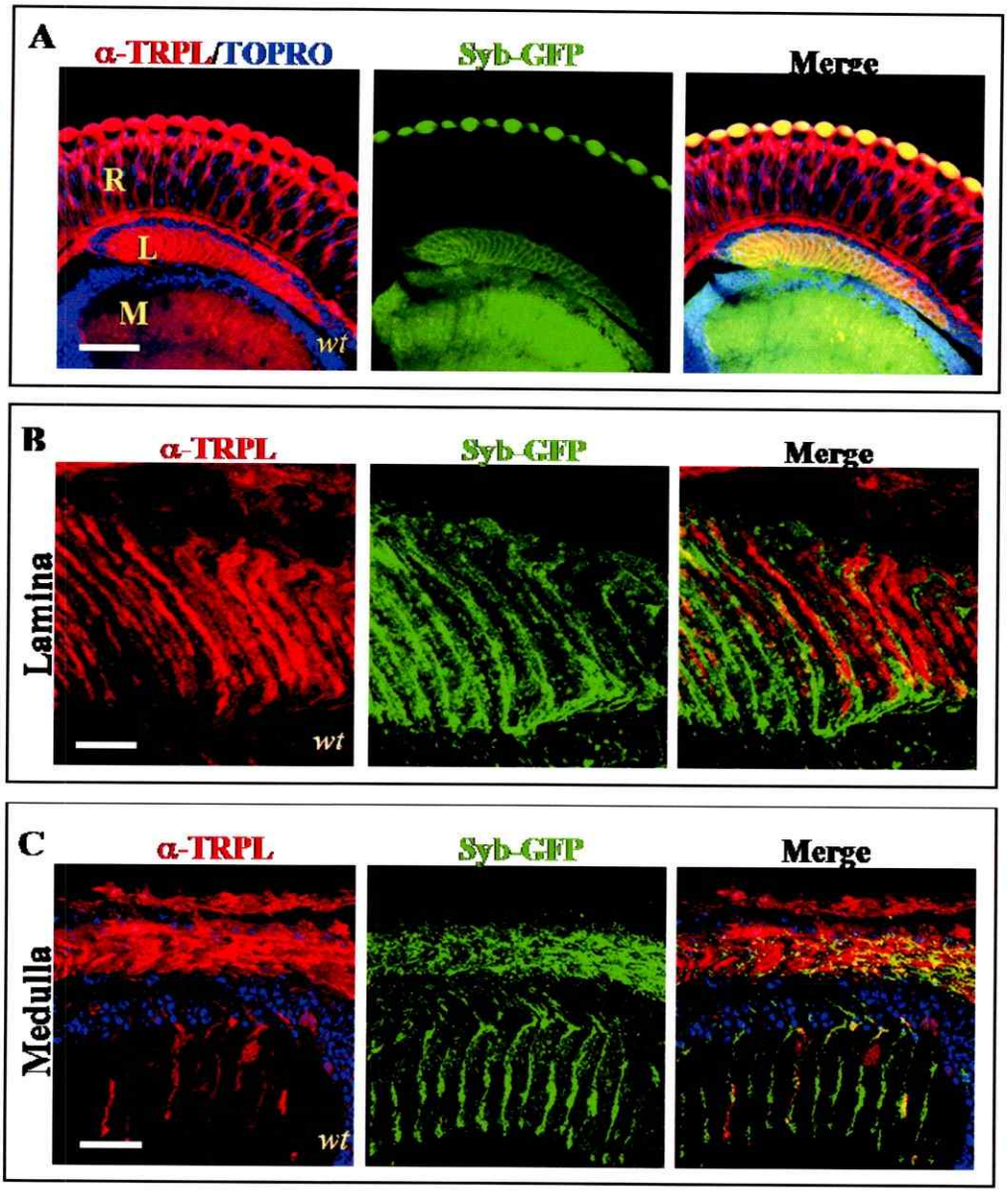

Figure 6. Distribution of TRPL channels in photoreceptors active zone in the lamina and medulla. Confocal images of immunofluorescently labelled synaptic terminals within the lamina and medulla in *Drosophila* brain slices. **A.** TRPL channel distribution in the retina and lamina (red) detected by monoclonal α-TRPL antibody reactivity. Cell nuclei are stained with TOPRO (blue). Photoreceptors present ectopic expression of GFP fused to the synaptic vesicle protein, synaptobrevin (Syb-GFP). Bar: 50 μm. **B.** Magnification of a detail from A of the TRPL channel distribution in synaptic terminals of the lamina. Bar: 10 μm. **C.** Detail of TRPL channel distribution in synaptic terminals in the medulla of images in A. Bar: 15 μm.

PLC_β and G_q-protein are essential for TRP and TRPL channel activation in the rhabdomers. PKC, on the other hand, has an essential role in response termination, as it is proposed to inhibit PLC_β activity by phosphorylation as part of an unidentified mechanism (Gu *et al.*, 2005). The scaffolding protein InaD has a structural function, assembling the signalling proteins together in a signalplex. To test whether these proteins are also present in the photoreceptors axons and in the synapse, their immunoreactivity in the lamina and medulla was explored. In *wt* flies, a strong staining for these proteins was observed in the retina and lamina, especially for PLC and PKC antisera. At higher magnification it was also possible to distinguish them in defined structures, likely to be axonal projections (Fig. 7A-D).

If G_q-protein is effectively expressed in axonal projections, an important question concerns its activation pathway at the synapse. Rhodopsin (Rh1) immunostaining was also explored, however it was only found in the retina, with no detectable expression in the neuropiles (Fig. 7E-G). This was further confirmed using the UAS-GAL4 system. Rh1-Gal4 flies (drives Gal4 under Rhodopsin 1 promoter) were crossed to UAS-mCD8-GFP. The GFP expression pattern of the progeny showed an intense labelling in the retina, while the lamina and medulla exhibited only few scarce spots. A very different situation was seen in GMR-Gal4/UAS-mCD8-GFP progeny, where GFP expression was clearly observed in the photoreceptors axonal projections both in the lamina and medulla. These results suggest that G_q-protein, PKC, PLC and INAD are found in axonal projections in the lamina and medulla, whereas rhodopsin is not present in such cellular structures.

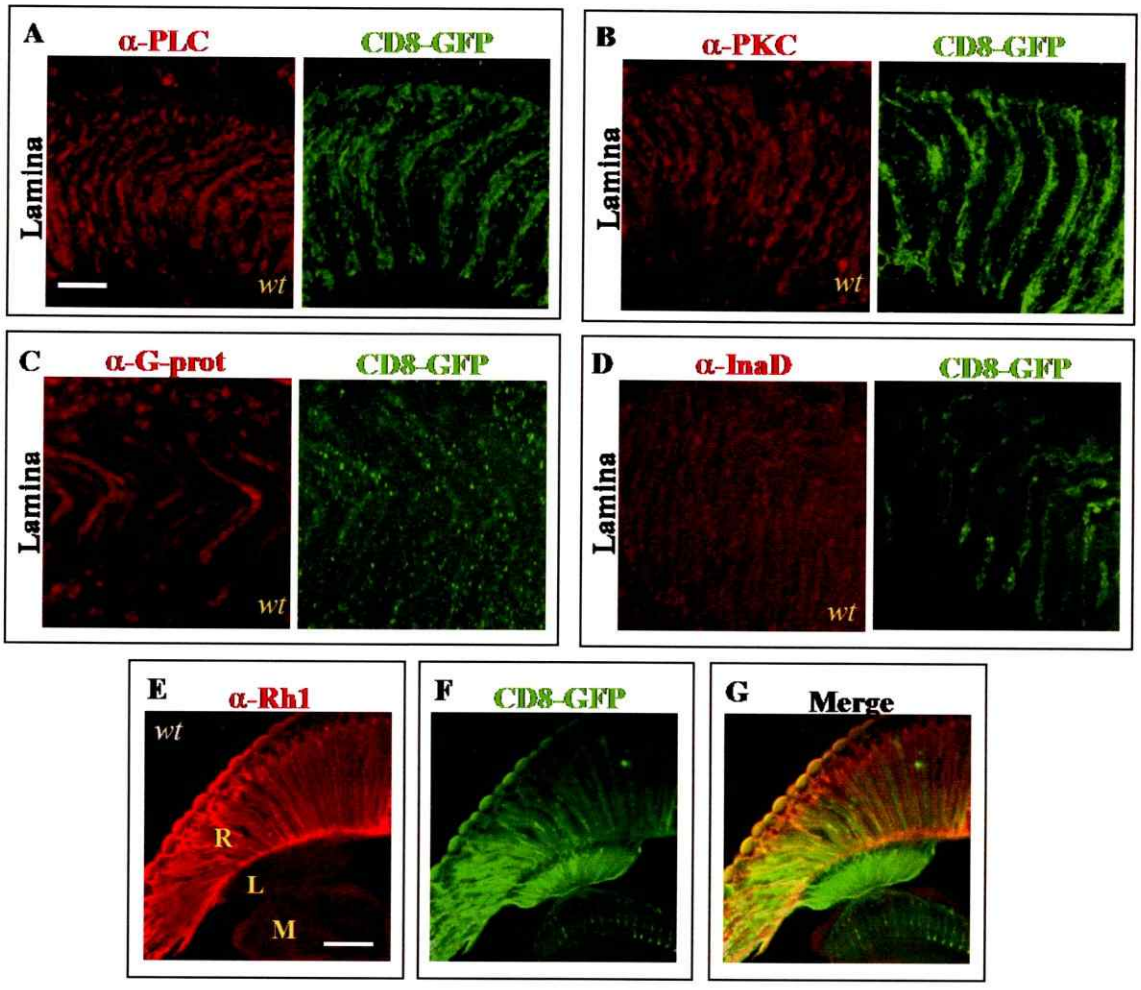

Figure 7. Distribution of transduction proteins in photoreceptor terminals. Confocal images of immunofluorescently labelled photoreceptor terminals within the lamina and medulla in *wt* brain slices. **A.** PLC distribution (red) within photoreceptors terminals in the lamina. For this an all the other images in the green channel, photoreceptors are labelled with ectopic CD8-GFP expression. Bar: 10 μm. **B.** PKC distribution (red) in photoreceptors terminals in the lamina. **C.** G_q-Protein distribution (red) in photoreceptors terminals in the lamina. **D.** InaD distribution (red) in photoreceptors terminals in the lamina. **E.** Rhodopsin Rh1 distribution in photoreceptors in the retina detected by a polyclonal α-Rh1 antibody. This reactivity is not seen in the lamina or medulla. **F.** Photoreceptors are labelled with ectopic CD8-GFP expression. **G.** Superposition of the image in A and B. Bar: 50 μm.

5.5 Quantification of TRP, TRPL and signalling proteins localization in photoreceptor axonal projections

The distribution of TRP, TRPL and the signalling proteins (described in section 5.4) within the photoreceptors axonal projections in the lamina was evaluated by comparing their expression pattern with that of ectopically expressed mCD8-GFP and Syb-GFP, as previously described. A novel colocalization analysis was performed in order to find an accurate method to quantify protein localization in the active zones and within the boundaries of the photoreceptors axonal projections.

Visual inspection of fluorescent signals in different channels may only be feasible for large structures, where their patterns can be easily correlated. For intermediate and small and highly packed structures such as the axons in the lamina, this is not feasible. In order to precisely determine the colocalization of the proteins of interest with photoreceptors expressing GFP within the lamina, it was essential to employ a quantitative method, capable to discriminate between true and random colocalization. This is a critical point in small structures with a high density of fluorescent signals, because the probability of random overlap between two channels increases with signal density. An algorithm to quantify true from random colocalization in small sub-cellular compartments has recently been developed (Omar Ramírez & Härtel, 2010). This confined displacement algorithm (CDA) is based on Costes *et al*, 2004 (Costes *et al.*, 2004) and image correlation spectroscopy. Manders Colocalization Coefficients, MI and M2 are calculated in defined regions of interest (ROIs). These coefficients ($M1/2_{ROI}$) determine the ratio between colocalizing signal to total signal in a channel-specific manner (Eq. 1A and B). A rigorous colocalization analysis must

include: (i) good quality two-channel confocal fluorescent images, (ii) two binary images with channel specific ROIs and (iii) one binary image that define the ROI of a confined cellular compartment.

Photoreceptor terminals in the lamina exhibit small diameters (~1 μm) and are highly compacted in the cartridge structures. For structures like these terminals, which are slightly above the resolution limit of the confocal microscope (~0.4 μm), it is crucial to optimize the resolution of the images. Good quality two-channel confocal fluorescent images are achieved by deconvolution. Deconvolution removes photon noise and is essential to enhance the S/N ratio in order to resolve defined structures. Information in the Z-axis significantly improves deconvolution. For this reason, images were acquired as Z-stacks (8-11 images) and then projected into one image for further analysis.

Two binary images with channel specific ROIs are subsequently obtained by segmentation. This procedure is crucial to define the structures to be further analyzed for colocalization. Segmentation routines, including Laplace filters and manual threshold settings, provided satisfactory binary images preserving the structures of interest. The specific morphology of the subcellular compartment must also be considered and defined for the subsequent analysis. The membrane of axon terminals was segmented to provide the confined area for the randomization algorithm (Fig. 8A).

The area of the segmented ROIs in each channel was quantified to calculate M1 and M2. In CDA, M1 refers to fluorescent signals in the red channel and M2 to those in the green channel. The medulla is a very dense neuropile and since the axonal projections are not organized in cartridges as in the lamina, it is very difficult to clearly distinguish structures from the background tissue. For this reason, data were only taken

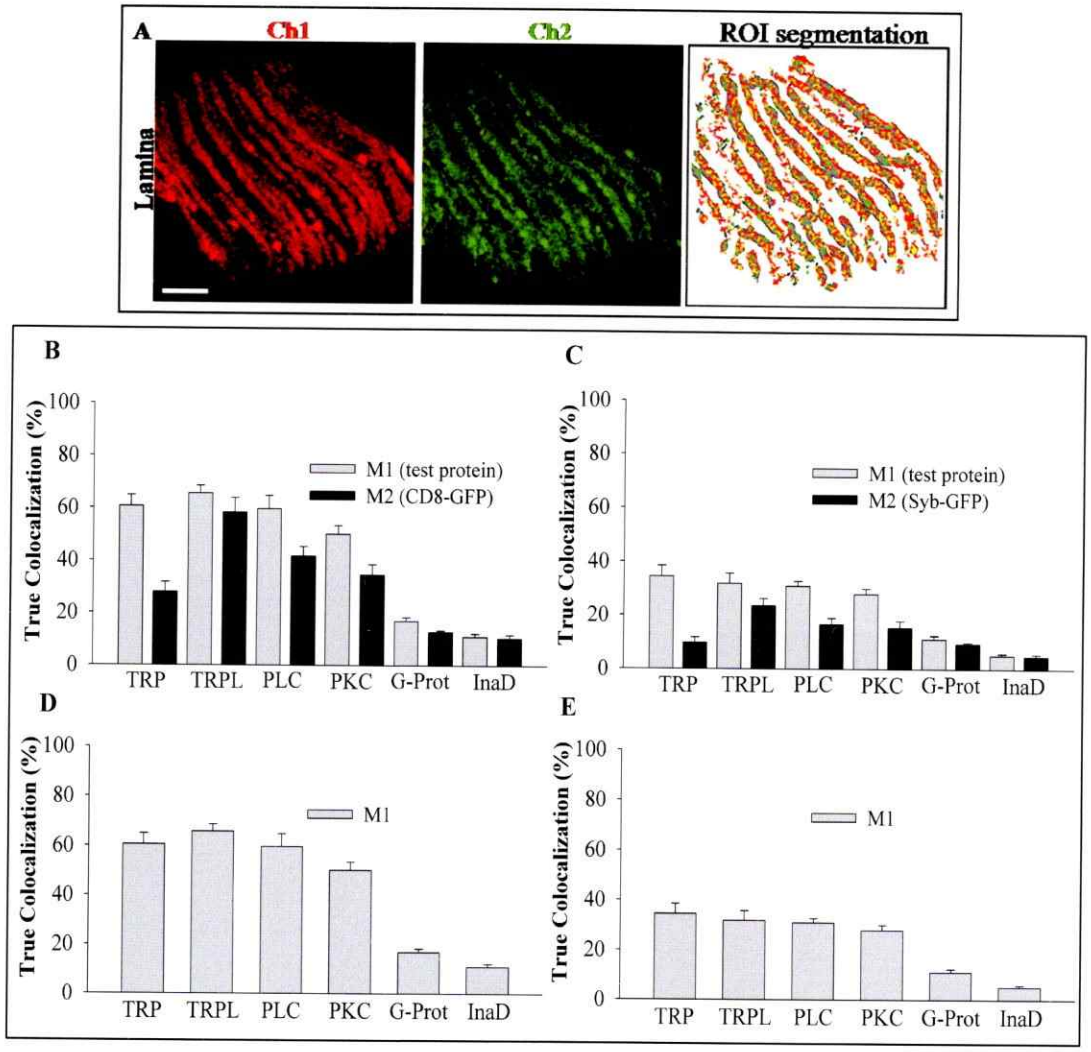

Figure 8. Localization of TRP, TRPL and transduction proteins in photoreceptor terminals.

A. Representative confocal images of a two channel immunofluorescence in the *Drosophila* lamina neuropile. The image in the left (red) corresponds to Channel 1 (Ch1); the image in the middle (green) to Channel 2 (Ch2). The right image is the merge of the segmented ROIs in each channel. **B.** True colocalization of TRP, TRPL and transduction proteins with CD8-GFP ectopically expressed in photoreceptors. Results are expressed as percentage of colocalization, obtained through the confined displacement algorithm (CDA) using Manders coefficients M1 and M2. M1 sums the contribution of the colocalized pixels in the red channel with respect to the total red fluorescent signal. M2 sums the contribution of the colocalized pixels in the green channel with respect to the total green fluorescent signal. Randomization was performed within the ROI area selected from the segmented image in A. The radius of the displacement is 20 pixels for all cases. At least 20 individual images were analysed with the CDA for all the proteins evaluated. Percentages are expressed as mean ± SD. **C.** Colocalization of TRP, TRPL and transduction proteins with Syb-GFP ectopically expressed in photoreceptors. Results are expressed as described in B. **D-E**. True colocalization of interest proteins from B and C respectively.

from the lamina, while the medulla was not considered for the analysis. It is worth mentioning that only preparations with a well preserved fine structure were considered for analysis.

CDA introduces radial displacements in the xy-plane, leading to random scenarios in each channel, without comprising the spatial correlation of fluorescent signal patterns. Reliable detection of true against random colocalization can be achieved when CDA is performed inside confined compartments such as the photoreceptors terminals in the lamina. Validation of true versus random colocalization is achieved by probability density functions (PDF), which reflect the probability to obtain certain colocalization coefficients under random conditions. The maximum colocalization achievable with this algorithm is restricted by the basal random colocalization in each image, which is determined by the signal density in the axons of the lamina. The maximal theoretical colocalization percentage was determined from one image applied in two channels (Ch1 and Ch2). Assuming that this approach would give the highest percent colocalization, the contribution of random colocalization for the axonal structures was calculated for this ideal situation. A random colocalization value of 35% was determined. This means that the theoretical maximum of percent colocalization of this method is 65%. The data obtained from the CDA analysis considers only the effective colocalization, excluding random values. Therefore, data were normalized by the calculated theoretical maximum (Figs. 8B and 8C). In Figure 8B, M1 sums the contribution of the colocalizing pixels in the red channel (TRP, TRPL and the signalling proteins), while M2 sums the contribution of colocalizing pixels in the green channel (mCD8-GFP). TRP and TRPL channels exhibit a mean colocalization close to 60% with

mCD8-GFP expressed in photoreceptors. This suggests that these channels may be expressed in other cell types in the lamina as well.

The colocalization values obtained for the immunofluorescent pattern of the evaluated signalling proteins in the photoreceptors axonal projections in the lamina, evidenced by mCD8-GFP expression, varies in each case. PLC and PKC exhibited the highest percent colocalization (59 and 50%, respectively), while Gq_{α}-protein and InaD presented less significant values (16 and 10%, respectively).

As mentioned above, it was also important to determine whether the channels and proteins of interest are present in the active zone of the photoreceptors terminals. To this aim, Syb-GFP driven to photoreceptors (as mentioned in section 5.3) was taken for the CDA analysis. In Figure 8C, M1 is referred to the red channel (TRP, TRPL and the signalling proteins), while M2 refers to Syb-GFP. The colocalization values observed between the immunofluorescent signal of TRP, TRPL and the signalling proteins with that of Syb-GFP in the photoreceptors active zones falls to one half of the colocalization observed with mCD8-GFP. The colocalization analysis performed presented the following colocalization percentages: TRP 34%, TRPL 31%, PLC 30 %, PKC 28%, Gq_{α}-protein 11%, and the scaffolding protein InaD, 4.7%. It appears that these components are not particularly expressed in the active zones of the photoreceptors axonal projections in the lamina. It seems more likely that they are uniformly distributed along the photoreceptors axonal projections. The speckled distribution of the TRP channel immunostaining within the axonal projections, especially in the medulla, suggests that these channels may associate in functional protein complexes. If this is the

case, the spatial distribution of these complexes is not expected to match the active zones, where the SV are released. It is possible that TRP and TRPL channels form signalling complexes with PLC_{β}, PKC, G_q-protein or InaD in the lamina. However, in contrast to the high immunoreactivity observed for TRP antibodies both, in the retina and in the lamina, InaD showed weaker immunofluorescence reactivity in the lamina than in the retina. For this reason, if the signalling components are grouped in signalplexes in the lamina, these complexes might include several TRP channels and a few molecules of InaD and G_q-proteins.

Regarding the relative proportion between the colocalization values between the red immunofluorescent signals and the GFP expression patterns and vice versa, additional information about the surface disposition of the components in the lamina was obtained. M1 colocalization values for all the proteins studied in the red channel are more prominent than M2 either for mCD8-GFP or Syb-GFP in the lamina. This result can be interpreted as a difference between the surface occupied by photoreceptors axonal projections and active zones and the surface covered by TRP, TRPL and the signalling proteins. It is possible that TRP channels are localized in confined microdomains within the photoreceptors terminals not equivalent to the active zones. In this scenario, the disposition of the signalling proteins in the photoreceptors axonal projections in the lamina is more constricted than that observed for TRP and TRPL channels.

Altogether, these results show that TRP and TRPL channels, together with the signalling cascade proteins required for their activation are present in confined regions

within photoreceptor axons in the lamina. In the active zone, this location is less significant.

5.6 Voltage-activated Ca^{2+} channels in the lamina

The Ca^{2+}-permeant channels TRP and TRPL are present in photoreceptor terminals in the lamina. With the aim to evaluate the possible existence of a second pathway for Ca^{2+} influx in these neurons, the presence of voltage-gated Ca^{2+} channels (VGCC) in this neuropile was examined by immunofluorescence. A screening for R, P/Q, T, L and N-type channels in *Drosophila* brain slices, revealed only the presence of the latter type in the retina (Fig. 9A) and lamina (Fig. 9B). The analysis showed a colocalization of 51% for mCD8-GFP with N-type channels and a 34% with Syb-GFP in the lamina. Both expression patterns, mCD8-GFP and Syb-GFP, presented a smaller percentage of colocalization than N-type channels. This may be the consequence of a significant difference between the surface occupied by photoreceptors axonal projections and active zones and the surface covered by N-type channels in the lamina.

In the fly genome, the *cacophony* gene encodes for a VGCC whose amino acidic sequence shares about 60% identity with vertebrate N-type channels, depending on the species. It was therefore possible that the vertebrate α-N-type channel antibody may recognize a conserved epitope present in these two channels. These results suggest that a VGCC with high sequence similarity to N-type channels, likely to be Cacophony, might be present in the lamina.

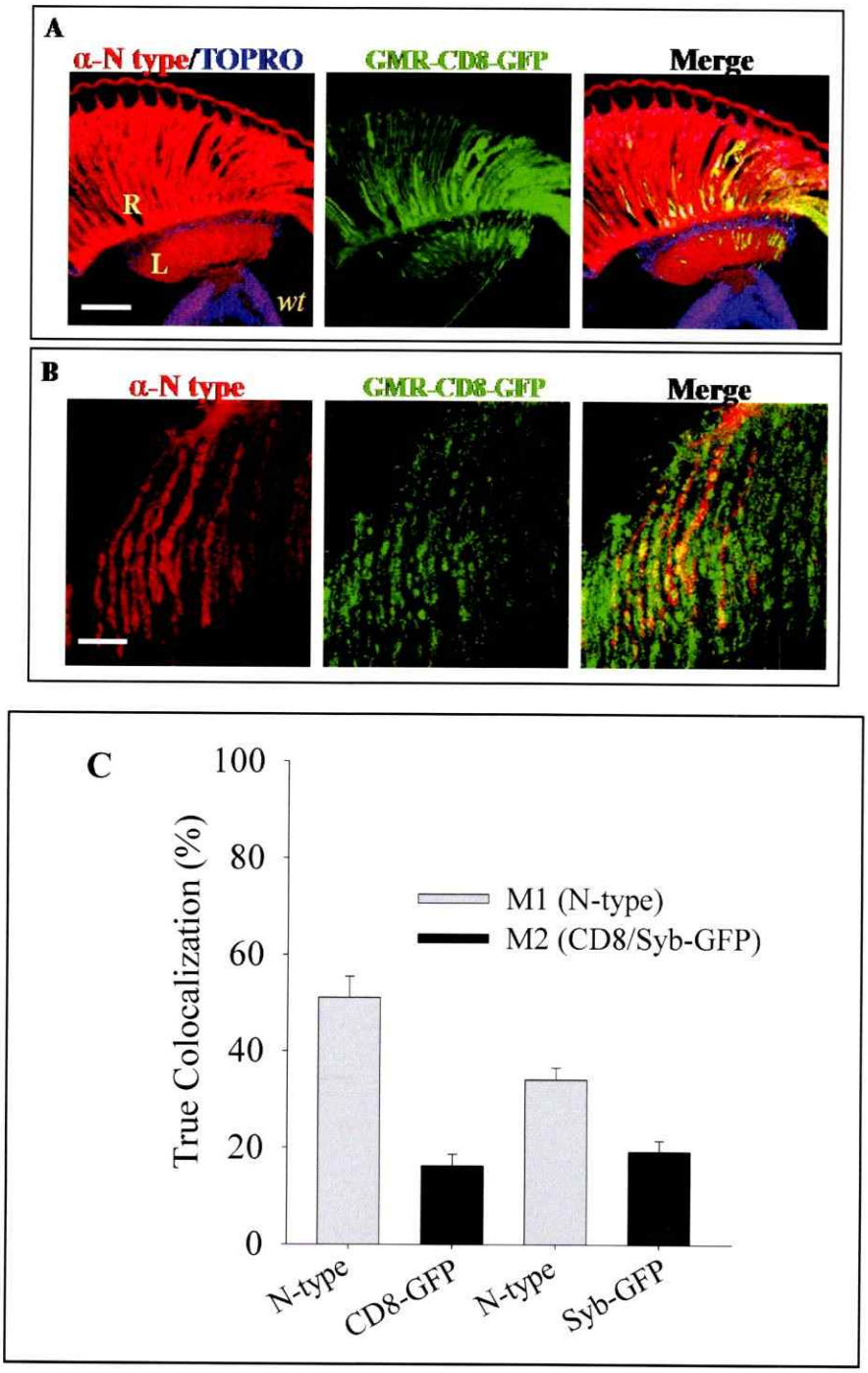

Figure 9. α-N type VGCC immunoreactivity in the lamina. A. Confocal images of polyclonal α-N type antibody immunofluorescence (red) in the visual system in *wt Drosophila* brain slices. Cell nuclei are stained with TOPRO (blue). Photoreceptors are labelled by CD8-GFP ectopic expression (green). Bar: 50 μm. **B.** Magnification of the α-N type channel antibody immunoreactivity in synaptic terminals of the lamina, for images in A. Bar: 10 μm.

5.7 Ca^{2+} signalling in photoreceptor axons

TRP and TRPL are Ca^{2+}-permeant channels and this ion is essential for synaptic vesicle exocytosis. In order to evaluate if these channels take part in Ca^{2+} signalling in photoreceptor terminals in the lamina, *in vivo* imaging in *wt* and $trp^{343};trpl^{302}$ *Drosophila* brain slices was performed. With the aim of imaging Ca^{2+} specifically in photoreceptor terminals, the Ca^{2+}-binding protein G-CaMP (Nakai *et al.*, 2001) was ectopically expressed in these cells by means of the GMR promoter. This is a fusion protein between the Ca^{2+}-binding site of Calmodulin and GFP that is efficiently used as an indicator for this ion (Nakai *et al.*, 2001). GMR-Gal4/UAS-GCaMP flies express the G-CaMP protein in the eyes (Fig. 10A). With higher amplification (63x objective) G-CaMP can be resolved in photoreceptor axons in the lamina and the medulla (Fig. 10B). The axonal projections in these neuropiles appeared with an intense G-CaMP signal. In the lamina, discrete and defined structures that might correspond to axonal projections could be identified (Fig. 10C) and were imaged to monitor Ca^{2+} transients upon application of various types of stimuli.

5.7.1 Ca^{2+} signals induced by PLC-dependent pathway in photoreceptor axons in the lamina

The first candidates tested as possible activators of TRP and TRPL channels were PUFAs. These lipids are the metabolic products of DAG metabolism by PLC. Linolenic acid (LNA) is a PUFA that has been previously shown to induce TRP and TRPL channel activity (Chyb *et al.*, 1999; Delgado & Bacigalupo, 2009). In order to evaluate a potential effect of LNA on channel activation in the lamina, a procedure for

local pressure-application of this lipid was implemented. This was achieved by positioning on the lamina a glass micropipette filled with extracellular solution (ES), supplemented with LNA (20 μM) while the slices were constantly perfused at a rate of 2mL/min. Under these conditions, LNA application in the lamina of *wt* slices induced an average reversible relative increase in G-CaMP fluorescence, $\Delta F/F_0$=1.8 ± 0.22 (results are expressed as mean ± standard error). Confocal time lapse images were obtained from the lamina, where individual terminals were scanned for 12 minutes (Fig. 10D) and were further quantified (Fig. 10E, red trace; n=4). Control experiments applying the vehicle (ethanol) to the lamina (n=3) did not show a significant increase in G-CaMP fluorescence (Fig. 10E, blue trace; n=3). In brain slices of $trp^{343};trpl^{302}$ double mutants, application of this lipid did not produce a significant change in the fluorescence intensity of the Ca^{2+} fluorophore Rhod-2 (Fig. 10E, gray trace; n=5). These observations are consistent with the possibility that LNA activates laminar TRP and TRPL channels, producing a Ca^{2+} increment in the terminals.

The next component tested as potentially implicated in the activation of TRP and TRPL channels in the lamina was PLC. For this purpose, the PLC activator, *m*-3M3FBS (80 μM), was applied to the lamina in brain slices. Topical application of this compound in *wt* brain slices induced a strong and reversible Ca^{2+} rise in this neuropile with a mean $\Delta F/F_0$ of 0.88 ± 0.11 (Fig. 11A, upper panels). Confocal images were acquired as z-stacks, before, during and after exposure to *m*-3M3FBS. For image analysis, z-stacks were projected as a single image and its integrated density was quantified in an area of

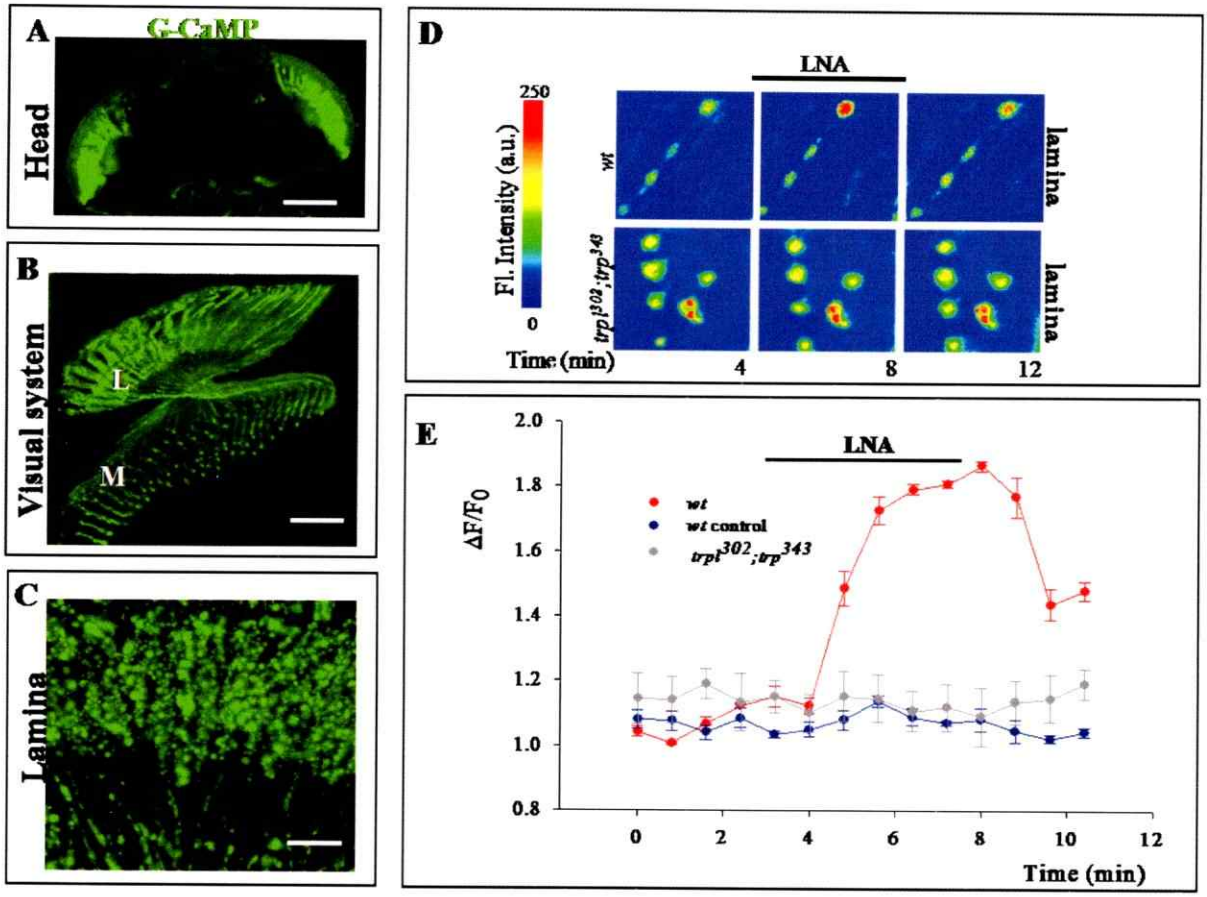

Figure 10. Ca^{2+} signals in photoreceptor synaptic terminals in the lamina.
A-C: Confocal images of brain slices from GMR-Gal4/UAS-GCaMP transgenic flies showing expression of the Ca^{2+} binding fluorescent protein, G-CaMP in *Drosophila* photoreceptors. **A**. G-CaMP expression in the head is restricted to the eyes. Bar: 200 μm. **B**. G-CaMP expression in the retina, lamina and medulla. Bar: 50 μm. **C**. G-CaMP expression in synaptic terminals in the lamina. Bar: 10 μm. **D**. Time lapse confocal images screening changes in G-CaMP/Ca^{2+} fluorescence. in response to local application of Linolenic Acid (LNA) in the lamina of *wt* and $trpl^{302};trp^{343}$ mutant flies (upper and lower panels respectively). This mutant was imaged with the fluorophore Rhod2. Bar: 3 μm. **E**. Quantification of G-CaMP/Ca^{2+} and Rhod-2 fluorescence in *wt* and $trpl^{302};trp^{343}$ from images shown in D.

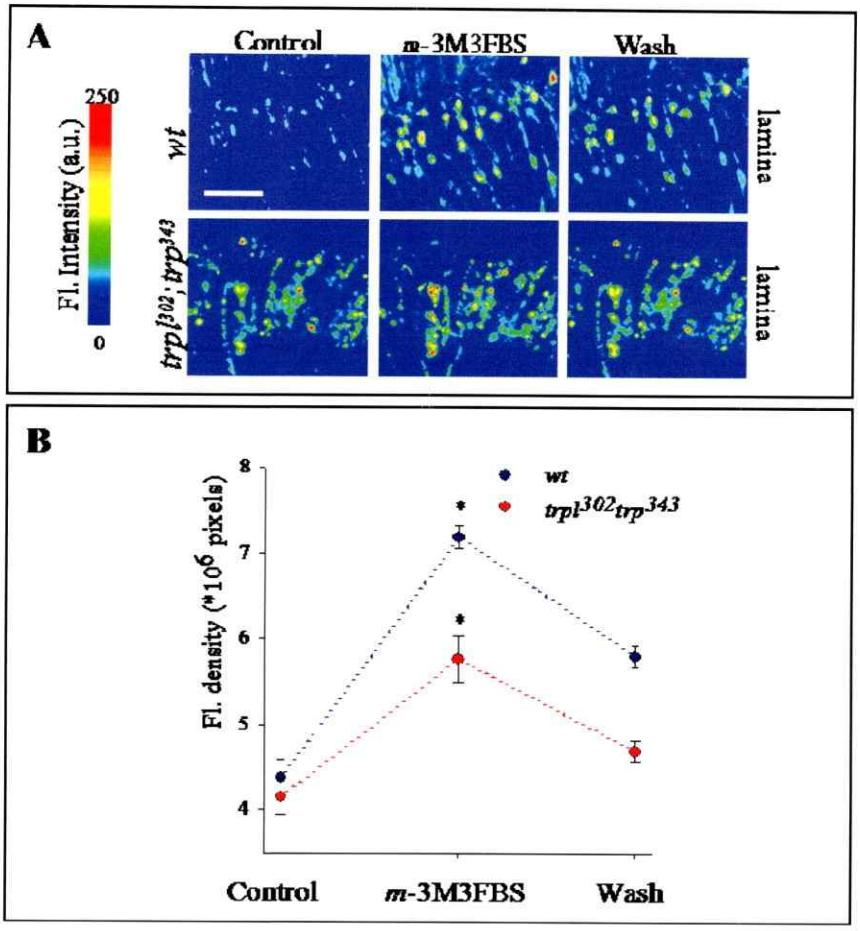

Figure 11. PLC-induced Ca^{2+} signals in *Drosophila* visual system.
A. Time lapse confocal images of brain slices from GMR-Gal4/UAS-GCaMP transgenic flies screening changes in G-CaMP/Ca^{2+} fluorescence, in response to application of the PLC activator, *m*-3M3FBS 100 μM in *wt* and $trpl^{302};trp^{343}$ (upper and lower panels respectively). This mutant was imaged with the fluorophore Rhod-2. **B.** Quantification of G-CaMP/Ca^{2+} and Rhod-2 fluorescence changes in response to *m*-3M3FBS 100 μM application in *wt* and $trpl^{302};trp^{343}$ flies. The integrated density of fluorescence (Fl.) intensity within a predetermined area was calculated in each image. (*) Two way anova, Bonferroni post-test; $p<0.05$.

36.56 x 36.56 μm in x/y axis (Fig. 11B). These results suggest that PLC activity generates Ca^{2+} signals in photoreceptors axonal projections in the lamina.

5.7.2 Ca^{2+} signals induced by depolarization in photoreceptor axons in the lamina

With the purpose of evaluating whether photoreceptor depolarization is sufficient to induce Ca^{2+} transients at these axonal projections, an extracellular solution containing 90 mM KCl was applied to brain slices. In *wt* slices, a reversible rise in G-CaMP fluorescence was observed after high K^+ application; the mean $\Delta F/F_0$ was 0.68 ± 0.8 (Fig. 12A upper panels). For quantification, ten z-stack confocal images were acquired before, during and after high K^+ treatment. These images were projected and the integrated density (in an area of 36 x 36 μm in x/y) was calculated for each case (Fig. 12B). In the presence of the Cacophony VGCC specific blocker, PLTX-II, these depolarization-induced Ca^{2+} transients were significantly reduced to a mean $\Delta F/F_0 = 0.36$ ± 0.6. In

$trp^{343};trpl^{302}$ double mutants, application of high K^+ induced a similar raise in Rhod-Ca^{2+} fluorescence than in *wt*. In this case, the mean $\Delta F/F_0$ was 0.63 ± 0.6. (Fig. 12B). These results suggest that depolarization induces an intracellular increase in Ca^{2+} in photoreceptors terminals in the lamina which is independent of TRP and TRPL channels.

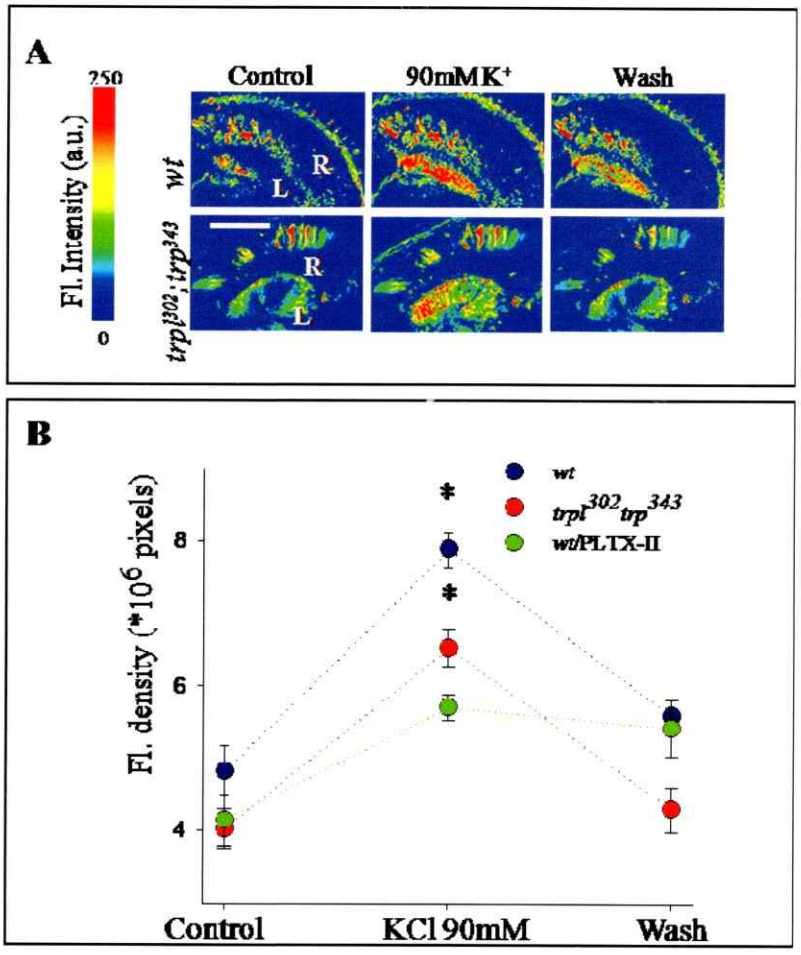

Figure 12. Voltage-dependent Ca^{2+} signals in *Drosophila* visual system.
A. Time lapse confocal images of brain slices from GMR-Gal4/UAS-GCaMP transgenic flies screening changes in G-CaMP/Ca^{2+} fluorescence in response to application of KCl 90 mM in *wt* and in $trpl^{302};trp^{343}$ (upper and lower panels respectively). This mutant was imaged with the fluorophore Rhod-2. **B.** Quantification of G-CaMP/Ca^{2+} and Rhod-2 fluorescence changes in response to KCl 90 mM application in *wt* and $trpl^{302};trp^{343}$ flies. The integrated density of fluorescence (Fl.) intensity within a predetermined area was calculated in each image. (*) Two way anova, Bonferroni post-test; $p<0.05$.

5.8 Vesicle exocytosis in synaptic terminals in the lamina

Synaptic vesicle exocytosis is a Ca^{2+}-dependent process. To assess whether TRP and TRPL channel activities contribute to vesicle exocytosis in the lamina, *in vivo* imaging with the fluorescent dye FM4-64 was performed in *Drosophila* brain slices. After FM4-64 (10 μM) exposure, the synaptic terminals in the lamina and medulla were fluorescently labelled in an activity-dependent manner. In the former neuropile, these functional units are arranged in high density columnar structures, and discrete boutons are clearly distinguished. In the medulla, synaptic terminals appear in high density arrangements, but in this case it was not possible to distinguish discrete boutons. For this reason, vesicle exocytosis in synaptic terminals was only scrutinized in the lamina. The confocal images were captured in the lamina of brain slices from *wt* and different fly mutants, as well as under diverse experimental conditions. In all cases, 10 z-stack images (with a fixed size of 36.56 μm in x/y and 0.3 μm in the z axis) were projected as a single image and were further analyzed for quantification with IDL. Deconvoluted confocal fluorescence images were segmented (Fig. 13A and 13B) to select binary ROIs by application of two different filters:

1) *Gradient filter*, to select high S/N objects from background. This procedure was used to determine object contours and to separate contiguous regions within a 10 pixel radius.

2) *Size selection filter* to choose objects within the range of interest. The diameter of the FM4-64 labelled synaptic boutons observed in *Drosophila* lamina varies from 0.9 to 1.1 μm. Based on this observation, object areas within the range from 0.6 to 1.0 μm^2 were selected from the rest (Fig. 13C) with this filter. The selected ROIs were automatically

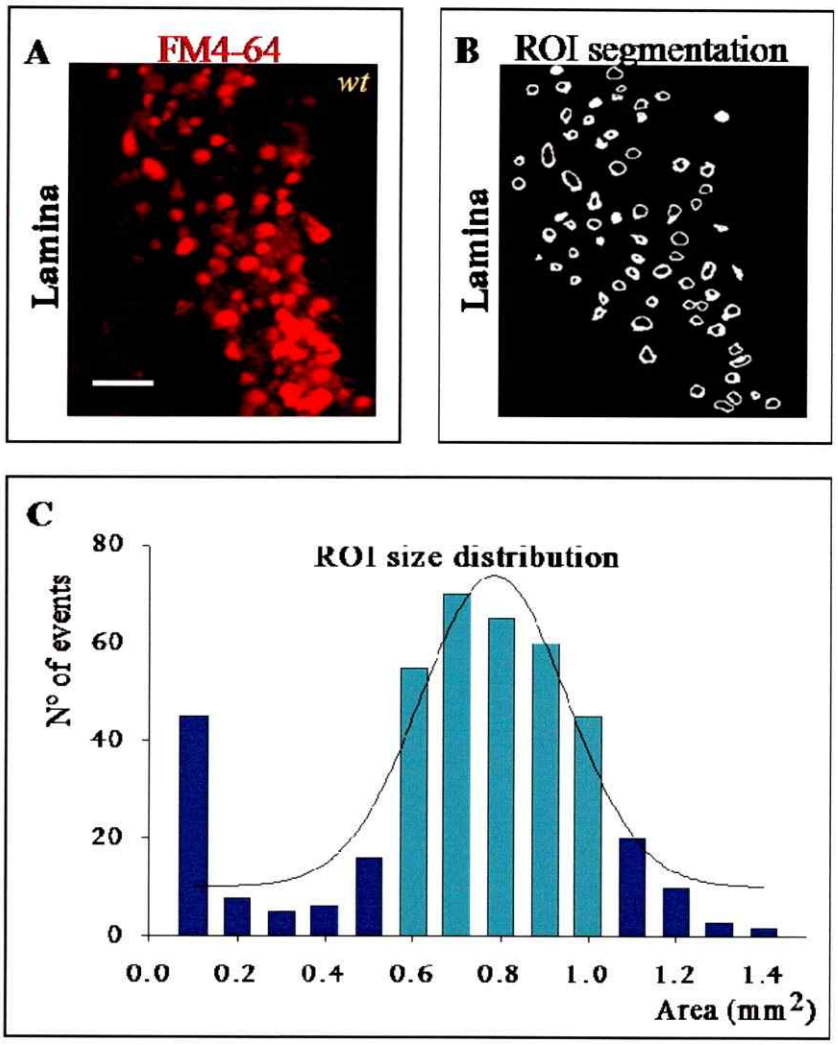

Figure 13. ROI segmentation in confocal images of FM4-64 labelled synaptic boutons in the lamina. A. Representative image of FM4-64 loaded boutons in the lamina of *wt* flies. **B.** Binary ROI segmentation for the boutons in the image shown in A. Bar: 5 µm. **C.** ROI quantification for objects segmented in B. The histogram shows the size distribution of the segmented ROIs. A size filter was applied to select objects within the range of synaptic terminals size.

quantified by IDL. For subsequent analysis, the results were expressed as the mean number of synaptic terminals (or ROIs) in each image (expressed as mean ± standard error) for all the mutants and conditions evaluated.

5.8.1 Depolarization-induced vesicle exocytosis in the lamina

In *wt* brain slices, exposure to a depolarizing stimulus (KCl 90 mM) for 10 minutes in the presence of FM4-64, induced massive vesicle exocytosis and a large number of fluorescently labelled synaptic boutons were observed in the lamina (199 ± 22; n=17) after treatment, indicating an active vesicle cycle. A representative image of this condition is shown in Figure 14A, and bouton quantification in Figure 15A.

As a control to measure spontaneous vesicle exocytosis in the absence of a depolarizing stimulus, brain slices were exposed to FM4-64 in normal extracellular solution (5 mM KCl) at two different temperatures: on ice and room temperature (RT). The reason to perform these controls at two different temperatures was that the FM4-64 experiments with high K^+ were performed in ice and the rest, at RT. The number of FM4-64-labeled synaptic boutons at these two temperatures was not significantly different (15 ± 2; n=10 and 20 ± 3, n=5 respectively; Fig. 15F), however both were significantly smaller (Anova; $p<0.05$) from that captured after depolarization by high K^+ (199 ± 22; Figs. 14C and 15A). This observation confirms that the observed FM4-64 labelling in the lamina corresponds to activity-dependent dye uptake into synaptic boutons. In brain slices from TRP (trp^{343}) or TRPL ($trpl^{302}$) channel mutants, the number of labelled boutons after exposure to high K^+ (150 ± 19, n=7 and 122 ± 16;

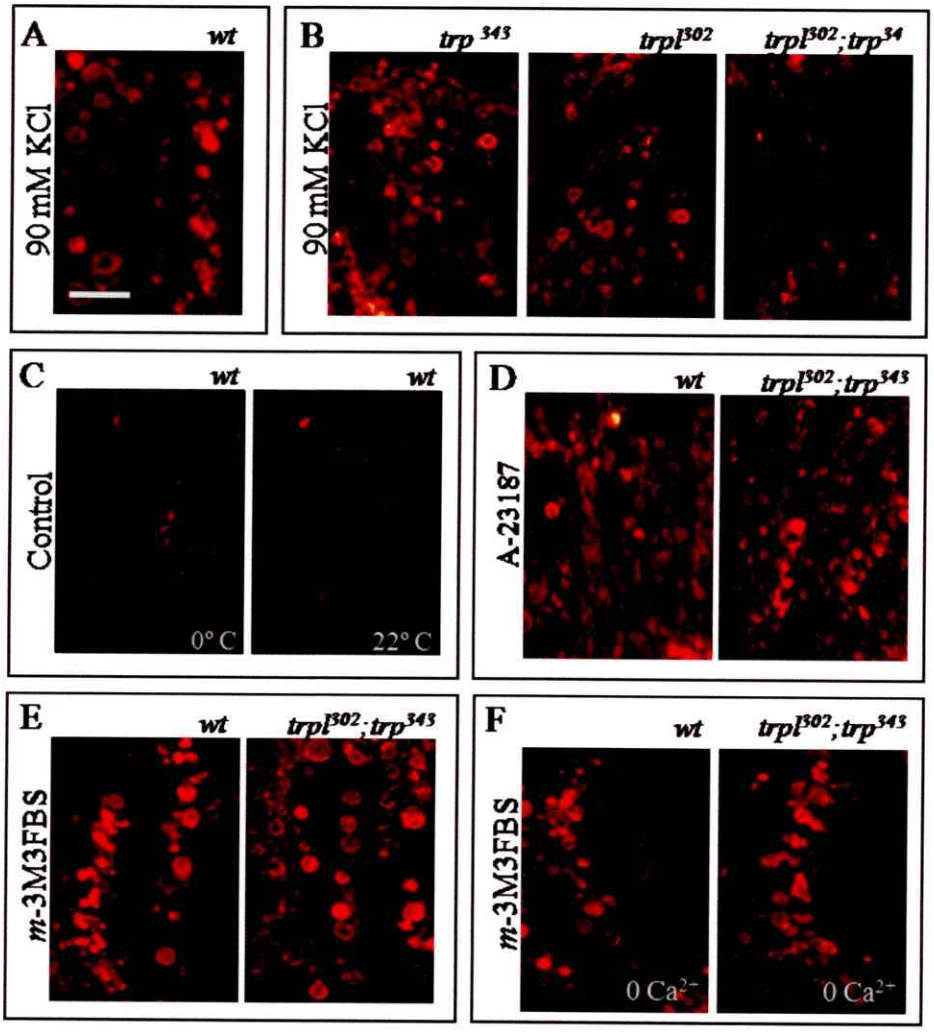

Figure 14. External and internal Ca^{2+}, TRP and TRPL are required for vesicle exocytosis in ribbon synapses of the lamina. Confocal images of *Drosophila* brain slices for *wt* and mutant flies stimulated in the presence of FM4-64 with the following agents: **A.** 90 mM KCl in *wt* flies. Bar: 5 μm **B.** 90 mM KCl in trp^{343}, $trpl^{302}$ and $trpl^{302};trp^{343}$ mutant flies. **C.** Ca^{2+} ionophore, A-23187 in normal KCl in *wt* and $trpl^{302};trp^{343}$. **D.** FM4-64 loading control in brain slices in ice and at room temperature (RT). No other stimulus was applied. **E.** *m*-3M3FBS in normal extracellular solution (1.5 mM Ca^{2+}) in *wt* and $trpl^{302};trp^{343}$ flies. **F.** *m*-3M3FBS in 0 extracellular Ca^{2+} in *wt* and $trpl^{302};trp^{343}$ flies.

n=9 respectively) was not significantly different from that observed in *wt* flies (Anova; p>0.05; Figs. 14B and 15A). On the contrary, brain slices from the $trpl^{302};trp^{343}$ double mutant presented a significantly smaller FM4-64 loading into synaptic boutons (40 ± 5, n=16, Anova; p<0.01; Figs. 14B and 15A) than *wt*. These observations indicate a severe defect in vesicle exocytosis in this mutant. This condition might be the result of synaptic terminals degeneration due to the absence of light induced activity in this mutant (as can be seen in its ERG). However, this is not the case for these synapses (Hiesinger *et al.*, 2006). In a series of electron micrographies, Hiesinger *et al* 2006 reported that $trpl^{302};trp^{343}$ as well as other mutants with disrupted generation of electrical potentials exhibit normal synaptic morphology (number of SV and contacts per terminal) and axon projections into the lamina and medulla. Consistent with this observation, application of the Ca^{2+} ionophore, A-23187 (250 nM, in normal extracellular solution) in the presence of FM4-64 induced a strong dye labelling in $trpl;trp^{343}$ mutants (Fig. 14D). The number of synaptic boutons in this case (90 ± 18; n=5) was significantly higher than those labelled under high K^+ in this mutant (Anova; p<0.05) and comparable to A-23187 induced labelling in *wt* flies (130 ± 15, n=5). These observations suggest that exocytosis in photoreceptor synaptic terminals can be experimentally activated by an increase in intracellular Ca^{2+} and rules out the possibility that they are degenerated. Moreover, they show that the presence of TRP and TRPL channels in photoreceptor axons is required for a normal (depolarization- induced) vesicle exocytosis in the lamina. From the results obtained in the single channel mutants (trp^{343} or $trpl^{302}$), it can be

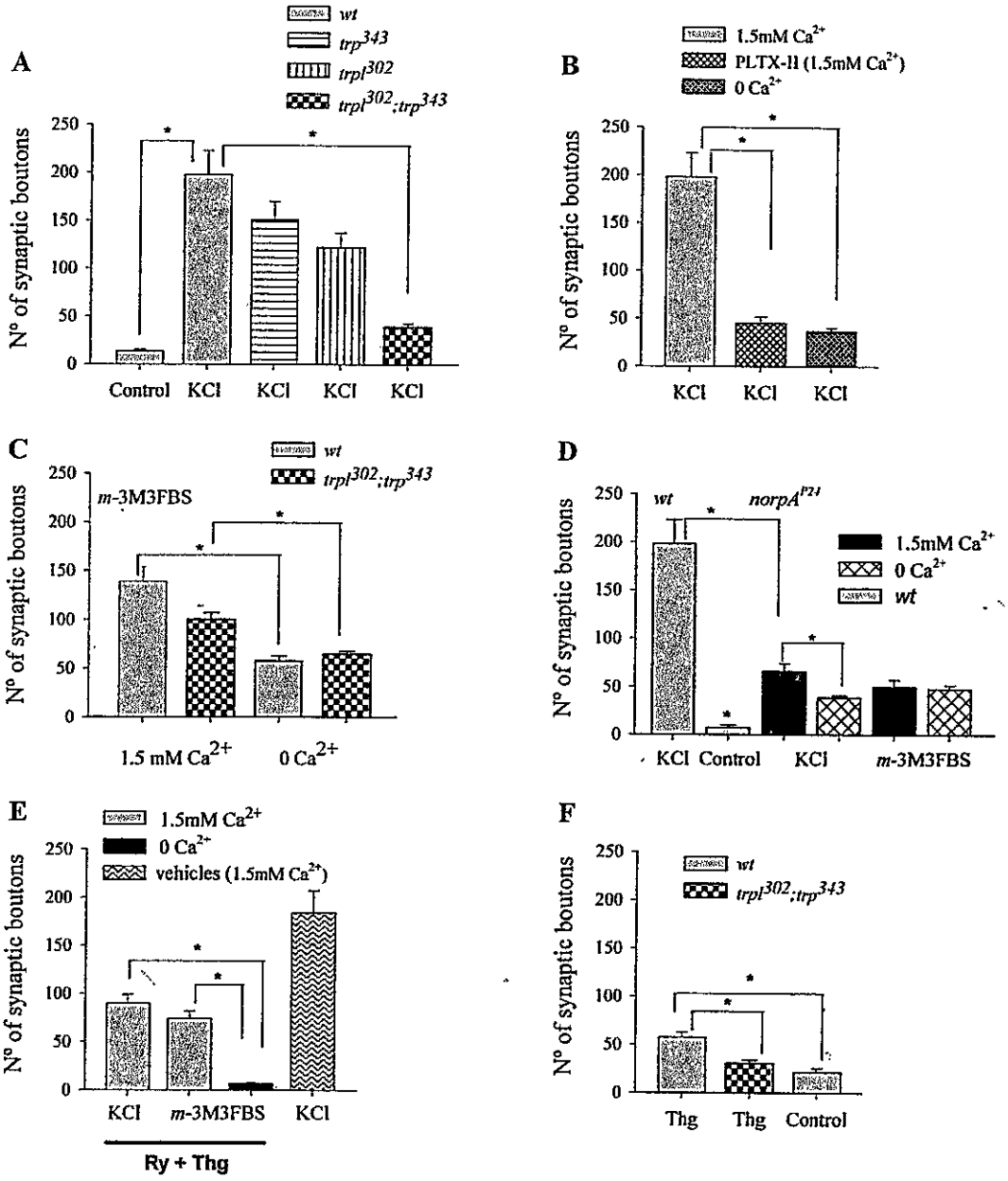
A
wt
trp343
trpl302
trpl302;trp343
N° of synaptic boutons
Control
KCl
KCl
KCl
KCl
B
1.5mM Ca2+
PLTX-II (1.5mM Ca2+)
0 Ca2+
N° of synaptic boutons
KCl
KCl
KCl
C
wt
trpl302;trp343
m-3M3FBS
N° of synaptic boutons
1.5 mM Ca2+
0 Ca2+
D
wt
norpAP24
1.5mM Ca2+
0 Ca2+
wt
N° of synaptic boutons
KCl
Control
KCl
m-3M3FBS
E
1.5mM Ca2+
0 Ca2+
vehicles (1.5mM Ca2+)
N° of synaptic boutons
KCl
m-3M3FBS
KCl
Ry + Thg
F
wt
trpl302;trp343
N° of synaptic boutons
Thg
Thg
Control

Figure 15. Synaptic activity in the *Drosophila* visual system. Number of FM4-64 labelled synaptic boutons in the lamina in brain slices, under the following conditions:
A. Depolarization by KCl 90 mM in *wt* and *trp* and *trpl* mutants. **B.** Depolarization by KCl in *wt* slices in Ca^{2+} free conditions or in addition to the Cacophony channel blocker, PLTX-II (100nM). **C.** Application of the PLC activator *m*-3M3FBS (80μM) in normal (1.5 mM) and Ca^{2+} free conditions in *wt* and $trpl^{302};trp^{343}$. **D.** KCl 90 mM and *m*-3M3FBS application in $norpA^{P24}$ mutants, in normal and Ca^{2+} free conditions. **E.** KCl 90 mM and *m*-3M3FBS application in *wt* slices, previously treated with Thapsigargin (Thg) and Ryanodine (Ry). **F.** Normal extracellular Ca^{2+} application after Thg treatment in Ca^{2+} free conditions, in *wt* slices. Bars represent mean values ± standard error in z-projections of 10 images, each one of size: x/y/z = 36/36/0.3 μm. One- and two-way ANOVA with Dunnett's and Bonferroni post test, respectively; $p<0.05$.

deduced that either one of them is sufficient to support the exocytic activity in the synaptic terminals in the lamina.

5.8.2 Voltage-gated Ca^{2+} channels-mediated exocytosis in the lamina

As a general rule, Ca^{2+} influx required for vesicle exocytosis at synaptic terminals is mediated by voltage-gated Ca^{2+} channels. In the *Drosophila* genome, the *cacophony* gene codes for one of such channels. With the aim to determine if the Ca^{2+} influx required for depolarization-induced exocytosis in the lamina is dependent on Cacophony channels, the specific Cacophony channel blocker PLTX-II (100nM) was applied. In the presence of this toxin, the number of boutons labelled in *wt Drosophila* brain slices in response to depolarization by high K^+ was 47 ± 8 (n= 7), significantly reduced compared to toxin-free conditions (Anova; $p<0.01$, Fig. 15B). This result suggests that Cacophony VGCCs are implicated in the depolarization-induced exocytosis in the lamina.

5.8.3 *m*-3M3FBS induced vesicle exocytosis in the lamina

Rhabdomeric TRP and TRPL channel activity is tightly related to PLC_β. In order to identify the activation pathway of these channels in photoreceptor axons in the lamina, their activation downstream to this enzyme was tested. The PLC activator, *m*-3M3FBS (80 μM) was used to induce vesicle exocytosis. In *wt Drosophila* brain slices, exposure to this drug for 10 minutes triggered exocytosis in the lamina and a large number of synaptic boutons were fluorescently labelled (140 ± 13; n= 18; Figs. 14E and 15C). The intensity, shape, spatial distribution and number of labelled boutons in the

lamina in this condition were not different from those induced by depolarization. Noteworthy, in the null double mutant, $trpl^{302};trp^{343}$ (where KCl failed to trigger massive exocytosis in the lamina), *m*-3M3FBS induced a similar synaptic bouton labelling than *wt* (101 ± 12; n= 20; Figs. 14E and 15C). While this observation confirms that the exocytic machinery in $trpl^{302};trp^{343}$ mutants is not degenerated, it also suggests that *m*-3M3FBS stimulated exocytosis involves a different Ca^{2+}-permeant channel than TRP or TRPL in the lamina. One plausible mechanism is that the PLC product IP_3, could be acting upon IP_3 receptors (IP_3R) in the ER and hence, inducing Ca^{2+} release from intracellular reservoirs. This Ca^{2+} release would support exocytosis in the lamina synaptic terminals in the absence of TRP and TRPL. As a consequence of this Ca^{2+} release from intracellular reservoirs, Ryanodine receptors (RyR) located in proximity to IP_3R in the ER membrane might be activated by this Ca^{2+}. This idea is supported by the fact that both, IP_3 and RyRs are abundantly expressed in the lamina (Vazquez-Martinez *et al.*, 2003). Moreover, given the fact that this neuropile is primarily composed of axo-axonic synaptic terminals, it is highly probable that these receptors are located in proximity to the synaptic vesicle exocytic machinery in the terminals.

Previous observations raise special concern regarding a possible parallel effect of *m*-3M3FBS on Ca^{2+} mobilization from intracellular stores by an unidentified mechanism, apparently independent of PLC activity (Krjukova *et al.*, 2004). If this occurred in the lamina, intracellularly released Ca^{2+} might supply the requirements for exocytosis in the terminals in the absence of Ca^{2+} influx through TRP and TRPL (as seen in the $trpl^{302};trp^{343}$ mutant). To evaluate the possibility to induce exocytosis in the

absence of extracellular Ca^{2+} ($[0Ca^{2+}]_e$), *wt* brain slices were treated with high K^+. In these conditions, bouton labelling induced by depolarization with KCl was significantly reduced (36 ± 5; n=11) compared to normal (1.5 mM) extracellular Ca^{2+} (Fig. 15B). These results show that extracellular Ca^{2+} is necessary for a normal vesicle exocytosis in the lamina.

To further evaluate this proposal, *m*-3M3FBS was also applied in $[0Ca^{2+}]_e$ to examine whether there was FM4-64 loading in this condition. In *wt* brain slices, vesicle exocytosis induced by this drug is significantly diminished with respect to normal Ca^{2+} conditions (57 ± 3, n=10; Anova; $p<0.01$; Figs. 14F and 15C). Nevertheless, there was a remnant exoc<ytic activity which was significantly higher than basal conditions in absence of stimulus (Anova; $p<0.01$). $trpl^{302};trp^{343}$ double mutants under $[0Ca^{2+}]_e$, also exhibited bouton labelling (63 ± 4, n= 9; Fig. 14F and 15C). Although this value is significantly smaller to normal $[Ca^{2+}]_e$ conditions, it is higher than basal labelling (Anova; $p<0.01$), thus indicating an active exocytic process, independent of extracellular Ca^{2+}. These observations are consistent with those made in slices depolarized by means of high K^+, in $[0Ca^{2+}]_e$.

These results suggest that there are two Ca^{2+} sources for exocytosis in the synaptic terminals in the lamina: one relying on external Ca^{2+} and the second, on internal reservoirs. As a control for additional secondary effects of *m*-3M3FBS, this drug was tested on a PLC_β mutant. Unfortunately, null mutants for this enzyme are lethal; consequently only hypomorphic phenotypes could be used. In $norpA^{P24}$, both depolarization by high K^+ or *m*-3M3FBS treatment induced a significantly smaller

number of labelled boutons in comparison to *wt* (66 ± 9; n=8 and 49 ± 6 n=9 respectively; (Anova; $p<0.05$; Fig. 15D). Therefore, PLC_β activity seems to be required for a normal synaptic activity in the lamina. In Ca^2-free ES, KCl-dependent exocytosis was significantly altered in this mutant (Fig. 15D), but a significant number of terminals was still labelled, confirming that extracellular Ca^{2+} is required for this process and that intracellular reservoirs also contribute to it.

Remarkably, exocytosis triggered by *m*-3M3FBS in $[0Ca^{2+}]_e$ was not different in $norpA^{P24}$ (46 ± 5, n=8) than under normal $[Ca^{2+}]_e$ (Fig. 15D). This observation strongly supports the idea that *m*-3M3FBS stimulates Ca^{2+} mobilization from intracellular reservoirs. Unfortunately, due to the residual PLC_β activity in the hypomorphic mutant $norpA^{P24}$, it is not possible to discriminate if this effect is dependent or not on PLC_β. In any case, it seems that the PLC activator produces an unspecific effect that disturbs the analysis of these data. For this reason, these results were treated with caution.

Taken together, these results show that besides the essential role of TRP and TRPL in SV exocytosis in the lamina, extracellular Ca^{2+}, PLC activity and Ca^{2+} release from intracellular reservoirs are also required.

5.8.4 Contribution of intracellularly released Ca^{2+} to synaptic transmission in the lamina

Intracellular Ca^{2+} is significantly regulated by the sarcoplasmic/endoplasmic reticulum Ca^{2+}/ATPase (SERCA) and RyR. SERCA replenishes the ER lumen with this ion, while RyRs mediates Ca^{2+} release. The former process can be blocked by the SERCA inhibitor thapsigargin (Thg), causing depletion of the ER Ca^{2+} stores.

Alternatively, Ca^{2+} release through the RyRs can be inhibited (Wingertzahn & Ochs, 1998) by high (100 μM) ryanodine (Ry) concentrations (Thastrup *et al.*, 1990). In combination, both drugs can be effectively used to abolish Ca^{2+} release from intracellular reservoirs.

In *Drosophila*, it has been reported that the thapsigargin-sensitive Ca^{2+} ATPase, together with IP_3R and RyR, are strongly expressed in the lamina (Vazquez-Martinez *et al.*, 2003). In the $trp^{343};trpl^{302}$ double mutant, the exocytosis induced by depolarization was highly reduced in this neuropile. However, the synaptic exocytic machinery was activated in a voltage and TRP-TRPL independent manner, by means of *m*-3M3FBS. Since this drug has been reported to induce Ca^{2+} mobilization from intracellular stores independently of PLC activity in other cell systems (Krjukova *et al.*, 2004), it is reasonable to explore whether this may also occur in *Drosophila* synaptic terminals.

With the aim of exploring whether Ca^{2+} release from intracellular reservoirs supplies the exocytic machinery in synaptic terminals of the lamina, Thg and Ry were used in combination to abolish this process. Incubation of *wt* brain slices, with Thg (10 μM) and Ry (100 μM) previous to high K^+ or *m*-3M3FBS exposure, significantly reduced bouton labelling caused by both treatments (87 ± 9, n=7, Anova; $p<0.01$ $p<0.01$, and 73 ± 10, n=6, $p<0.05$ respectively; Fig.15E). When extracellular Ca^{2+} was removed in addition to intracellular store depletion, drug-stimulated exocytic activity fell to nominal values (6 ± 3, n=6; Anova; $p<0.01$). This result confirms that the FM4-64 labelling observed in the lamina (in the previous set of experiments) was due to a Ca^{2+}-dependent exocytic mechanism. In order to evaluate whether the solvents for Thg

(DMSO) and Ry (methanol) exerted any effect on vesicle exocytosis, a control experiment was done with high K^+ in the presence of both vehicles. In these conditions the number of labelled boutons (182 ± 14; n= 5; Fig. 15E) did not differ from that observed with normal KCl stimulation.

These results support a role of intracellularly released Ca^{2+} in vesicle exocytosis in synaptic terminals of the lamina. It seems likely that Ca^{2+} levels controlling vesicle exocytosis in the lamina synaptic terminals is regulated by two complementary processes. One of them is dependent on depolarization and implies extracellular Ca^{2+} influx into the terminals through Cacophony VGCC and a second process involves Ca^{2+} release from intracellular reservoirs, where TRP/TRPL channels may take part in a SOC mechanism.

5.8.5 SOC stimulated Ca^{2+} activity in synaptic terminals in the lamina

In the absence of TRP and TRPL channels, exocytosis in response to depolarization is impaired. As induced intracellular Ca^{2+} release can sustain exocytosis by itself, it is possible that TRP and TRPL channels are implicated in Ca^{2+} refilling of internal stores by a SOC mechanism.

In a number of reports, SOC channels are studied with a widely used 'depletion protocol' that consists of emptying Ca^{2+} stores in 0 Ca^{2+} ES supplemented with 10 μM thapsigargin (Szikra *et al.*, 2008). After 10 minutes under these conditions, intracellular stores are depleted. Exposure to normal $[Ca^{2+}]_e$ induces a large Ca^{2+} influx into the

cytoplasm, restoring luminal concentrations of this ion, when a SOC mechanism is present in the model of study (Szikra *et al.*, 2008; Szikra *et al.*, 2009).

If TRP and TRPL channels are indirectly involved in Ca^{2+} release from intracellular reservoirs in the lamina, an essential issue concerns its activation pathway and a potential coupling to the ER. The previous protocol was used to examine if exocytosis in the lamina can be triggered by Thg treatment. In *wt* brain slices treated with Thg in [0 $Ca^{2+}]_e$, a shift to 1.5 mM Ca^{2+} triggered substantial FM4-64 labelling (58 ± 7, n=7; Fig. 15F). The number of boutons labelled under such conditions was significantly smaller (Anova; $p< 0.01$) than after KCl depolarization in normal $[Ca^{2+}]_e$. Nevertheless, it was comparable to the previous data obtained under 0 Ca^{2+}. These results are consistent with the proposed role of intracellularly released Ca^{2+} in synaptic transmission. Moreover, they suggest a SOC-related mechanism for this Ca^{2+} release into the cytosol.

The experiments with KCl were conducted on ice and the series described above, at room temperature (RT). As a control, to evaluate the effect of temperature on exocytosis in the lamina, *wt* slices were exposed to FM4-64 at RT. In these conditions the basal number of stained boutons was small (20 ± 3, n=5; Fig. 15F) and not significantly different from that observed in ice (Fig. 13F). This confirms that the observed Thg-induced bouton labelling is not a consequence of temperature facilitation.

In $trpl^{302};trp^{343}$ double mutants, vesicle exocytosis induced by this "depletion protocol" was significantly reduced with respect to *wt* flies (29 ± 4, n=6; Fig. 15F).

These results strongly support a role for TRP and TRPL channels in Ca^{2+} release from intracellular stores that might involve SOCE for refilling of these stores.

In order to determine if the mentioned vesicle exocytosis triggered by the "depletion protocol" is accompanied by an intracellular Ca^{2+} rise in the lamina, *in vivo* imaging was performed to evaluate SOCE. In *wt* brain slices, a significant Ca^{2+} rise was observed after application of this protocol, with a mean $\Delta F/F_0$ of 0.38 ± 0.06 (Fig. 16A, upper panels; n= 5). In $trpl^{302};trp^{343}$ double mutants, this treatment failed to induce Ca^{2+} signals in the lamina (Fig. 16A, lower panels; n=4). For image analysis, z-stacks of 10 images acquired in the lamina from *wt* and $trpl^{302};trp^{343}$ flies (in an area of 36.56 x 36.56 μm in the x/y axis) were projected into one for quantification (Fig. 16B). Taken together, these results show that intracellular Ca^{2+} stores are an important source of this ion for vesicle exocytosis in the lamina and that TRP and TRPL channels are implicated in this process, mediating SOCE.

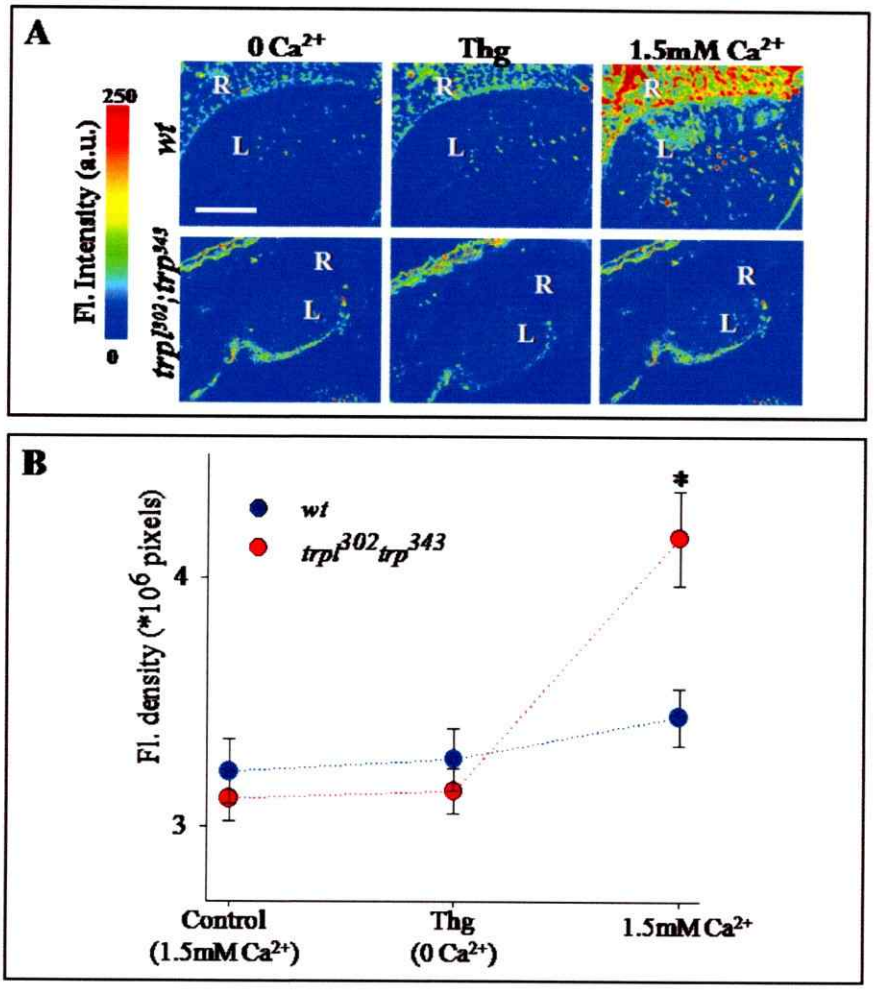

Figure 16. Store depletion-induced Ca^{2+} signals in *Drosophila* visual system.
A. Time lapse confocal images of brain slices from screening changes in G-CaMP/Ca^{2+} fluorescence in *wt* and Rhod-2 in $trpl^{302};trp^{343}$ (upper and lower panels respectively) in response to the 'depletion protocol'. This consists of emptying Ca^{2+} stores in 0 Ca^{2+} ES supplemented with 10 μM Thg, followed by re-exposure to normal ES. **B.** Quantification of G-CaMP/Ca^{2+} and Rhod-2 fluorescence changes in response to the depletion protocol in *wt* and $trpl^{302};trp^{343}$ flies. The integrated density of fluorescence (Fl.) intensity within a predetermined area was calculated in each image. One- and two-way ANOVA with Dunnett's and Bonferroni post test respectively, $p<0.05$.

6. DISCUSSION

6.1 TRP and TRPL channels and other phototransduction proteins are present in the lamina and medulla

TRP channels have been widely studied, principally in relation to their role in sensory transduction. However, in recent years an increasing number of investigations have related TRP channels also with synaptic transmission. This role is of special interest, due to their Ca^{2+} permeability and the multiple factors that are known to regulate their activity. Synapses are the key elements for neuronal communication and thus the relation between their inputs and outputs is essential to regulate network circuitry. For this reason, regulation of synaptic transmission at any level (pre- or post-synaptically) is a matter of paramount importance.

In vertebrate rod synapses, VGCC are not the only source for Ca^{2+} influx into the terminals. Like invertebrate photoreceptors and some other sensory neurons, rods exhibit graded synapses, which extend their physiological range of synaptic responses beyond the operational voltage range of VGCC. In graded synapses this property has a special significance as they constantly respond to voltage changes and release neurotransmitter in a tonic and regulated manner. At membrane potentials where VGCC are not activated, an alternative mechanism for Ca^{2+} influx into the synaptic terminals must operate, since Ca^{2+} is crucial for synaptic vesicle exocytosis. It was recently shown that this mechanism involves the Ca^{2+}-permeant channel TRPC1 in rod synapses, which is essential to sustain high rates of neurotransmitter release (Szikra *et al.*, 2008).

In *Drosophila* photoreceptors, Ca^{2+} homeostasis in the synaptic terminals has not been investigated so far. However, like their vertebrate counterparts, these sensory neurons must also maintain a high rate of neurotransmitter release (Uusitalo *et al.*, 1995a; Uusitalo *et al.*, 1995b). In the present work, the presence of TRP and TRPL channels was demonstrated in the lamina and medulla of the *Drosophila* visual system, where the photoreceptors make synapses with postsynaptic neurons. As these are Ca^{2+} permeant channels, this work aimed to evaluate the presence of TRP channels in photoreceptor axons and their possible physiological function in synaptic transmission. We propose that TRP and TRPL play a significant role in maintaining Ca^{2+} levels in intracellular reservoirs and that this Ca^{2+} source is required for normal SVexocytosis in the lamina. To determine whether these channels are present in photoreceptors axonal projections, a precise colocalization analysis was necessary, due to the high axonal density and connectivity of the lamina. It must be considered that, as a consequence of this high axonal density, fluorescence signals in one channel (Ch1) could randomly overlap those in the other channel (Ch2). The CDA allowed us to exclude random colocalization originated from the high signal density in the cartridges. This random colocalization may lead to an overestimation of true colocalization levels. Based on these observations, we confirmed the presence of TRP and TRPL channels in mCD8-GFP labelled photoreceptors, where they exhibited a mean true colocalization of ~60%. When the same analysis was applied to compare the expression pattern of TRP and TRPL channel with that of Syb-GFP (a presynaptic marker), the colocalization percentage dropped by half (~30%) in both cases, indicating that a considerable

proportion of these channels is closely related to the acive zones in photoreceptorsThe fluorescence signal of mCD8-GFP extends beyond the area ofthe TRP signals. One possibility to understand this scenario is that TRP channels are located in microdomains within photoreceptor axons or that a subset of photoreceptor types (Rh1-6 or Rh7-8, which cross the lamina into the medulla) selectively express TRP. On the other hand, we cannot exclude the possibility that TRP and TRPL channels are also postsynaptically expressed in the laminar interneurons, L1-L5. To precisely determine the cellular localization of these channels, an accurate study should include electronic microscopy. However, the development and interpretation of such technique in the lamina is highly demanding and exceeds the purpose of this work.

Comparison of the Manders coefficients may provide further information about channel distribution in the axons. M2 values calculated for mCD8-GFP signal in TRP immunofluorescences are significantly smaller than M1 (Anova; $p<0.05$). One possibility to understand this scenario is that TRP channels are distributed in small clusters within localized areas of the photoreceptors terminals. A different situation is observed in TRPL immunofluorescences, where M2 values are not significantly smaller than M1 (Anova; $p>0.05$). In this case, unlike TRP channels, it seems possible that TRPL are not clustered within the terminals, exhibiting a homogeneous distribution. This is consistent with the defined segregation of the fluorescent signal in TRP immunofluorescences observed in the medulla terminals (Fig. 4A). In contrast, TRPL channels appeared uniformly distributed within the photoreceptor axonal projections. These observations are reminiscent of the rhabdomeric situation, where TRP channels are recruited into signalplexes in tight relation to InaD, whereas TRPL channels are not

part of these structures and are able to translocate from the rhabdomers to the cell body depending on light (Bahner *et al.*, 2002; Cronin *et al.*, 2006; Meyer *et al.*, 2006). In consequence, under invariable light conditions, TRPL channels are also uniformly distributed in the photoreceptors cell bodies and rhabdomers. Most of the signalling proteins of the phototransduction cascade in the rhabdomers are also found in photoreceptors axonal projections in the lamina and medulla. PLC and PKC display an intense immunofluorescence with a wide distribution in different cell types in the lamina, including photoreceptors axonal projections. In these structures, PLC exhibited a mean colocalization of 59% with the mCD8-GFP signal and a similar value was observed for PKC (50%). The $G_{q\alpha}$-protein presented a smaller degree of colocalization (16%) than the other two proteins in these projections. The scaffolding protein InaD, on the other hand, showed a small percentage of colocalization (10%). In contrast, the G_q-protein coupled receptor, Rhodopsin (Rh1), was not found in the lamina in this study. This observation opens the question concerning the signalling mechanism that triggers TRP and TRPL channel opening in photoreceptors axonal projections in the lamina.

In this thesis, VGCC were also found to be expressed in the photoreceptor axonal projections in the lamina by immunofluorescence. This observation was further confirmed by functional studies on the lamina with the PLTX-II toxin, which is specific for Cacophony VGCC. These observations suggest that TRP and TRPL channels, together with the signalling proteins, might function in addition to VGCC for Ca^{2+} influx in photoreceptor terminals in the lamina.

channels blockade by PLTX-II. These results confirm that in addition to Cacophony channels, there may be a secondary Ca^{2+} source that supplies the exocytic machinery of the lamina.

In *Drosophila* genome there are merely four different genes that code for α1 subunits of voltage-gated Ca^{2+} channels (in contrast to ten in mammals). These are the pore forming subunits and determine the channel ion selectivity and pharmacological properties (Takahashi *et al.*, 1987). The *cacophony* gene (*cac*) encodes for a Cav2-type channel (named CAC, Dmca1A, Nightblind A or No-on-transient B) which is the only homologue of vertebrate N-, P/Q- and R-type VGCC, essential for neurotransmitter release in excitable cells (Catterall, 2000). Splicing of the *cac1* subunit mRNA contributes to the diversity of Cacophony channels in *Drosophila*. The other three genes in *Drosophila* represent homologues for L-type (Dmca1D) *(Eberl et al., 1998)* and T-type channels (Dmca1T) (http://fl ybase.bio.indiana.edu/) and an invertebrate-specific subunit (Dmalpha1U, also known as narrow abdomen and halothane resistance) (Nash *et al.*, 2002). Cacophony is the primary VGCC subunit involved in neurotransmission in *Drosophila* and *cac* mutants display a marked reduction in synaptic release and visual functional defects (not morphological) (Smith *et al.*, 1996). Moreover, it has been proposed that these channels mediate vesicle exocytosis in non-spiking neurons at central excitatory synapses in the adult fly brain (Lee & O'Dowd, 1999). According to these data, the PLTX-II sensitive and voltage-dependent Ca^{2+} pathway monitored by optical imaging in the lamina may rely on Cacophony channels.

6.2 Ca^{2+} influx and vesicle exocytosis in *Drosophila* lamina

The physiological implications of TRP and TRPL channels in the lamina terminals were also studied in this work. This aim was attained by optical imaging of Ca^{2+} signals and vesicle exocytosis (by means of FM4-64) in *Drosophila* brain slices. According to the results found in this thesis, different Ca^{2+} pathways appear to interact in order to cooperatively regulate vesicle exocytosis at the lamina. Strikingly, these pathways seem to be interconnected and regulated by Ca^{2+}. In summary, the key factors identified in this thesis to participate in vesicle exocytosis at the lamina are the following: external Ca^{2+} influx through Cacophony VGCC, Ca^{2+} release from intracellular reservoirs, TRP/TRPL channels, probably functioning as SOCs and PLC activity.

6.2.1 Voltage-dependent Ca^{2+} influx and vesicle exocytosis in *Drosophila* lamina

In *wt* slices, Ca^{2+} influx into the terminals and vesicle exocytosis was induced by depolarization with high K^+ saline (Figs. 14A, 15A). The specific Cacophony channel toxin PLTX-II significantly reduced depolarization-induced Ca^{2+} influx and vesicle exocytosis in photoreceptor axonal projections and terminals at the lamina (Fig. 15B). However, neither of these two processes was completely abolished. This observation suggests that although Cacophony channels are essential for a normal vesicle exocytosis, a second pathway may also contribute to supply the Ca^{2+} requirements for exocytosis in the lamina. In the same way, application of high K^+ in 0 external Ca^{2+} in *wt* slices strongly reduced, but did not abolish, exocytic activity in the lamina (Fig. 15B). Under these conditions, vesicle loading was comparable to that observed after Cacophony

6.2.2 TRP/TRPL-dependent Ca^{2+} influx and vesicle exocytosis in *Drosophila* lamina

As discussed in section 6.2.1, in *wt* slices, Ca^{2+} influx into the terminals and vesicle exocytosis was induced by depolarization with high K^+ saline. However, activity-dependent FM4-64 loading induced by high K^+ treatment in $trp^{343};trpl^{302}$ mutants, was considerably lower than in *wt* (Figs. 14A-B, 15A). These results indicate that in the absence of TRP and TRPL, depolarization-induced exocytosis is dramatically altered. It is notable that in $trp^{343};trpl^{302}$ double mutants it was still possible to observe depolarization-induced Ca^{2+} signals (Fig. 12). This observation suggests that Ca^{2+} influx through Cacophony VGCC is not altered in the absence of TRP and TRPL channels. In fact, vesicle exocytosis is decreased to the same extent by blockade of Cacophony channels, removal of extracellular Ca^{2+} or by the absence of TRP/TRPL channels (Fig. 15A-B). One plausible explanation for this observation is that Ca^{2+} influx through VGCCs may act as a trigger for further Ca^{2+} amplification by a process that requires normal TRP/TRPL activity. As it will be discussed later (section 6.2.4) such mechanism may involve Ca^{2+} release from intracellular stores and TRP/TRPL channels operating as SOCs.

Vesicle exocytosis in $trp^{343};trpl^{302}$ double mutants was induced by the Ca^{2+} ionophore, A-23187 (Fig. 14D). This indicates that the exocytic deficiency of this mutant is not the product of a morphological defect, but it rather reflects a physiological impairment. Consistent with this observation, retinal degeneration evaluated in a series of electron micrographs in this mutant (Hiesinger *et al.*, 2006) revealed a normal synaptic morphology (both in the number of SV as well as in the number of contacts per terminal) and axon projections into the lamina and medulla. Furthermore, development

of *Drosophila* visual connectivity is complete at about 50% of pupal life, prior to the expression of rhodopsin at 78% (Kumar & Ready, 1995), suggesting that R1–R6 sorting is independent of light-evoked activity in the photoreceptors. These evidence highlight that the nominal neurotransmitter release observed in $trp^{343};trpl^{302}$ mutants is not due to morphological defects.

The significant contribution of TRP/TRPL channels to neurotransmitter release raises the question concerning the gating mechanism of these channels in the lamina. In the rhabdomere, diverse PUFAs such as LNA, have been shown to activate TRP and TRPL channels by an unknown mechanism that might involve direct gating or changes in the physicochemical properties of the plasma membrane (Chyb *et al.*, 1999; Delgado & Bacigalupo, 2009). In *wt Drosophila* slices, local application of this lipid induced Ca^{2+} influx into photoreceptor terminals at the lamina (Fig. 10D-E). In $trp^{343};trpl^{302}$ double mutants this effect was not observed, suggesting that the Ca^{2+} influx induced by LNA at the lamina might be carried by TRP and TRPL channels. These results show that laminar TRP and TRPL might be subjected to lipid modulation, resembling their rhabdomeric counterparts. Moreover, this observation suggests that the PLC_{β} signalling pathway might be involved in TRP/TRPL channel activation in the lamina.

6.2.3 PLC_{β}-dependent Ca^{2+} influx and vesicle exocytosis in *Drosophila* lamina

The enzymatic products of PLC_{β} activity are the second messenger molecules DAG and IP_3. The former stays inside the plasma membrane, while IP_3 is a soluble ligand that activates IP_3R on the ER membrane. Opening of these Ca^{2+} permeant

receptors results in an increase in cytoplasmic Ca^{2+}, which activates RyR by Ca^{2+}-induced Ca^{2+} release (CICR), enhancing Ca^{2+} signals (Ferris & Snyder, 1992).

The relevance of PLC activity in depolarization-induced exocytosis in the lamina was confirmed in PLC_β hypomorphic mutants (*norpA*^{p24}). Since null PLC_β mutants are not viable, *norpA*^{p24} flies preserving between 5-10% of normal PLC_β activity were used (www.flybase.org). In these mutants, depolarization-induced bouton labelling was significantly reduced, to approximately 30%, of *wt* values, suggesting an essential role of PLC in vesicle exocytosis in the lamina (Fig. 15D). Application of the PLC activator, *m*-3m3FBS, in *wt Drosophila* slices induced Ca^{2+} signals and vesicle exocytosis at the lamina, consistent with a role of this enzyme in this process (Figs. 11, 14E, 15C). In 0 Ca^{2+} ES, this value was significantly reduced, indicating that vesicle exocytosis induced by PLC_β activation in part relies on extracellular Ca^{2+} in the lamina. However, exocytosis still remained in these conditions, suggesting a contribution from intracellular stores.

While the results of experiments with *m*-3m3FBS are suggestive, there are reasons to be cautious in their interpretation at a quantitative level of analysis. This issue emerged from the results obtained upon application of this drug in PLC_β hypomorphic mutants. As expected, bouton labelling in response to *m*-3m3FBS treatment was reduced in *norpA*^{p24} mutants compared to *wt* flies. However, substantial labelling was still observed and this signal was similar to that induced by the drug in Ca^{2+}-free ES, suggesting that the remaining effect was mediated by intracellular Ca^{2+} (Fig. 15D).

These observations may be explained by two different possibilities:

1) Residual PLC activity in the hypomorphic mutants may be sufficient to trigger intracellular Ca^{2+} release through IP_3R, which can be potentiated by CICR.
2) PLC-independent side effects previously reported for *m*-3m3FBS involving Ca^{2+} release from intracellular reservoirs.

While it seems unlikely that the low PLC_β activity preserved in these flies could account for the substantial SV release remaining, the second proposal is based on previous reports regarding unspecific Ca^{2+} mobilization from intracellular stores (including mitochondria and ER) induced by *m*-3m3FBS (Bae *et al.*, 2003; Krjukova *et al.*, 2004). Although the exact mechanism underlying this unspecific effect has not been identified, the possibility that this substantial contribution to SV release would be present in every experiment performed with this drug, makes it difficult to interpret results in a quantitative way. In fact, the same effect may give an explanation for the unexpectedly high vesicle exocytosis observed in $trp^{343};trpl^{302}$ double mutants after *m*-3m3FBS treatment in normal external Ca^{2+} (Figs. 14E, 15C). For this reason, these experiments must be carefully interpreted. However,it is important to remark that, the experiments performed with this compound in $trp^{343};trpl^{302}$ constitute further evidence to rule out the possibility that the terminals are degenerated in this mutant.

It is also remarkable that the experiments in $norpA^{P24}$ mutants show that the PLC-dependent vesicle exocytosis requires extracellular Ca^{2+}.. In addition, a secondary PLC-dependent pathway involving Ca^{2+} release from intracellular stores cannot be ruled out as a mechanism to induce exocytosis in the lamina. As a result of PLC activation, IP_3

may induce intracellular release of this ion from the ER through IP_3R. In this case, Ca^{2+} release from intracellular reservoirs might be additionally potentiated by Ca^{2+}-induced Ca^{2+} release (CICR) from Ry sensitive stores in the ER.

6.2.4 Extracellular and intracellular Ca^{2+} is required for normal vesicle exocytosis in *Drosophila* lamina

In *Drosophila* photoreceptors Ca^{2+} stores play a controversial but essential role in the photoresponse (Hardie, 1996). Receptors for both IP_3 and Ry have been reported in the retina, lamina and medulla (Hasan & Rosbash, 1992; Yoshikawa *et al.*, 1992; Hardie, 1996; Vazquez-Martinez *et al.*, 2003). Inhibition of IP_3R by heparin or depletion of Ry stores blocks the voltage signals in photoreceptor axons, indicating that internal Ca^{2+} stores are required in *Drosophila* vision (Hasan & Rosbash, 1992; Arnon *et al.*, 1997). It has been proposed that release of Ca^{2+} from the IP_3-sensitive stores triggers CICR from Ry-sensitive stores, resulting in amplification of the light-induced current in photoreceptors (Arnon *et al.*, 1997). While diverse evidence have ruled out a substantial role of IP_3R in phototransduction, the role of intracellular reservoirs in the subsequent signal processing remains highly controversial. The initial activation of the light-dependent conductance is induced by a very rapid mechanism independent of the stores, while the sustained response may involve the internal stores (Montell, 1997). The IP_3-sensitive Ca^{2+} stores have been proposed to mediate sustained cation influx for an extended duration.

The FM4-64 optical imaging experiments in *Drosophila* lamina were done under sustained stimulation (minutes), either with high K^+ or the PLC activator, implying that

vesicle exocytosis might have reached a steady state. Under these conditions, it is reasonable to propose that Ca^{2+} influx through VGCC is complemented by intracellular release of this ion from internal reservoirs in order to sustain high rates of vesicle exocytosis in the lamina.

In order to asses a possible contribution to SV exocytosis of Ca^{2+} released from intracellular Ca^{2+} stores, exocytosis was scrutinized under Ca^{2+}-depleted store conditions in the lamina. In *wt* slices, acute store depletion (caused by Thg + Ry treatment in normal extracellular Ca^{2+}) reduced KCl-induced vesicle exocytosis by approximately 50% (Fig. 15E). This is indicative of an important role of intracellular Ca^{2+} reservoirs in depolarization-induced exocytosis and suggests that extracellular Ca^{2+} influx and intracellular Ca^{2+} release contribute similarly to this process. When release is stimulated by *m*-3m3FBS in depleted store conditions, there is also a 50% reduction in signal. Such reduction may reflect removal of unspecific effect (that depends on internal reservoirs), plus a possible contribution of IP_3 receptor-dependent Ca^{2+} increase. Importantly, in Ca^{2+}-depleted stores and extracellular Ca^{2+}-free conditions, application of *m*-3m3FBS did not induce vesicle exocytosis, highlighting the contribution of a PLC-dependent Ca^{2+} influx to the cell. Taken together, these results suggest that vesicle exocytosis at the lamina terminals is supported by both, internal and external Ca^{2+}.

Ca^{2+} release from internal reservoirs in response to depolarization might be stimulated by two complementary pathways. One may be related to PLC activity (whose activation mechanism in the lamina remains elusive), by IP_3-induced Ca^{2+} release through IP_3R on the ER. It is also possible that Ca^{2+} influx into the terminals through Cacophony VGCC is potentiated by Ca^{2+}-induced Ca^{2+} release (CICR) from Ry sensitive

stores in the ER. These interrelated pathways might be activated downstream of Cacophony channels in response to depolarization.

The physiological implications of Ca^{2+} release from presynaptic internal stores in photoreceptor graded synapses might be essential to support a sustained neurotransmitter release. Ca^{2+}-dependent exocytosis in vertebrate rod terminals is strongly regulated by Ca^{2+} release from Ry sensitive stores (Cadetti *et al.*, 2006; Suryanarayanan & Slaughter, 2006). On the other hand, intracellular recordings in *Drosophila* LMC in the lamina (Weckstrom *et al.*, 1995) have revealed that the amplitude of the postsynaptic response is nonlinearly related to the intensity of the light stimuli, related to a presynaptic enhancement of neurotransmitter release. These authors showed that light-adapted photoreceptors exposed to an intense illumination exhibit a presynaptic facilitation that has been related to an IP_3-induced intracellular Ca^{2+} release. Moreover, by intracellular recordings from photoreceptor terminals (Matti Weckstrom, 1992), it has been demonstrated that the presynaptic enhancement (due to intracellular Ca^{2+} release) directly regulates neurotransmitter release. It is noteworthy that these terminals have unique electrical properties not seen in the somata that produce amplified transients typical of transmission in the fly lamina.

6.2.5 Store operated Ca^{2+} entry (SOCE) can induce vesicle exocytosis in *Drosophila* lamina

Assuming that activation of IP_3R in the ER membrane causes transient Ca^{2+}-release from internal stores in this organelle, we propose that a more sustained plasma

membrane Ca^{2+} conductance is activated by depletion of Ca^{2+} from these stores (SOCE), which may correspond to TRP/TRPL in *Drosophila* photoreceptor axons.

An increasing number of mammalian TRP homologues, such as TRPC 1, 2, 4 and 6, specially TRPC1, are implied in SOCE in a diversity of cell types (Itagaki *et al.*, 2009; Pani *et al.*, 2009). In these reports, TRPCs channels were shown to form structural and functional complexes with the two main SOCE proteins, namely STIM1 and Orai1. These proteins are the Ca^{2+} sensor and Ca^{2+} channel, respectively (Soboloff *et al.*, 2006). STIM1 is thought to sense the Ca^{2+} loading state of the ER stores and interact with plasma membrane store-operated TRPC and/or Orai channels (Worley *et al.*, 2007). TRPC1 forms functional SOCs when coexpressed with STIM1 (Liao *et al.*, 2007; Yuan *et al.*, 2007) and SOCE is clearly compromised in TRPC1 knockout animals (Liu *et al.*, 2007b). In addition, these functional SOCs have been found in signalling microdomains enriched in lipid rafts and caveolae in the plasma membrane of human glandular cells (Pani & Singh, 2009). These molecular interactions are important for SOC regulation and distribution. However, the molecular mechanism that regulates channel activity and protein assembly in these SOC complexes remains elusive.

In the *Drosophila* genome, there is one gene coding for Stim1 and one for Orai1 (www.flybase.org). Although SOC regulation of TRP and TRPL channels has been a matter of intense debate, heterologously expressed TRP and TRPL channels exhibit SOC activity that can be gated by Thg-induced store depletion (Vaca *et al.*, 1994; Sinkins *et al.*, 1996; Xu *et al.*, 1997).

A "Ca^{2+} depletion protocol" is commonly used to identify SOCE by depleting ER stores in Ca^{2+}-free solutions followed by re-exposure of cells to normal Ca^{2+} ES (Bird *et*

al., 2008). In case of a SOCE mechanism, a Ca^{2+} transient signal is observed upon restoring normal Ca^{2+} inside the ER. This protocol was applied to *Drosophila* slices in order to assess whether SOCE can support exocytosis at the lamina, in the absence of depolarizing stimulation. Optical imaging revealed Ca^{2+} signals and vesicle exocytosis when normal ES was applied under store-depleted conditions (Fig. 15F, 16). It is remarkable that in the absence of any other stimulus, Ca^{2+} entry by means of a SOCE mechanism appears to be capable of supporting significant vesicle exocytosis and Ca^{2+} signals at the lamina in *wt* slices. Although the number of labelled boutons under such conditions is smaller than under KCl depolarization (in normal ES), it is significantly higher than basal release. In $trp^{343};trpl^{302}$ flies Ca^{2+} signals and exocytosis elicited by the "Ca^{2+} depletion protocol" was negligible and not different from basal vesicle exocytosis. These results indicate that TRP and TRPL channels are involved in the observed SOCE and that this mechanism is sufficient to partially support detectable vesicle exocytosis. According to these observations, TRP and TRPL channels would be essential for ER replenishment after high levels of stimulation. Therefore, vesicle exocytosis in $trp^{343};trpl^{302}$ double mutants could be highly impaired due to irreversible ER Ca^{2+} depletion.

An interesting question to resolve, concerns TRP and TRPL location within the axonal projections in the lamina. If these channels behave as SOC in photoreceptor synaptic terminals, they might be coupling the plasma and ER membranes. Therefore, it might be expected to find them in the plasma membrane in proximity to this organelle. Further work is necessary to precisely determine their allocation.

In other cell systems, functional SOCs channels have been found in the plasma membrane within microdomains enriched in lipid rafts and caveolae (Pani & Singh, 2009). In *Drosophila*, TRP channel coupling to plasma and ER membranes may involve a cluster of other proteins that might be implicated in regulating channel gating. The signalling proteins such as PKC might regulate PLC activity and therefore, to modulate Ca^{2+} release from intracellular reservoirs.

In the rhabdomere, TRP channel anchoring by the scaffolding InaD is required for retention of the signalplex in photoreceptors (Li & Montell, 2000). It has also been reported that SOC activity in heterologously expressed TRP channels is suppressed by coexpression with InaD (Harteneck *et al.*, 2002). This observation is consistent with the scarce InaD abundance found in the lamina (Figs. 7D, 8B-C). If InaD is effectively clustering TRP channels in SOC complexes in the lamina, it might be expected that TRP channels would be in mayor proportion than InaD. By this subtle regulation, the SOC activity of TRPs in the lamina may not be inhibited by InaD.

6.3 Role of TRPC1 and intracellular Ca^{2+} in neurotransmitter release at vertebrate photoreceptors ribbon synapses

Visual perception in diurnal animals is constrained by the sensitivity and operating range of retinal photoreceptors (Szikra *et al.*, 2009). In vertebrate cones, light-evoked signals are regulated by two different mechanisms that control the input and output gain respectively: the phototransduction pathway and the release rate of SV at the synaptic terminals. Tonic synapses are specialized for sustained Ca^{2+} entry and transmitter release, allowing them to operate in a graded fashion over a wide dynamic

range. The output range of rods and cones is wider than voltage-operated calcium entry, which is determined by the threshold for channel activation, suggesting that other Ca^{2+} influx mechanism operates in addition to VGCCs. Closure of cone L-type channels appears to be complete as cells hyperpolarize beyond -50 mV (Maricq & Korenbrot, 1988) however cone synapses continue to transmit at hyperpolarized membrane potentials closer to -70 mV (Vessey *et al.*, 2005; Szikra *et al.*, 2009). At membrane potentials beyond the activation threshold of VGCC, Ca^{2+} influx may reach saturation. A novel plasma membrane mechanism that exhibits the molecular and physiological characteristics of SOCE has been reported to modulate Ca^{2+} homeostasis and light-evoked neurotransmission in rods and cones (Szikra *et al.*, 2008; Szikra *et al.*, 2009). This voltage-independent Ca^{2+} influx pathway is mediated by TRPC1 channels and is activated in light-adapted, strongly hyperpolarized cells. This supported by recent studies documenting the essential role for Ca^{2+} stores at low light levels at which Ca^{2+} release is indispensable for maintaining exocytosis in vertebrate rods (Cadetti *et al.*, 2006; Suryanarayanan & Slaughter, 2006). Pharmacological suppression of voltage-operated Ca^{2+} entry in cones and rods leaves a component of Ca^{2+} entry that is mediated by intracellular reservoirs. This Ca^{2+} influx was potentiated by strong hyperpolarization and depolarization, facilitated by depletion of intracellular Ca^{2+} stores and suppressed by SOC inhibitors. SOC represent a main Ca^{2+} entry pathway in non-excitable cells (Parekh, 2006) and have been increasingly identified as contributors to neuronal Ca^{2+} homeostasis in excitable cells, such as vertebrate photoreceptors (Borges *et al.*, 2008; Szikra *et al.*, 2008) and sensory cells of the dorsal root ganglia (Usachev & Thayer, 1999).

In vertebrate photoreceptors, the "Ca^{2+} depletion protocol" induces Ca^{2+} overshoots in depolarized cells that are comparable in amplitude to overshoots measured in hyperpolarized cells (Szikra *et al.*, 2008), suggesting that SOCE can be activated across the operating range of cone function. The authors show that store depletion and the subsequent Ca^{2+} influx directly stimulate exocytosis in rods terminals and modulate sustained release. Similarly, a previous capacitance study in chromaffin cells directly demonstrated that SOCE plays a significant role in exocytosis (Fomina & Nowycky, 1999).

Pharmacological suppression of the SOCE produces a dramatic reduction (50%) on the slow and sustained component of evoked EPSCs in postsynaptic horizontal basal cells, while the initial fast burst was not affected. This component is associated with a fast depletion of the presynaptic vesicle pool induced by voltage-operated Ca^{2+} entry at the ribbon or Ca^{2+} release from Ry sensitive stores (Cadetti *et al.*, 2006; Suryanarayanan & Slaughter, 2006). In addition, the time-course of depletion-dependent $[Ca^{2+}]i$ changes in cones is significantly slower than voltage-dependent raises (Szikra *et al.*, 2009). Moreover, the authors noted that the amplitude and kinetics of SOCE responses were much more variable than the conserved responses of voltage-operated Ca^{2+} channels, suggesting that SOCE is susceptible to modulation by intracellular signalling cascades.

Both TRPC and Orai channels are regulated by STIM1 (Soboloff et al. 2006; Yuan et al. 2007) and it is possible that SOCE in rods is regulated by coactivation of endogenous Orai1, STIM1 and TRPC1 protein complexes (Ong *et al.*, 2007; Cheng *et al.*, 2008). TRPC1 represents a signalling element in communication between Ca^{2+}

stores and the plasma membrane, however the mechanism whereby rod ER stores interact with TRPC1 channels remains elusive.

6.4 Model for Ca^{2+} and neurotransmitter release regulation in *Drosophila* photoreceptor ribbon synapses

The present study proposes a novel Ca^{2+} influx pathway for neurotransmitter release in *Drosophila* photoreceptors mediated by TRP and TRPL and activated by depletion of intracellular Ca^{2+} stores. The physiological implication of the presence of these channels in lamina synapses is related to Ca^{2+} refilling of intracellular reservoirs when they are depleted. Ca^{2+} influx through presynaptic SOCs may increase presynaptic $[Ca^{2+}]i$ and refill internal stores at high light levels, when activation of IP_3R and/or CICR has caused store depletion and can no longer potentiate Ca^{2+} influx through Cacophony channels. It is reasonable to propose (as in vertebrate photoreceptors) (Szikra *et al.*, 2008; Szikra *et al.*, 2009) that the initial burst of vesicle exocytosis evoked by strong depolarization may be controlled by the opening of Cacophony channels, while sustained transmitter release would be maintained by internal Ca^{2+} stores. This intracellular pathway might be essential to modulate neurotransmitter release at the photoreceptors synapse and may play a central role in tonic signalling. Following a regime of high rate of vesicle exocytosis, this activity may be indispensable to sustain exocytosis in the lamina.

The model is as follows: low levels of light stimulation (or depolarization) would trigger Ca^{2+} influx through Cacophony VGCC. At higher levels of stimulation, Ca^{2+} influx may trigger CICR from RyR in the ER. PLC activity (see below) could also

contribute to Ca^{2+} release by an IP_3R-dependent process. Under prolonged high stimulation this process would lead to store depletion, stimulating TRP/TRPL-mediated SOCE. In addition, TRP/TRPL channel function might also be regulated by the PLC-associated cascade (Fig. 17).

An open question concerns PLC_β activation in the lamina. Activation of PLC by micromolar Ca^{2+} has been reported for many tissues and cell types (Eberhard & Holz, 1988; Guillon *et al.*, 1992). In *Drosophila* photoreceptors, a high level of basal PLC activity has been reported in diverse biochemical and *in vivo* experiments (Ferreira *et al.*, 1993; Running Deer *et al.*, 1995; Willars *et al.*, 1998; Hardie *et al.*, 2004). PLC activity is stimulated by incrementing free Ca^{2+} from 10 nM to 1 μM (Running Deer *et al.*, 1995). PLC activity is maximal at 1 μM free Ca^{2+}, and at these levels it is not sensitive to light. These authors report that PLC regulation by G-protein depends on the substrate environment, as high levels of PLC activity are achievable independently of light and G-protein. Ca^{2+} dependence of PLC activity in *Drosophila* heads is consistent with a positive feedback model of PLC activation in which light-induced Ca^{2+} mobilization accelerates the response to light. In the lamina, basal PLC activity may be incremented by cytosolic Ca^{2+} influx through Cacophony.

A novel protein named rolling blackout (RBO) has recently been implicated in PLC regulation (Huang *et al.*, 2004). RBO is a DAG lipase enriched in the nervous system, where it is restricted to neuropiles and sensory neurons, including photoreceptors. RBO presents a strong signal in the lamina.

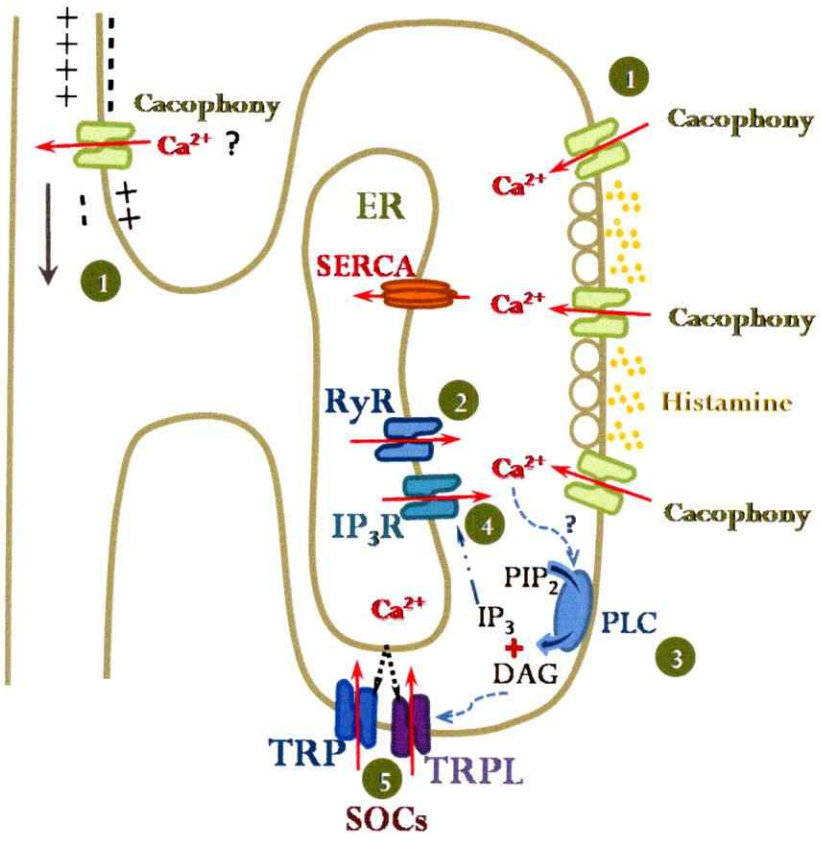

Figure 17. Model for neurotransmitter release in *Drosophila* photoreceptors.
Depolarization propagates from the soma to the axon terminals by an unidentified mechanism (probably by Cacophony channels). In the terminals, depolarization-induced Ca^{2+} influx through Cacophony channels (1) is potentiated by CICR from RyR in the ER (2). PLC activation (3) produces further Ca^{2+} amplification by IP_3, which activates Ca^{2+} efflux from the ER (4). Under a prolonged period of activity, sustained Ca^{2+} efflux from the ER would decrease the stores content of this ion. This would cause the opening of the SOCs TRP and TRPL (5), allowing the ER to restore its Ca^{2+} content. PLC may also regulate TRP/TRPL channels by DAG pathway.

Null *rbo* mutants are embryonically lethal, and temperature-sensitive *rbo* mutants show a complete blockade of phototransduction. The accumulation of PIP-PIP_2 and depletion of DAG after conditional blockade of RBO function suggest that RBO is required for PLC activity. Interestingly, RBO is localized to presynaptic boutons and is essential for neurotransmission in *Drosophila* neuromuscular junction (NMJ). At restrictive temperature, *rbo* mutants display a complete, reversible block of synaptic transmission and accumulate docked SV at the presynaptic active zone (Vijayakrishnan & Broadie, 2006). This acute role in exocytosis is related to SV priming and fusion in a syntaxin-dependent mechanism.

The results obtained in this thesis provide novel evidence for TRP/TRPL channel function in *Drosophila* photoreceptors. For the first time, we show that these paradigmatic channels have different functions and are activated by distinct mechanisms in the same cell depending on their location. In the rhabdomere they participate in phototransduction and function as lipid-modulated channels, but in the synaptic terminal they may be store-operated channels. We utilized a variety of genetic and fluorescence tools on a novel *Drosophila* slice preparation to describe the molecular mechanism of synaptic vesicle release, for which we propose a specific model. Further investigation is required to elucidate PLC activation in the lamina. However, the novel intracellular Ca^{2+} signalling pathway described in this work may give some lights for understanding presynaptic regulation of information flow in graded synapses.

7. CONCLUSIONS

1. VGCCs, TRP and TRPL channels are present in photoreceptors axonal projections in the lamina and medulla.
2. G_q-protein, PLC and PKC (but not rhodopsin) are present in photoreceptors axonal projections, in the lamina. The scaffolding protein InaD is scarcely found in these axons.
3. VGCC, TRP, TRPL channels and PLC_β are required for Ca^{2+} influx and a normal vesicle exocytosis in the lamina.
4. Ca^{2+} entry (Cacophony, TRP and TRPL) and release from internal reservoirs support vesicle exocytosis in the lamina.
5. TRP/TRPL appear to function as SOCs in the lamina and play an essential role in Ca^{2+} refilling of internal stores.

6. REFERENCES

Acharya JK, Jalink K, Hardy RW, Hartenstein V & Zuker CS. (1997). InsP3 receptor is essential for growth and differentiation but not for vision in Drosophila. *Neuron* **18,** 881-887.

Arnon A, Cook B, Montell C, Selinger Z & Minke B. (1997). Calmodulin regulation of calcium stores in phototransduction of Drosophila. *Science* **275,** 1119-1121.

Bae YS, Lee TG, Park JC, Hur JH, Kim Y, Heo K, Kwak JY, Suh PG & Ryu SH. (2003). Identification of a compound that directly stimulates phospholipase C activity. *Mol Pharmacol* **63,** 1043-1050.

Bahner M, Frechter S, Da Silva N, Minke B, Paulsen R & Huber A. (2002). Light-regulated subcellular translocation of Drosophila TRPL channels induces long-term adaptation and modifies the light-induced current. *Neuron* **34,** 83-93.

Betz WJ & Bewick GS. (1992). Optical analysis of synaptic vesicle recycling at the frog neuromuscular junction. *Science* **255,** 200-203.

Bird GS, DeHaven WI, Smyth JT & Putney JW, Jr. (2008). Methods for studying store-operated calcium entry. *Methods* **46,** 204-212.

Bloomquist BT, Shortridge RD, Schneuwly S, Perdew M, Montell C, Steller H, Rubin G & Pak WL. (1988). Isolation of a putative phospholipase C gene of Drosophila, norpA, and its role in phototransduction. In *Cell*, 1988/08/26 edn, pp. 723-733.

Borges S, Lindstrom S, Walters C, Warrier A & Wilson M. (2008). Discrete influx events refill depleted Ca2+ stores in a chick retinal neuron. *J Physiol* **586,** 605-626.

Cadetti L, Bryson EJ, Ciccone CA, Rabl K & Thoreson WB. (2006). Calcium-induced calcium release in rod photoreceptor terminals boosts synaptic transmission during maintained depolarization. *Eur J Neurosci* **23,** 2983-2990.

Catterall WA. (2000). Structure and regulation of voltage-gated Ca2+ channels. *Annu Rev Cell Dev Biol* **16,** 521-555.

Cosens DJ & Manning A. (1969). Abnormal electroretinogram from a Drosophila mutant. *Nature* **224,** 285-287.

Costes SV, Daelemans D, Cho EH, Dobbin Z, Pavlakis G & Lockett S. (2004). Automatic and quantitative measurement of protein-protein colocalization in live cells. *Biophys J* **86,** 3993-4003.

Cronin MA, Lieu MH & Tsunoda S. (2006). Two stages of light-dependent TRPL-channel translocation in Drosophila photoreceptors. *J Cell Sci* **119,** 2935-2944.

Cheng KT, Liu X, Ong HL & Ambudkar IS. (2008). Functional requirement for Orai1 in store-operated TRPC1-STIM1 channels. *J Biol Chem* **283,** 12935-12940.

Chevesich J, Kreuz AJ & Montell C. (1997). Requirement for the PDZ domain protein, INAD, for localization of the TRP store-operated channel to a signaling complex. *Neuron* **18,** 95-105.

Chyb S, Raghu P & Hardie RC. (1999). Polyunsaturated fatty acids activate the Drosophila light-sensitive channels TRP and TRPL. *Nature* **397,** 255-259.

De Petrocellis L & Di Marzo V. (2009). Role of endocannabinoids and endovanilloids in Ca2+ signalling. *Cell Calcium* **45,** 611-624.

Delgado R & Bacigalupo J. (2009). Unitary recordings of TRP and TRPL channels from isolated Drosophila retinal photoreceptor rhabdomeres: activation by light and lipids. *J Neurophysiol* **101,** 2372-2379.

Eberhard DA & Holz RW. (1988). Intracellular Ca2+ activates phospholipase C. *Trends Neurosci* **11,** 517-520.

Eberl DF, Ren D, Feng G, Lorenz LJ, Van Vactor D & Hall LM. (1998). Genetic and developmental characterization of Dmca1D, a calcium channel alpha1 subunit gene in Drosophila melanogaster. *Genetics* **148,** 1159-1169.

Espinosa A, Garcia A, Hartel S, Hidalgo C & Jaimovich E. (2009). NADPH oxidase and hydrogen peroxide mediate insulin-induced calcium increase in skeletal muscle cells. *J Biol Chem* **284,** 2568-2575.

Ferreira PA, Shortridge RD & Pak WL. (1993). Distinctive subtypes of bovine phospholipase C that have preferential expression in the retina and high homology to the norpA gene product of Drosophila. *Proc Natl Acad Sci U S A* **90,** 6042-6046.

Ferris CD & Snyder SH. (1992). IP3 receptors. Ligand-activated calcium channels in multiple forms. *Adv Second Messenger Phosphoprotein Res* **26,** 95-107.

Fomina AF & Nowycky MC. (1999). A current activated on depletion of intracellular Ca2+ stores can regulate exocytosis in adrenal chromaffin cells. *J Neurosci* **19,** 3711-3722.

Gaffield MA & Betz WJ. (2006). Imaging synaptic vesicle exocytosis and endocytosis with FM dyes. *Nat Protoc* **1,** 2916-2921.

Gengs C, Leung HT, Skingsley DR, Iovchev MI, Yin Z, Semenov EP, Burg MG, Hardie RC & Pak WL. (2002). The target of Drosophila photoreceptor synaptic transmission is a histamine-gated chloride channel encoded by ort (hclA). *J Biol Chem* **277,** 42113-42120.

Gillo B, Chorna I, Cohen H, Cook B, Manistersky I, Chorev M, Arnon A, Pollock JA, Selinger Z & Minke B. (1996). Coexpression of Drosophila TRP and TRP-like proteins in Xenopus oocytes reconstitutes capacitative Ca^{2+} entry. *Proc Natl Acad Sci U S A* **93,** 14146-14151.

Greenspan RJ. (2007). An introduction to nervous systems. Cold Spring Harbour Laboratory Press.

Gu Y, Oberwinkler J, Postma M & Hardie RC. (2005). Mechanisms of light adaptation in Drosophila photoreceptors. *Curr Biol* **15,** 1228-1234.

Guillon G, Mouillac B & Savage AL. (1992). Modulation of hormone-sensitive phospholipase C. *Cell Signal* **4,** 11-23.

Hardie RC. (1989). A histamine-activated chloride channel involved in neurotransmission at a photoreceptor synapse. *Nature* **339,** 704-706.

Hardie RC. (1996). Excitation of Drosophila photoreceptors by BAPTA and ionomycin: evidence for capacitative Ca2+ entry? *Cell Calcium* **20,** 315-327.

Hardie RC, Gu Y, Martin F, Sweeney ST & Raghu P. (2004). In vivo light-induced and basal phospholipase C activity in Drosophila photoreceptors measured with genetically targeted phosphatidylinositol 4,5-bisphosphate-sensitive ion channels (Kir2.1). *J Biol Chem* **279,** 47773-47782.

Hardie RC, Martin F, Cochrane GW, Juusola M, Georgiev P & Raghu P. (2002). Molecular basis of amplification in Drosophila phototransduction: roles for G protein, phospholipase C, and diacylglycerol kinase. *Neuron* **36,** 689-701.

Hardie RC & Minke B. (1992). The trp gene is essential for a light-activated Ca2+ channel in Drosophila photoreceptors. *Neuron* **8,** 643-651.

Hardie RC, Peretz A, Suss-Toby E, Rom-Glas A, Bishop SA, Selinger Z & Minke B. (1993). Protein kinase C is required for light adaptation in Drosophila photoreceptors. *Nature* **363,** 634-637.

Harteneck C, Kuchta SN, Huber A, Paulsen R & Schultz G. (2002). The PDZ scaffold protein INAD abolishes apparent store-dependent regulation of the light-activated cation channel TRP. *FASEB J* **16,** 1668-1670.

Harteneck C, Plant TD & Schultz G. (2000). From worm to man: three subfamilies of TRP channels. *Trends Neurosci* **23,** 159-166.

Hasan G & Rosbash M. (1992). Drosophila homologs of two mammalian intracellular Ca(2+)-release channels: identification and expression patterns of the inositol 1,4,5-triphosphate and the ryanodine receptor genes. *Development* **116,** 967-975.

Hiesinger PR, Zhai RG, Zhou Y, Koh TW, Mehta SQ, Schulze KL, Cao Y, Verstreken P, Clandinin TR, Fischbach KF, Meinertzhagen IA & Bellen HJ. (2006). Activity-independent prespecification of synaptic partners in the visual map of Drosophila. *Curr Biol* **16,** 1835-1843.

Huang FD, Matthies HJ, Speese SD, Smith MA & Broadie K. (2004). Rolling blackout, a newly identified PIP2-DAG pathway lipase required for Drosophila phototransduction. *Nat Neurosci* **7,** 1070-1078.

Itagaki K, Barton BE, Murphy TF, Taheri S, Shu P, Huang H & Jordan ML. (2009). Eicosanoid-Induced Store-Operated Calcium Entry in Dendritic Cells. *J Surg Res.*

Jiang CY, Fujita T, Yue HY, Piao LH, Liu T, Nakatsuka T & Kumamoto E. (2009). Effect of resiniferatoxin on glutamatergic spontaneous excitatory synaptic transmission in substantia gelatinosa neurons of the adult rat spinal cord. *Neuroscience* **164,** 1833-1844.

Juusola M, French AS, Uusitalo RO & Weckstrom M. (1996). Information processing by graded-potential transmission through tonically active synapses. *Trends Neurosci* **19,** 292-297.

Juusola M, Uusitalo RO & Weckstrom M. (1995). Transfer of graded potentials at the photoreceptor-interneuron synapse. *J Gen Physiol* **105,** 117-148.

Kedei N, Szabo T, Lile JD, Treanor JJ, Olah Z, Iadarola MJ & Blumberg PM. (2001). Analysis of the native quaternary structure of vanilloid receptor 1. *J Biol Chem* **276,** 28613-28619.

Kim YH, Park CK, Back SK, Lee CJ, Hwang SJ, Bae YC, Na HS, Kim JS, Jung SJ & Oh SB. (2009). Membrane-delimited coupling of TRPV1 and mGluR5 on presynaptic terminals of nociceptive neurons. *J Neurosci* **29,** 10000-10009.

Kosugi M, Nakatsuka T, Fujita T, Kuroda Y & Kumamoto E. (2007). Activation of TRPA1 channel facilitates excitatory synaptic transmission in substantia gelatinosa neurons of the adult rat spinal cord. *J Neurosci* **27,** 4443-4451.

Krjukova J, Holmqvist T, Danis AS, Akerman KE & Kukkonen JP. (2004). Phospholipase C activator m-3M3FBS affects Ca2+ homeostasis independently of phospholipase C activation. *Br J Pharmacol* **143,** 3-7.

Kumar JP & Ready DF. (1995). Rhodopsin plays an essential structural role in Drosophila photoreceptor development. *Development* **121,** 4359-4370.

Kuzhikandathil EV, Wang H, Szabo T, Morozova N, Blumberg PM & Oxford GS. (2001). Functional analysis of capsaicin receptor (vanilloid receptor subtype 1) multimerization and agonist responsiveness using a dominant negative mutation. *J Neurosci* **21,** 8697-8706.

Lee D & O'Dowd DK. (1999). Fast excitatory synaptic transmission mediated by nicotinic acetylcholine receptors in Drosophila neurons. *J Neurosci* **19,** 5311-5321.

Li HS & Montell C. (2000). TRP and the PDZ protein, INAD, form the core complex required for retention of the signalplex in Drosophila photoreceptor cells. *J Cell Biol* **150,** 1411-1422.

Liao Y, Erxleben C, Yildirim E, Abramowitz J, Armstrong DL & Birnbaumer L. (2007). Orai proteins interact with TRPC channels and confer responsiveness to store depletion. *Proc Natl Acad Sci U S A* **104,** 4682-4687.

Liu CH, Wang T, Postma M, Obukhov AG, Montell C & Hardie RC. (2007a). In vivo identification and manipulation of the Ca2+ selectivity filter in the Drosophila transient receptor potential channel. *J Neurosci* **27,** 604-615.

Liu X, Cheng KT, Bandyopadhyay BC, Pani B, Dietrich A, Paria BC, Swaim WD, Beech D, Yildrim E, Singh BB, Birnbaumer L & Ambudkar IS. (2007b). Attenuation of store-operated Ca2+ current impairs salivary gland fluid secretion in TRPC1(-/-) mice. *Proc Natl Acad Sci U S A* **104,** 17542-17547.

Maricq AV & Korenbrot JI. (1988). Calcium and calcium-dependent chloride currents generate action potentials in solitary cone photoreceptors. *Neuron* **1,** 503-515.

Matti Weckstrom MJaSBL. (1992). Presynaptic Enhancement of Signal Transients in Photoreceptor Terminals in the Compound Eye. *Proceedings: Biological Sciences* **250,** 83-89

Meinertzhagen IA & O'Neil SD. (1991). Synaptic organization of columnar elements in the lamina of the wild type in Drosophila melanogaster. *J Comp Neurol* **305,** 232-263.

Meyer NE, Joel-Almagor T, Frechter S, Minke B & Huber A. (2006). Subcellular translocation of the eGFP-tagged TRPL channel in Drosophila photoreceptors requires activation of the phototransduction cascade. *J Cell Sci* **119,** 2592-2603.

Michaely P & Bennett V. (1993). The membrane-binding domain of ankyrin contains four independently folded subdomains, each comprised of six ankyrin repeats. *J Biol Chem* **268,** 22703-22709.

Miller R & Ripps H. (2001). Concepts and challenges in retinal biology. A tribute to John E. Dowling. Introduction. *Prog Brain Res* **131,** xxiii-xxix.

Minke B. (1977). Drosophila mutant with a transducer defect. *Biophys Struct Mech* **3,** 59-64.

Minke B & Cook B. (2002). TRP channel proteins and signal transduction. *Physiol Rev* **82,** 429-472.

Montell C. (1997). New light on TRP and TRPL. *Mol Pharmacol* **52,** 755-763.

Montell C, Jones K, Hafen E & Rubin G. (1985). Rescue of the Drosophila phototransduction mutation trp by germline transformation. *Science* **230,** 1040-1043.

Nakai J, Ohkura M & Imoto K. (2001). A high signal-to-noise Ca(2+) probe composed of a single green fluorescent protein. *Nat Biotechnol* **19,** 137-141.

Nash HA, Scott RL, Lear BC & Allada R. (2002). An unusual cation channel mediates photic control of locomotion in Drosophila. *Curr Biol* **12,** 2152-2158.

Niemeyer BA, Suzuki E, Scott K, Jalink K & Zuker CS. (1996). The Drosophila light-activated conductance is composed of the two channels TRP and TRPL. *Cell* **85,** 651-659.

Niven JE, Anderson JC & Laughlin SB. (2007). Fly photoreceptors demonstrate energy-information trade-offs in neural coding. *PLoS Biol* **5,** e116.

Omar Ramírez AG, Rodrigo Rojas, Andrés Couve & Härtel aS. (2010). Confined Displacement Algorithm Determines True and Random Colocalization in Fluorescence Microscopy. *Journal of Microscopy*. In Press.

Ong HL, Cheng KT, Liu X, Bandyopadhyay BC, Paria BC, Soboloff J, Pani B, Gwack Y, Srikanth S, Singh BB, Gill DL & Ambudkar IS. (2007). Dynamic assembly of TRPC1-STIM1-Orai1 ternary complex is involved in store-operated calcium influx. Evidence for similarities in store-operated and calcium release-activated calcium channel components. *J Biol Chem* **282,** 9105-9116.

Pak WL & Leung HT. (2003). Genetic approaches to visual transduction in Drosophila melanogaster. *Receptors Channels* **9,** 149-167.

Pani B, Ong HL, Brazer SC, Liu X, Rauser K, Singh BB & Ambudkar IS. (2009). Activation of TRPC1 by STIM1 in ER-PM microdomains involves release of the channel from its scaffold caveolin-1. *Proc Natl Acad Sci U S A* **106,** 20087-20092.

Pani B & Singh BB. (2009). Lipid rafts/caveolae as microdomains of calcium signaling. *Cell Calcium* **45,** 625-633.

Pantazis A, Segaran A, Liu CH, Nikolaev A, Rister J, Thum AS, Roeder T, Semenov E, Juusola M & Hardie RC. (2008). Distinct roles for two histamine receptors (hclA and hclB) at the Drosophila photoreceptor synapse. *J Neurosci* **28,** 7250-7259.

Parekh AB. (2006). On the activation mechanism of store-operated calcium channels. *Pflugers Arch* **453,** 303-311.

Phillips AM, Bull A & Kelly LE. (1992). Identification of a Drosophila gene encoding a calmodulin-binding protein with homology to the trp phototransduction gene. *Neuron* **8,** 631-642.

Pollock JA, Assaf A, Peretz A, Nichols CD, Mojet MH, Hardie RC & Minke B. (1995). TRP, a protein essential for inositide-mediated Ca2+ influx is localized adjacent to the calcium stores in Drosophila photoreceptors. *J Neurosci* **15,** 3747-3760.

Raghu P, Colley NJ, Webel R, James T, Hasan G, Danin M, Selinger Z & Hardie RC. (2000). Normal phototransduction in Drosophila photoreceptors lacking an InsP(3) receptor gene. *Mol Cell Neurosci* **15,** 429-445.

Reuss H, Mojet MH, Chyb S & Hardie RC. (1997). In vivo analysis of the drosophila light-sensitive channels, TRP and TRPL. *Neuron* **19,** 1249-1259.

Running Deer JL, Hurley JB & Yarfitz SL. (1995). G protein control of Drosophila photoreceptor phospholipase C. *J Biol Chem* **270,** 12623-12628.

Sanchez G, Escobar M, Pedrozo Z, Macho P, Domenech R, Hartel S, Hidalgo C & Donoso P. (2008). Exercise and tachycardia increase NADPH oxidase and ryanodine receptor-2 activity: possible role in cardioprotection. *Cardiovasc Res* **77,** 380-386.

Sedgwick SG & Smerdon SJ. (1999). The ankyrin repeat: a diversity of interactions on a common structural framework. *Trends Biochem Sci* **24,** 311-316.

Sinkins WG, Vaca L, Hu Y, Kunze DL & Schilling WP. (1996). The COOH-terminal domain of Drosophila TRP channels confers thapsigargin sensitivity. *J Biol Chem* **271,** 2955-2960.

Smith DP, Ranganathan R, Hardy RW, Marx J, Tsuchida T & Zuker CS. (1991). Photoreceptor deactivation and retinal degeneration mediated by a photoreceptor-specific protein kinase C. *Science* **254,** 1478-1484.

Smith LA, Wang X, Peixoto AA, Neumann EK, Hall LM & Hall JC. (1996). A Drosophila calcium channel alpha1 subunit gene maps to a genetic locus associated with behavioral and visual defects. *J Neurosci* **16,** 7868-7879.

Soboloff J, Spassova MA, Dziadek MA & Gill DL. (2006). Calcium signals mediated by STIM and Orai proteins--a new paradigm in inter-organelle communication. *Biochim Biophys Acta* **1763,** 1161-1168.

Sun B, Bang SI & Jin YH. (2009). Transient receptor potential A1 increase glutamate release on brain stem neurons. *Neuroreport* **20,** 1002-1006.

Suryanarayanan A & Slaughter MM. (2006). Synaptic transmission mediated by internal calcium stores in rod photoreceptors. *J Neurosci* **26,** 1759-1766.

Szikra T, Barabas P, Bartoletti TM, Huang W, Akopian A, Thoreson WB & Krizaj D. (2009). Calcium homeostasis and cone signaling are regulated by interactions between calcium stores and plasma membrane ion channels. *PLoS One* **4,** e6723.

Szikra T, Cusato K, Thoreson WB, Barabas P, Bartoletti TM & Krizaj D. (2008). Depletion of calcium stores regulates calcium influx and signal transmission in rod photoreceptors. *J Physiol* **586,** 4859-4875.

Takahashi M, Seagar MJ, Jones JF, Reber BF & Catterall WA. (1987). Subunit structure of dihydropyridine-sensitive calcium channels from skeletal muscle. *Proc Natl Acad Sci U S A* **84,** 5478-5482.

Thastrup O, Cullen PJ, Drobak BK, Hanley MR & Dawson AP. (1990). Thapsigargin, a tumor promoter, discharges intracellular Ca2+ stores by specific inhibition of the

endoplasmic reticulum Ca2(+)-ATPase. *Proc Natl Acad Sci U S A* **87,** 2466-2470.

Tominaga M & Caterina MJ. (2004). Thermosensation and pain. *J Neurobiol* **61,** 3-12.

Tsunoda S, Sun Y, Suzuki E & Zuker C. (2001). Independent anchoring and assembly mechanisms of INAD signaling complexes in Drosophila photoreceptors. *J Neurosci* **21,** 150-158.

Usachev YM & Thayer SA. (1999). Ca2+ influx in resting rat sensory neurones that regulates and is regulated by ryanodine-sensitive Ca2+ stores. *J Physiol* **519 Pt 1,** 115-130.

Uusitalo RO, Juusola M, Kouvalainen E & Weckstrom M. (1995a). Tonic transmitter release in a graded potential synapse. *J Neurophysiol* **74,** 470-473.

Uusitalo RO, Juusola M & Weckstrom M. (1995b). Graded responses and spiking properties of identified first-order visual interneurons of the fly compound eye. *J Neurophysiol* **73,** 1782-1792.

Vaca L, Sinkins WG, Hu Y, Kunze DL & Schilling WP. (1994). Activation of recombinant trp by thapsigargin in Sf9 insect cells. *Am J Physiol* **267,** C1501-1505.

Vazquez-Martinez O, Canedo-Merino R, Diaz-Munoz M & Riesgo-Escovar JR. (2003). Biochemical characterization, distribution and phylogenetic analysis of Drosophila melanogaster ryanodine and IP3 receptors, and thapsigargin-sensitive Ca2+ ATPase. *J Cell Sci* **116,** 2483-2494.

Venkatachalam K, Long AA, Elsaesser R, Nikolaeva D, Broadie K & Montell C. (2008). Motor deficit in a Drosophila model of mucolipidosis type IV due to defective clearance of apoptotic cells. *Cell* **135,** 838-851.

Venkatachalam K & Montell C. (2007). TRP channels. *Annu Rev Biochem* **76,** 387-417.

Vessey JP, Stratis AK, Daniels BA, Da Silva N, Jonz MG, Lalonde MR, Baldridge WH & Barnes S. (2005). Proton-mediated feedback inhibition of presynaptic calcium channels at the cone photoreceptor synapse. *J Neurosci* **25,** 4108-4117.

Vijayakrishnan N & Broadie K. (2006). Temperature-sensitive paralytic mutants: insights into the synaptic vesicle cycle. *Biochem Soc Trans* **34,** 81-87.

Weckstrom M, Juusola M, Uusitalo RO & French AS. (1995). Fast-acting compressive and facilitatory nonlinearities in light-adapted fly photoreceptors. *Ann Biomed Eng* **23,** 70-77.

Willars GB, Nahorski SR & Challiss RA. (1998). Differential regulation of muscarinic acetylcholine receptor-sensitive polyphosphoinositide pools and consequences for signaling in human neuroblastoma cells. *J Biol Chem* **273,** 5037-5046.

Wingertzahn MA & Ochs RS. (1998). Control of calcium in skeletal muscle excitation-contraction coupling: implications for malignant hyperthermia. *Mol Genet Metab* **65,** 113-120.

Worley PF, Zeng W, Huang GN, Yuan JP, Kim JY, Lee MG & Muallem S. (2007). TRPC channels as STIM1-regulated store-operated channels. *Cell Calcium* **42,** 205-211.

Wrigley PJ, Jeong HJ & Vaughan CW. (2009). Primary afferents with TRPM8 and TRPA1 profiles target distinct subpopulations of rat superficial dorsal horn neurones. *Br J Pharmacol* **157,** 371-380.

Xu XZ, Chien F, Butler A, Salkoff L & Montell C. (2000). TRPgamma, a drosophila TRP-related subunit, forms a regulated cation channel with TRPL. *Neuron* **26,** 647-657.

Xu XZ, Li HS, Guggino WB & Montell C. (1997). Coassembly of TRP and TRPL produces a distinct store-operated conductance. *cell* **89,** 1155-1164.

Yang K, Kumamoto E, Furue H & Yoshimura M. (1998). Capsaicin facilitates excitatory but not inhibitory synaptic transmission in substantia gelatinosa of the rat spinal cord. *Neurosci Lett* **255,** 135-138.

Yoshikawa S, Tanimura T, Miyawaki A, Nakamura M, Yuzaki M, Furuichi T & Mikoshiba K. (1992). Molecular cloning and characterization of the inositol 1,4,5-trisphosphate receptor in Drosophila melanogaster. *J Biol Chem* **267,** 16613-16619.

Yuan JP, Zeng W, Huang GN, Worley PF & Muallem S. (2007). STIM1 heteromultimerizes TRPC channels to determine their function as store-operated channels. *Nat Cell Biol* **9,** 636-645.